

INFORMATION TO USERS

The most advanced technology has been used to photograph and reproduce this manuscript from the microfilm master. UMI films the text directly from the original or copy submitted. Thus, some thesis and dissertation copies are in typewriter face, while others may be from any type of computer printer.

The quality of this reproduction is dependent upon the quality of the copy submitted. Broken or indistinct print, colored or poor quality illustrations and photographs, print bleedthrough, substandard margins, and improper alignment can adversely affect reproduction.

In the unlikely event that the author did not send UMI a complete manuscript and there are missing pages, these will be noted. Also, if unauthorized copyright material had to be removed, a note will indicate the deletion.

Oversize materials (e.g., maps, drawings, charts) are reproduced by sectioning the original, beginning at the upper left-hand corner and continuing from left to right in equal sections with small overlaps. Each original is also photographed in one exposure and is included in reduced form at the back of the book.

Photographs included in the original manuscript have been reproduced xerographically in this copy. Higher quality 6" x 9" black and white photographic prints are available for any photographs or illustrations appearing in this copy for an additional charge. Contact UMI directly to order.

U·M·I

University Microfilms International
A Bell & Howell Information Company
300 North Zeeb Road, Ann Arbor, MI 48106-1346 USA
313 761-4700 800 521-0600

Order Number 9110948

**Geometric nonlinear filtering theory with application to the
maneuvering aircraft tracking problem**

Bishop, Robert H., Ph.D.

Rice University, 1990

U·M·I
300 N. Zeeb Rd.
Ann Arbor, MI 48106

RICE UNIVERSITY

GEOMETRIC NONLINEAR FILTERING THEORY WITH APPLICATION TO
THE MANEUVERING AIRCRAFT TRACKING PROBLEM


by

ROBERT H. BISHOP


A THESIS SUBMITTED
IN PARTIAL FULFILLMENT OF THE
REQUIREMENTS FOR THE DEGREE

DOCTOR OF PHILOSOPHY


APPROVED, THESIS COMMITTEE:



A. C. Antoulas, Associate Professor in
Electrical and Computer Engineering,
Director



G. B. Pearson, Abercrombie Professor in
Electrical and Computer Engineering



A. Miele, Professor of Aerospace
Sciences and Mathematical Sciences



B. Aazhang, Assistant Professor in
Electrical and Computer Engineering

Houston, Texas
April 1990

Abstract

Geometric Nonlinear Filtering Theory with Application to the Maneuvering Aircraft Tracking Problem

by

Robert H. Bishop

A geometric nonlinear filter (GNF) is designed for application to the problem of tracking a maneuvering aircraft. The aircraft tracking problem is a state estimation problem and a state prediction problem. A nonlinear aircraft maneuver model is proposed for use in the state estimation as well as the state prediction. This nonlinear model is based on the so-called coordinated turn and describes planar trajectories.

The GNF design approach involves state transformations with output injection to transform the nonlinear system model to a linear form, known as the observer canonical form. For many nonlinear systems, such as the proposed aircraft maneuver model, this linearizing transformation does not exist. Therefore, for the maneuvering aircraft model, a transformation to an approximate observer canonical form is given.

Utilizing a Lyapunov stability approach, sufficient conditions for stability of the GNF estimation error are derived. No such conditions exist for the extended Kalman filter (EKF).

The GNF was found to be stable in cases where the EKF was not stable. The tracking performance of the GNF compares favorably with the EKF for various levels of measurement noise. However, the GNF offers a substantial savings in computational time making it more attractive than the EKF for use in a fire control computer.

Acknowledgements

I wish to express my gratitude to my advisor Professor A. C. Antoulas for his support and guidance throughout this research. I would like to thank Professor J. B. Pearson, Professor A. Miele, and Professor B. Aazhang for serving on my thesis committee and for their comments. I would also like to thank Heinz Piccolruaz and Jürg Weilenmann of Contraves Ltd., Zurich for suggesting this problem and for their input.

I would like to acknowledge my wife, Lynda, for our many technical discussions and for typing and reviewing this dissertation.

I would like to thank my wife, my parents and my son, Robert Emerson, for their love and support.

Table of Contents

Chapter 1 Introduction	1
Chapter 2 The Aircraft Maneuver Model	10
2.1 Introduction	10
2.2 The Coordinated Turn Model	12
2.3 Geometric Interpretation	14
2.4 Maneuver Plane Equations	17
2.5 Model Uncertainties	19
2.6 The Maneuver Model	23
2.7 Observability	25
Chapter 3 Geometric Nonlinear Filter (GNF) Design	27
Chapter 4 Approximate Observer Canonical Form	35
4.1 Introduction	35
4.2 Transformation	38
Chapter 5 GNF Gain Calculation	44
5.1 Introduction	44
5.2 Designing the Gain in the Scalar Output Case	47
5.3 Special Cases of Theorem 5.1	52
5.4 Designing the Gain in the Multi-Output Case	55
5.5 The GNF Gain	57
Chapter 6 Sufficient Stability Conditions	62
6.1 Introduction	62
6.2 Deterministic Stability	63
6.3 Deterministic Stability Computations	69
6.4 Stochastic Stability	70

Chapter 7 The Extended Kalman Filter	75
7.1 Introduction	75
7.2 Aircraft Maneuver Model EKF	77
Chapter 8 Aircraft Tracking Results	79
8.1 Introduction	79
8.2 Simulated Aircraft Trajectories	81
8.2.1 Stability Analysis	82
8.2.2 Measurement Noise	89
8.3 Actual Aircraft Trajectories	93
Chapter 9 Conclusions	123
Appendix A Reference Frames	126
Appendix B Theory of Nonlinear Geometric Estimation ..	131
Appendix C Proof of Theorem 5.1	140
Appendix D GNF Gain Calculations	143
Appendix E EKF Gain Calculations	148
Appendix F Actual Aircraft Trajectories	152
Bibliography	166

Chapter 1

Introduction

This thesis deals with the problem of tracking a maneuvering aircraft. The approach presented here differs significantly from previous work in the following two areas,

- (i) the aircraft maneuver model, and
- (ii) the filter design method.

The aircraft maneuver model, which is described in detail in Chapter 2, is derived by assuming that the aircraft is executing a coordinated turn. This maneuver model is nonlinear and the three spatial directions are coupled. In previous work, evasive maneuvers were viewed as a response to a random noise. The resulting maneuver models were linear and the three spatial directions were uncoupled. The filter designs associated with these linear models generally consisted of three separate filters, one for each spatial direction. The individual filters are usually Kalman filters. The developmental history of the aircraft maneuver models and their associated filters is presented in more detail in the discussion that follows.

The filter design presented here is geometric and is based on the so-called Lie algebraic methods. The basic idea is to transform the nonlinear maneuver model to a linear form through the use of nonlinear state transformations so that the well

developed linear filtering theory can be utilized. This filter design technique results in what will be referred to here as a geometric nonlinear filter (GNF). In this thesis the GNF will be compared to the extended Kalman filter (EKF). Comparison of any nonlinear filter results with the EKF is inevitable since the EKF has been used with great success in practical nonlinear filter design for the last twenty years and filter designers usually look first to the EKF for a solution to their nonlinear problem.

The EKF has the advantages that it has stood the test of time and it works. Its disadvantages are that there is no stability theory associated with it and that it requires an on-line solution of a matrix Riccati equation, which is computationally slow.

The underlying problem which motivates the problem of tracking a maneuvering aircraft is that of anti-aircraft gun fire control. The primary functions of the fire control computer are to compute an accurate target state vector, maintain target tracking by aligning the radar boresight, and estimate target position at projectile arrival time in order to compute gun pointing angles. Of interest here are the first two functions, namely, state estimation and short-interval prediction. The purpose of the short-interval prediction is to keep the radar boresight moving in the right direction to insure that tracking is maintained.

Much effort has been spent over the years developing algorithms for tracking maneuvering aircraft. This effort has been summarized in the survey paper by Chang and Tabaczynski [4]. The historical development of the maneuver models, taken from Moose [24] et al., is shown in Figure 1.1.

The perturbations can be modelled as zero mean, white Gaussian disturbances (see Figure 1.1a). In this case, the aircraft acceleration is modelled by

$$\dot{a}(t) = w(t), \quad (1.1)$$

where $w(t)$ is a white driving function. The strength of the noise corresponds roughly to the maneuver magnitude. The filter performance for nonmaneuvering trajectories is severely degraded.

The perturbations can also be modelled as a correlated random process (see Figure 1.1b). This was first proposed by Singer [29], wherein the aircraft acceleration $a(t)$ is modelled by

$$\dot{a}(t) = -\alpha a(t) + w(t), \quad (1.2)$$

where α is the reciprocal of the acceleration time constant.

Berg [1] added a term to this acceleration model which he called an adaptive estimate of the mean target jerk. Berg's model has the form

$$\dot{a}(t) = -\alpha a(t) + w(t) + \dot{a}^*, \quad (1.3)$$

where a' is the mean target jerk. The basic assumption leading to this additional term is that the maneuver is modelled as a coordinated turn. In a coordinated turn,

- (a) the change in the sum of the aerodynamic and propulsive accelerations acting on the aircraft is constant;
- (b) the aircraft body rate along the roll axis is zero;
- (c) the angles of attack and sideslip are zero.

Berg [1] makes the additional assumption that a' is constant and updated only at discrete times based on the state estimates at that time.

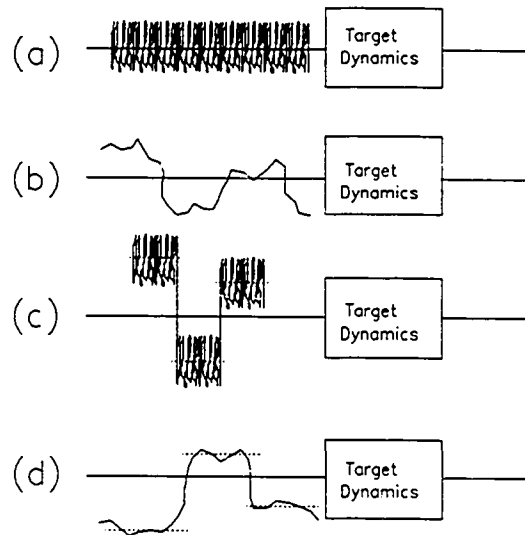


Figure 1.1. The Historical Development of Maneuver Models

The maneuvering target can also be modelled as a random process whose mean value switches randomly from among a finite

set of predefined values (see Figure 1.1c). An adaptive filter, due to Moose [23] and Gholson and Moose [9], can then be utilized.

Finally, Moose et al. [24] combined the maneuver models in Figures 1.1b and 1.1c to obtain the model illustrated in Figure 1.1d and developed an adaptive filter.

The common denominator in each of the maneuver models just described is that the resulting maneuver model is linear. Also, the acceleration models in the three spatial directions are uncoupled. The aircraft acceleration $a(t)$, hence the state noise, are in inertial coordinates. This is awkward since the state noise is more naturally described in the aircraft body coordinates. Based on one of the above maneuver models, the resulting tracking algorithm generally consists of three independent filters, one for each spatial direction. As previously remarked, it is common to use a Kalman filter, one for each direction, although other types of filters including constant gains filters (such as the Wiener filter) have been used. Thorp [32] introduced the idea of switching between two Kalman filters in response to a detected maneuver. Other common filter algorithms include the α - β and the α - β - γ filters. These filters generally have little capability to track severely maneuvering targets and are used in concert with a maneuver detection scheme (see e.g. Williams and Friedland [36]). Different variations of the above models include switching

between several filters in response to maneuvers of varying strengths. A comparison of these various filters can be found in Singer and Behrke [30].

The approach taken here is to model the aircraft maneuver as a coordinated turn. These assumptions lead to a set of nonlinear differential equations describing the maneuver. The use of these equations to track the aircraft trajectory was suggested by Contraves [5] as a more sophisticated alternative to linear models just described. The resulting filter is nonlinear and the three spatial disturbances are highly coupled. Perturbations to this maneuver model are modelled in the aircraft body frame as correlated random noise.

The coordinated turn model is also utilized for the short-term prediction. Since the coordinated turn model describes planar trajectories, the number of first-order differential equations that must be integrated is reduced from nine to four, thus reducing the computational burden.

Central to the GNF approach is the transformation of the nonlinear system to a linear form, known as the observer canonical form, through the use of a nonlinear state (possibly including the output) transformation and output feedback. The filter design is simplified in the observer canonical form coordinates since the wealth of linear theory is then available. This approach has recently attracted much attention (Bestle

and Zeitz [2], Frezza et al. [7], Krener [16], Krener and Isidori [17], Krener and Respondek [19], Phelps and Krener [27], and Walcott et al. [34]).

Bestle and Zeitz [2] show how a GNF design can be accomplished using the partial derivatives of the transformation to observer canonical form without actually computing the transformation. These derivatives, which are crucial in this method, can be computed in a straight-forward manner. Bestle and Zeitz [2] assume that a transformation to observer canonical form with output injection exists, and then based on a classical local linearization of the estimation error equation, they show how, using the partial derivatives, a nonlinear gain vector which insures asymptotic stability of the estimation error can be obtained. State and measurement noise and output coordinate changes are not considered.

Krener [16] developed the asymptotic GNF technique. This technique accounts for state and measurement noise and results in a solution very similar in nature to the Kalman filter, i.e. the optimal gains are computed off-line. Krener [16] introduces the modified observer canonical form. Although it is desirable to have a system in observer canonical form, this is not always possible. The modified observer canonical form allows the injection term to include states that are not measured directly but that can be estimated quickly and accurately. It applies when the state and measurement noises are small and when the state vector can be divided into fast and slow states.

The fast/slow terminology is derived from the respective time constants of the dynamics of the estimation errors. With this new canonical form, the GNF approach can then be applied to a larger family of nonlinear systems.

Frezza et al. [7] applied the asymptotic GNF technique to a one-dimensional tracking problem with success. The tracking performance compared favorably to the EKF but at a substantial savings in computational time.

The question of the existence of transformations to observer canonical form has been addressed by Krener and Isidori [17] and Krener and Respondek [19]. Krener and Isidori [17] considered only the scalar output case, no inputs, and no output coordinate changes. Krener and Respondek [19] considered the multi-output case with inputs and allowed for output coordinate changes as well as state coordinate changes. As previously remarked, not all nonlinear systems can be transformed into observer canonical form. Determining the existence of such transformations generally involves transforming the given nonlinear system to yet another canonical form, the so-called observable canonical form. This canonical form is not of direct use in constructing estimators. However, as shown in Krener and Respondek [19], it is very useful in determining the existence of transformations to observer canonical form. Using the observable canonical form, Phelps and Krener [27] give necessary conditions for the existence of transformations and algorithms to compute the transformation to observer form

without the usual Lie bracket calculations. The algorithms were implemented in Macsyma (a symbolic manipulation software package).

The coordinated turn model (on which the GNF design proposed in this thesis is based) cannot be transformed into observer canonical form. It is possible to transform the model into an approximate observer canonical form, thus making the GNF approach applicable to the aircraft tracking problem.

A GNF and an EKF are designed and evaluated in this thesis. Sufficient conditions for stability of the GNF are given. No such stability conditions exist for the EKF. It will be shown that the GNF is stable for a much wider range of initial conditions than the EKF. Also, the GNF requires less computational time, yet tracks at least as well as the EKF. This performance evaluation is done utilizing both simulated aircraft trajectories as well as "real-world" trajectories.

This thesis is organized as follows: Chapter 2 presents the derivation of the aircraft maneuver model. Chapter 3 describes the GNF design procedure. Chapter 4 describes the transformation of the aircraft maneuver model to approximate observer canonical form. The GNF design for the aircraft tracking problem is in Chapter 5. The deterministic and stochastic stability analyses of the GNF is presented in Chapter 6. Chapter 7 presents the EKF which will be used for comparison purposes. The results and conclusions are presented in Chapters 8 and 9, respectively.

Chapter 2

The Aircraft Maneuver Model

2.1 Introduction

The motion of a rigid aircraft travelling through the atmosphere is described by a set of nonlinear, coupled differential equations. These equations can be written in the form

$$\begin{aligned}\dot{x} &= f(x) + u_x \\ y &= h(x) + u_m.\end{aligned}$$

The (nonlinear) system dynamics are given by $f(x)$ and the (nonlinear) measurements are given by $h(x)$. The term u_x is the uncertainty in the system dynamics and is referred to as the state uncertainty. The term u_m is the measurement uncertainty. The purpose of this chapter is to derive a maneuvering aircraft model which describes the aircraft trajectories more accurately than the current state of the art maneuver models described in the introduction.

A general mathematical model of the aircraft maneuver consists of both dynamic and kinematic equations (see Etkin [6]), where the forces and torques acting on the aircraft are complex functions of the aircraft shape and its motion. The aerodynamic forces and torques are known only approximately. In addition, the pilot can alter the forces and torques acting on the aircraft. To reduce the complexity of the problem,

appropriate assumptions are made resulting in a simpler and yet realistic description of the aircraft motion. In the case of aircraft targets, it is the resulting aircraft motion in the atmosphere that should be modelled. The response of the aircraft to pilot and environmental inputs is not modelled (Singer and Behnke [30]).

An aircraft has many different operational modes: take-off and landings, steady-flight, turns, and evasive maneuvers, to name but a few. Since simplifying assumptions do not generally apply for all the different operational modes, it is necessary to restrict attention to one mode at a time. Of interest here are evasive maneuvers.

The purpose of this section is to present the aircraft maneuver model used in this thesis. The assumptions which lead to the maneuver model are consistent with the coordinated turn of a fixed-wing aircraft. The coordinated turn assumptions lead to a set of nonlinear, coupled differential equations which describe the aircraft trajectory. The derivation of the maneuver model is presented in Section 2.2. The trajectories described by the model have interesting geometric properties, as discussed in Sections 2.3 and 2.4. The model uncertainties are discussed in Section 2.5. The definition of the state vector is presented in Section 2.6 and the question of observability is discussed in Section 2.7. A description of all pertinent reference frames is given in Appendix A.

2.2 The Coordinated Turn

The aircraft maneuver is modelled here as a coordinated turn. The assumptions leading to a coordinated turn maneuver are

- (1) the change in the aerodynamic lift and thrust-drag accelerations (with respect to the body reference frame) is zero;
- (2) the aircraft body rate about the roll axis is zero;
- (3) $e_1^B = e_1^W$ (see Appendix A).

The coordinated turn assumptions reduce the problem of modelling the aircraft motion to a kinematics problem. There is no need to model the pilot response and also no need to try to estimate the aircraft angular attitude.

Letting a equal the sum of the aerodynamic and propulsive accelerations acting on the aircraft, by assumption (1)

$$\dot{a}_B = 0. \quad (2.1)$$

It is assumed that the aerodynamic accelerations include only lift along e_3^B and drag along e_1^B . Aerodynamic accelerations along e_2^B are assumed to be zero. Assumption (2) implies that

$$\dot{\phi} = \omega^B \cdot e_1^B = 0, \quad (2.2)$$

and assumption (3) implies that the angles of attack and of sideslip are zero (see Figure A3, Appendix A).

The aircraft angular velocity vector, ω^B , is computed by utilizing Poisson's formulas (Miele [22]) :

$$\dot{e}_i^B = \omega^B \times e_i^B, \quad i=1,2,3.$$

Forming the cross-product $\mathbf{e}_i^B \times \dot{\mathbf{e}}_i^B$ and using the identity

$$\mathbf{v}_1 \times (\mathbf{v}_2 \times \mathbf{v}_3) = (\mathbf{v}_1 \cdot \mathbf{v}_3) \mathbf{v}_2 - (\mathbf{v}_1 \cdot \mathbf{v}_2) \mathbf{v}_3$$

the formula for ω^B is,

$$\omega^B = (\omega^B \cdot \mathbf{e}_i^B) \mathbf{e}_i^B + \mathbf{e}_i^B \times \dot{\mathbf{e}}_i^B, \quad i=1,2,3. \quad (2.3)$$

By assumption (2), (2.3) reduces to

$$\omega^B = \mathbf{e}_1^B \times \dot{\mathbf{e}}_1^B \quad (2.4)$$

for the specific case where $i=1$. Using assumption (3) it follows that

$$\mathbf{e}_{1E}^B = \dot{\mathbf{r}}_E / |\dot{\mathbf{r}}_E|. \quad (2.5)$$

(2.5) is differentiated with respect to time, and together with $\mathbf{e}_1^B \cdot \dot{\mathbf{e}}_1^B = 0$ (Miele [22]), it follows that

$$\dot{\mathbf{e}}_{1E}^B = \frac{\ddot{\mathbf{r}}_E}{|\dot{\mathbf{r}}_E|} - \left(\frac{\ddot{\mathbf{r}}_E \cdot \dot{\mathbf{r}}_E}{|\dot{\mathbf{r}}_E|^3} \right) \dot{\mathbf{r}}_E. \quad (2.6)$$

Substituting equations (2.5) and (2.6) into equation (2.4) yields

$$\omega_E^B = \frac{\dot{\mathbf{r}}_E \times \ddot{\mathbf{r}}_E}{|\dot{\mathbf{r}}_E|^2}. \quad (2.7)$$

With respect to the inertial reference frame the accelerations acting on the aircraft are given by

$$\ddot{\mathbf{r}}_E = \mathbf{a}_E + \mathbf{g}_E \quad (2.8)$$

where \mathbf{g}_E is the constant gravity acceleration in the inertial reference frame. With respect to the body reference frame (2.8) becomes

$$\mathbf{L}_{BE}(\ddot{\mathbf{r}}_E - \mathbf{g}_E) = \mathbf{L}_{BE} \mathbf{a}_E = \mathbf{a}_B. \quad (2.9)$$

Differentiating (2.9), using the fact that

$$L_{EB} \dot{L}_{BE} v_E = -\omega_E^B \times v_E \quad \forall v_E,$$

using assumption (1) and (2.7) yields the kinematic equation of motion

$$\ddot{r}_E = \frac{\dot{r}_E \times \ddot{r}_E}{|\dot{r}_E|^2} \times (\ddot{r}_E - g_E). \quad (2.10a)$$

A condition on the aircraft trajectory is that the velocity, $|\dot{r}_E|$, must always be different from zero.

In this thesis the radar measurement set is taken to be the aircraft inertial position vector r_E in Cartesian coordinates (Figure A1, Appendix A). This leads to a linear measurement model. It is also common to have as a measurement set the spherical coordinates of range, elevation and azimuth angles which leads to a nonlinear measurement model. For the particular application studied here, the radar measurements that were available for the actual aircraft trajectories in the data base (Appendix F) are in inertial Cartesian coordinates. Therefore, for the measurement set used here, the (noise-free) measurement equation is

$$y = r_E. \quad (2.10b)$$

2.3 Geometric Interpretation

An aircraft trajectory through the atmosphere can be viewed as an arbitrary speed space curve. The aircraft velocity is assumed to be nonzero, hence the curve r is *regular*. See O'Neill [26] for more details on space curves.

THEOREM 2.1

Let r be a regular curve in R^3 . Then

$$e_1^F = \dot{r}/|\dot{r}|,$$

$$e_2^F = (\ddot{r} \times \dot{r})/|\ddot{r} \times \dot{r}|,$$

$$e_3^F = e_1^F \times e_2^F,$$

$$\kappa = |\ddot{r} \times \dot{r}|/|\dot{r}|^3, \text{ and}$$

$$\tau = (\ddot{r} \times \dot{r}) \cdot \ddot{r}/|\ddot{r} \times \dot{r}|^2.$$

The scalar κ is the curvature and the scalar τ is the torsion. If $\kappa=0$ the curve is a straight line; if $\tau=0$ the curve is planar. e_1^F is the unit tangent vector field, e_2^F is the binormal vector field and e_3^F is the principal normal vector field. (e_1^F, e_2^F, e_3^F) is the Frenet frame field on r , (see Figure 2.1). The Frenet frame field will be referred to here as the Frenet reference frame.

Computing the torsion, τ , using (2.10) and the formula in Theorem 2.1 yields

$$\tau=0.$$

Thus, the coordinated turn maneuver model describes planar trajectories in a *maneuver plane* (see Figure 2.1). The curvature, on the other hand, is in general not zero. This points out a major difference between the coordinated turn maneuver model proposed here and the previous maneuver models described in Chapter 1. Those maneuver models are characterized by having zero torsion and zero curvature (i.e. straight line paths).

The maneuver reference frame can be taken to be the Frenet reference frame at t_0 . Therefore, from Theorem 2.1, the transformation matrix from the maneuver reference frame to the inertial

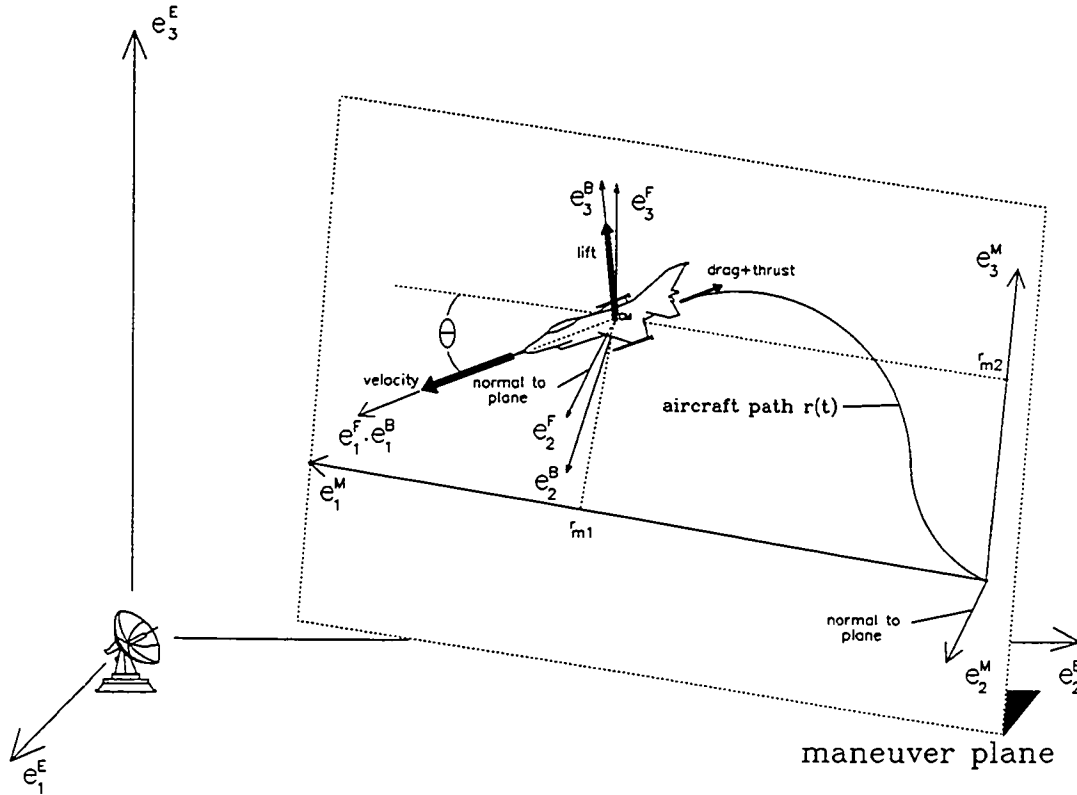


Figure 2.1. The Maneuver Plane Geometry

reference frame is the constant matrix

$$L_{EM} = \begin{pmatrix} \frac{\dot{r}}{|\dot{r}|} & \frac{\ddot{r} \times \dot{r}}{|\ddot{r} \times \dot{r}|} & \frac{\dot{r} \times (\ddot{r} \times \dot{r})}{|\dot{r} \times (\ddot{r} \times \dot{r})|} \end{pmatrix} \bigg|_{t=t_0}. \quad (2.11)$$

The transformation from the maneuver reference frame to the Frenet reference frame is

$$L_{FM} = \begin{pmatrix} \cos \theta & 0 & -\sin \theta \\ 0 & 1 & 0 \\ \sin \theta & 0 & \cos \theta \end{pmatrix}. \quad (2.12)$$

θ is the angle of the velocity vector measured from e_1^M (see Figure 2.1). By choosing the maneuver reference frame to be the Frenet reference frame at t_0 , it follows that θ is zero at $t=t_0$. From Theorem 2.1, it follows that the transformation from the Frenet reference frame to the inertial reference frame is

$$L_{EF} = L_{EM} L_{FM}^T = \begin{pmatrix} \frac{\dot{r}}{|\dot{r}|} & \frac{\ddot{r} \times \dot{r}}{|\ddot{r} \times \dot{r}|} & \frac{\dot{r} \times (\ddot{r} \times \dot{r})}{|\dot{r} \times (\ddot{r} \times \dot{r})|} \end{pmatrix}. \quad (2.13)$$

The transformation matrix from the body reference frame to the inertial reference frame is

$$L_{EB} = \begin{pmatrix} \frac{\dot{r}}{|\dot{r}|} & \frac{(\ddot{r} - g_E) \times \dot{r}}{|(\ddot{r} - g_E) \times \dot{r}|} & \frac{\dot{r} \times ((\ddot{r} - g_E) \times \dot{r})}{|\dot{r} \times ((\ddot{r} - g_E) \times \dot{r})|} \end{pmatrix}, \quad (2.14)$$

and the transformation from the body reference frame to the Frenet reference frame is

$$L_{FB} = \begin{pmatrix} 1 & 0 & 0 \\ 0 & \cos \phi & -\sin \phi \\ 0 & \sin \phi & \cos \phi \end{pmatrix}. \quad (2.15)$$

(2.15) follows from (2.13) and (2.14). ϕ is the aircraft roll angle (measured between e_3^B and e_3^F) and is assumed to be a constant in the coordinated turn model.

2.4 Maneuver Plane Equations

Consider the situation in the maneuver plane as shown in Figure 2.1. r_m and v_m denotes the position and velocity, respectively, of the center of mass (CM). The velocity of the aircraft in the maneuver plane is

$$\mathbf{v}_m = \dot{\mathbf{r}}_m = \begin{bmatrix} \cos\theta & 0 & \sin\theta \\ 0 & 1 & 0 \\ -\sin\theta & 0 & \cos\theta \end{bmatrix} \begin{pmatrix} v \\ 0 \\ 0 \end{pmatrix}, \quad (2.16)$$

where $v = |\dot{\mathbf{r}}_m|$. Taking the derivative of (2.16) yields the aircraft acceleration

$$\ddot{\mathbf{r}}_m = \begin{bmatrix} \cos\theta & 0 & \sin\theta \\ 0 & 1 & 0 \\ -\sin\theta & 0 & \cos\theta \end{bmatrix} \begin{pmatrix} \dot{v} \\ 0 \\ -v\dot{\theta} \end{pmatrix}, \quad (2.17)$$

and taking the derivative of (2.17) yields the aircraft jerk,

$$\dddot{\mathbf{r}}_m = \begin{bmatrix} \cos\theta & 0 & \sin\theta \\ 0 & 1 & 0 \\ -\sin\theta & 0 & \cos\theta \end{bmatrix} \begin{pmatrix} \ddot{v} - v\dot{\theta}^2 \\ 0 \\ -2\dot{v}\dot{\theta} - v\ddot{\theta} \end{pmatrix}. \quad (2.18)$$

Using (2.16), (2.17) and (2.7) the angular acceleration ω is

$$\omega = \begin{pmatrix} 0 \\ \dot{\theta} \\ 0 \end{pmatrix}. \quad (2.19)$$

Let

$$\mathbf{g}_m = \mathbf{L}_{M\mathcal{E}} \mathbf{g}_{\mathcal{E}} = \begin{pmatrix} g_{mx} \\ g_{my} \\ g_{mz} \end{pmatrix}$$

be the constant gravity acceleration. Substituting (2.17), (2.18) and (2.19) into (2.10a) yields

$$\ddot{v} = -\dot{\theta}(g_{mx}\sin\theta + g_{mz}\cos\theta), \text{ and} \quad (2.20a)$$

$$v\ddot{\theta} + \dot{v}\dot{\theta} = -\dot{\theta}(g_{mx}\cos\theta - g_{mz}\sin\theta). \quad (2.20b)$$

Integrating equation (2.20) yields

$$\dot{v} = -g_{mz}\sin\theta + g_{mx}\cos\theta + c_1, \text{ and} \quad (2.21a)$$

$$v\dot{\theta} = -g_{mz}\cos\theta - g_{mx}\sin\theta + c_2. \quad (2.21b)$$

The constant c_1 is the sum of the thrust and drag accelerations and as a consequence of the coordinated turn assumptions it is constant. The constant c_2 is the lift acceleration times the cosine of the roll angle and is also constant. Hence it follows that

$$\dot{c}_1 = 0, \text{ and} \quad (2.22a)$$

$$\dot{c}_2 = 0. \quad (2.22b)$$

The aircraft trajectory in the maneuver plane is described by (2.16), (2.21) and (2.22). Once a state estimate (i.e. position, velocity and acceleration) is available, the four equations (2.16) and (2.21) can be used to predict the state forward. Thus, the number of first-order differential equations needed for the prediction is reduced from nine to four. This prediction scheme was used successfully by Berg [1].

2.5 Model Uncertainties

The coordinated turn maneuver model was developed on the assumptions that the time-variation of the roll angle is zero and that the time-variation of the aerodynamic and propulsive accelerations is zero. The state uncertainties in the model follow directly from these assumptions.

The uncertainty in the time-variation of the aerodynamic and propulsive accelerations is naturally modelled in the aircraft body reference frame (under the assumption that the coordinated turn maneuver model assumption (3) is valid, i.e. $e_1^B = e_1^V$). From (2.1)

$$\dot{a}_B = 0.$$

The uncertainty in the aerodynamic and thrust accelerations is modelled by assuming that the time-variation in a_B is random. Thus, the uncertainty is modelled by

$$\dot{a}_B = u_a \quad (2.23)$$

where u_a is a random process. In practice, it has been found that (2.23) is a good model for filter design purposes, even though the time-variation may actually be deterministic in nature (Gelb [8]). u_a has the form

$$u_a = \begin{pmatrix} u_{a1} \\ 0 \\ u_{a3} \end{pmatrix}$$

where u_{a1} is the uncertainty in the thrust-drag direction and u_{a3} is the uncertainty in the lift direction. With the uncertainty in the body reference frame given by u_a , it is given in the inertial reference frame by $L_{EB} u_a$.

The uncertainty in the time-variation of the roll angle is modelled similarly. From (2.2)

$$\dot{\phi} = 0.$$

The roll rate uncertainty is modelled by assuming that the time-variation in $\dot{\phi}$ is random,

$$\dot{\phi} = \bar{u}_\phi, \quad (2.24)$$

where \bar{u}_ϕ is a random process. It follows from (2.3) that the random component of the angular velocity vector ω^B is $\bar{u}_\phi e_1^B$. The uncertainty with respect to the inertial reference frame due to the roll rate uncertainty is

$$u_\phi = \bar{u}_\phi e_1^B \times (\bar{r} - g_E) = -\bar{u}_\phi |e_1^B \times (\bar{r} - g_E)| e_2^B.$$

Define

$$u_\phi = -\bar{u}_\phi |(\bar{r} - g_E) \times e_1^B|.$$

Notice that u_ϕ is just a random process scaled by the magnitude of the aerodynamic accelerations. Thus, u_ϕ will be modelled as a random process where strength (characterized by the covariance matrix) has been adjusted to account for the maximum expected acceleration magnitudes. Although this is a (conservative) approximation, it will have a negligible effect on the final results after the "filter tuning" is complete. So, the roll rate uncertainty can be written as

$$u_\phi = L_{EB} \begin{pmatrix} 0 \\ u_\phi \\ 0 \end{pmatrix}. \quad (2.25)$$

Therefore, the total uncertainty (with respect to the inertial reference frame) is given by

$$L_{EB} u_B = L_{EB} \begin{pmatrix} u_{a1} \\ u_\phi \\ u_{a3} \end{pmatrix}. \quad (2.26)$$

The aircraft maneuver model, including the uncertainties, is

$$\dot{\bar{r}} = \frac{\bar{r} \times \dot{\bar{r}}}{|\dot{\bar{r}}|^2} \times (\bar{r} - g_E) + L_{EB} u_B. \quad (2.27a)$$

The measurement uncertainties, u_m , add directly to the measurements yielding

$$y = r_\varepsilon + u_m. \quad (2.27b)$$

Up to this point, the uncertainty u_B has been described only as a random process. It can be modelled as a white gaussian stochastic process or as a gauss-markov stochastic process, for example. Descriptions of other possible models can be found in any standard text on stochastic processes, such as Jazwinski [12] and Maybeck [21]. The model chosen here is the first-order gauss-markov stochastic process. The process is modelled by the first-order linear matrix differential equation

$$\dot{u}_B = -A_a u_B + w_B,$$

where

$$A_a = \begin{bmatrix} -\alpha_1 & 0 & 0 \\ 0 & -\alpha_2 & 0 \\ 0 & 0 & -\alpha_3 \end{bmatrix}.$$

The α_i 's are the reciprocals of the markov process time-constants and w_B is a white gaussian stochastic process with

$$E(w_B(t)w_B^T(\tau)) = \begin{bmatrix} 2\alpha_1\sigma_1^2 & 0 & 0 \\ 0 & 2\alpha_2\sigma_2^2 & 0 \\ 0 & 0 & 2\alpha_3\sigma_3^2 \end{bmatrix} \delta(t-\tau),$$

where

$$E(u_{a1}(t)u_{a1}(\tau)) = \sigma_1^2 \delta(t-\tau),$$

$$E(u_{a2}(t)u_{a2}(\tau)) = \sigma_2^2 \delta(t-\tau),$$

$$E(u_{a3}(t)u_{a3}(\tau)) = \sigma_3^2 \delta(t-\tau).$$

The measurement uncertainties, $u_m(t)$, are modelled as white gaussian stochastic processes with

$$E(u_m(t)u_m^T(\tau)) = \sigma_m^2 I \delta(t-\tau).$$

2.6 The Maneuver Model

The objective is to write the aircraft maneuver model (2.27) in the form

$$\dot{x} = f(x) + u_x \quad (2.28a)$$

$$y = h(x) + u_m.$$

To accomplish this, first define the state vector x as

$$x_{4i-3} = r_i,$$

$$x_{4i-2} = \dot{r}_i,$$

$$x_{4i-1} = \ddot{r}_i,$$

$$x_{4i} = u_{Bi} \quad \text{for } i=1,2,3.$$

Notice that the number of states is twelve. This is an increase of three over the number of states needed to represent the maneuver model (2.27a) when the state noise is modelled as a white gaussian stochastic process. This procedure of *state vector augmentation* results from modelling the uncertainty as a first-order markov process. Higher order markov process models will increase the number of states even further.

With the above definition of the state vector it follows that the nonlinear dynamics are

$$f(x) = \begin{pmatrix} x_2 \\ x_3 \\ f_1 + l_{11}x_4 + l_{12}x_8 + l_{13}x_{12} \\ -\alpha_1 x_4 \\ x_6 \\ x_7 \\ f_2 + l_{21}x_4 + l_{22}x_8 + l_{23}x_{12} \\ -\alpha_2 x_8 \\ x_{10} \\ x_{11} \\ f_3 + l_{31}x_4 + l_{32}x_8 + l_{33}x_{12} \\ -\alpha_3 x_{12} \end{pmatrix},$$

where the l_{ij} 's are the (i,j) th elements of L_{EB} and the functions f_i are given by

$$\begin{pmatrix} f_1 \\ f_2 \\ f_3 \end{pmatrix} = \frac{1}{\Delta_1} \begin{pmatrix} (x_3x_{10} - x_2x_{11})(x_{11} - g) - (x_2x_7 - x_3x_6)x_7 \\ (x_2x_7 - x_3x_6)x_3 - (x_6x_{11} - x_7x_{10})(x_{11} - g) \\ (x_6x_{11} - x_7x_{10})x_7 - (x_3x_{10} - x_2x_{11})x_3 \end{pmatrix},$$

where

$$\Delta_1^2 = x_2^2 + x_6^2 + x_{10}^2.$$

The (linear) measurements are

$$h(x) = \begin{pmatrix} x_1 \\ x_5 \\ x_9 \end{pmatrix}.$$

The state and measurement noise covariance matrices are

$$E[u_x(t)u_x^T(\tau)] = \Sigma \delta(t - \tau)$$

and

$$E[u_m(t)u_m^T(\tau)] = \sigma_m^2 I \delta(t - \tau),$$

where $\Sigma = (\Sigma_{11}, \Sigma_{22}, \Sigma_{33})$ is a block diagonal matrix with

$$\Sigma_{ii} = \begin{bmatrix} \sigma_a^2 & 0 & 0 & 0 \\ 0 & \sigma_b^2 & 0 & 0 \\ 0 & 0 & \sigma_c^2 & 0 \\ 0 & 0 & 0 & 2\alpha_i \sigma_1^2 \end{bmatrix}.$$

σ_a^2, σ_b^2 , and σ_c^2 are nominally zero but can be used as "tuning" parameters to alter the filter performance. The initial conditions $x(0)$ are modelled as normally distributed random variables with

$$E[(x(0) - \bar{x}(0))(x(0) - \bar{x}(0))^T] = P_0(0)$$

where $\bar{x}(0) = E[x(0)]$. If $u_x = 0$ and $u_m = 0$ for all t , then the system is *autonomous*, and

$$\dot{x} = f(x) \quad (2.28b)$$

$$y = h(x).$$

2.7 Observability

At this point, it is necessary to check the observability of the aircraft maneuver model. If it is not observable, it will not be possible to observe all the states using the aircraft position as the measurements. Observability of nonlinear systems can be determined using the

DEFINITION (Krener and Respondek [19]) : The system

$$\dot{x} = f(x)$$

$$y = h(x)$$

is observable at x_0 if there exists a neighborhood, U , of x_0 and p -tuple of integers (l_1, l_2, \dots, l_p) such that

$$\Theta = \begin{bmatrix} \theta_1 \\ \theta_2 \\ \cdot \\ \cdot \\ \cdot \\ \theta_p \end{bmatrix}$$

where

$$\theta_i = \begin{bmatrix} L_f^0 & (dh_i) \\ L_f^1 & (dh_i) \\ \cdot & \\ \cdot & \\ L_f^{l_i-1} & (dh_i) \end{bmatrix}$$

is nonsingular at each $x \in U$ and

$$l_1 + l_2 + \dots + l_p = n.$$

The definition of the Lie derivative utilized in the above definition can be found in Appendix B. The integers (l_1, l_2, \dots, l_p) are called the observability indices at x_0 . Several other definitions of observability have appeared in the literature (see e.g. Hermann and Krener [10] and Kou, et al. [15]).

Computing the determinant of the observability matrix associated with the aircraft maneuver model yields

$$\det \Theta = 1.$$

Hence, the aircraft maneuver model is observable for any x_0 .

The observability indices are $l_1 = 4, l_2 = 4, l_3 = 4$.

Chapter 3

Geometric Nonlinear Filter (GNF) Design

Suppose that the nonlinear system (2.28a) is given. Considered in this thesis are nonlinear filters of the form (Kou et al. [14] and Thau [31])

$$\hat{\mathbf{x}} = \mathbf{f}(\hat{\mathbf{x}}) + \mathbf{K}'(\hat{\mathbf{x}})(\mathbf{y} - \mathbf{h}(\hat{\mathbf{x}})) \quad (3.1)$$

associated with the nonlinear system (2.28a).

The objective of the filter is to provide *good* estimates of the state of the system at the current time. This objective is met if $\mathbf{K}'(\hat{\mathbf{x}})$ is properly computed. Of utmost importance is the stability of the estimation error. In other words, the estimated state approaches the actual state as time increases. Once stability is established, other issues such as tracking performance (i.e. time convergence, error bounds, etc.) can be addressed.

One possible solution to the nonlinear estimation problem is provided by the extended Kalman filter (EKF). In the EKF, $\mathbf{K}'(\hat{\mathbf{x}})$ depends on the on-line solution of a state-dependent matrix Riccati equation of dimension equal to the number of states. The EKF does not guarantee stability and, in general, is not optimal. However, the design process is straight-forward and similar to the widely used Kalman filter design (which is valid in the linear case). The filter gain computations are

highly algorithmic, lending themselves to computer implementation, although if the number of states is large the computational burden (i.e. CPU time) is very high.

In the GNF design proposed here, $K'(x)$ is computed to guarantee stability of the estimation error. As in the EKF, the GNF gains are state-dependent, although the state dependency manifests itself through algebraic manipulations, such as additions, multiplications, etc., rather than through the on-line integration of a state dependent matrix differential equation. The GNF design lends itself to computer implementation and the computational burden is very low relative to the EKF.

The GNF design process is comprised of the following four steps.

STEP 1: The first step in the GNF design process is to try to find a (bijective C^∞) transformation $T: R^n \rightarrow R^n$ which transforms the state x to z :

$$x = T(z) \quad (3.2)$$

in such a way that the system

$$\dot{x} = f(x)$$

$$y = h(x)$$

is transformed into observer canonical form

$$\dot{z} = Az + b(Cz)$$

$$y = Cz.$$

The main characteristics of the observer canonical form are that the output is linear in the state and that the (nonlinear) output injection term depends only on states that are measured. The advantage of this form over the original nonlinear form is that the process of computing the filter gains to insure stability of the estimation error is simplified. When a transformation to observer canonical form exists, a general theory exists for designing a stable filter. This theory is presented in Appendix B.

It appears that the family of nonlinear systems which can be brought to observer canonical form through use of a nonlinear transformation with output injection is not large. This fact is discussed in more detail in Chapter 4. The aircraft maneuver model presented in Chapter 2 cannot be transformed to observer canonical form. It can, however, be transformed to an approximate observer canonical form as shown in the next chapter.

When the transformation that takes (2.28b) to approximate observer canonical form is applied to the actual system model (2.28a), the state noise is also transformed. The transformed state noise is given by

$$u_z = \left(\frac{\partial T}{\partial z} \right)^{-1} u_x.$$

Since u_x is modelled as a white gaussian process, then in general, u_z is not a white gaussian process. However, the transformation proposed here (and presented in the next chapter)

has the property that the transformed state noise remains a white gaussian stochastic process. Similar problems arise with the measurement noise when output transformations are considered.

When considering transformations of the stochastic model, all differentials and integrals are defined in the sense of Stratonavich (see Jazwinski [12], for example).

Imbedded in the state transformation (3.2) is a (possible) transformation of the output. In general, nonlinear transformations of the output present difficulties in the estimation of the states of a system in the presence of measurement noise modelled as a white gaussian stochastic process. This is because the output transformation transforms the measurement noise as well as the output, and usually, a white gaussian stochastic process is not transformed to a white gaussian stochastic process. For the aircraft maneuver model, the outputs (radar measurements of the aircraft position in the inertial reference frame) will be transformed by a linear transformation represented by an orthogonal matrix. The orthogonal matrix coupled with the fact that the variance of the measurement noise is equal in all three inertial directions results in transforming the white gaussian stochastic process measurement noise model to a white gaussian stochastic process. This is described in detail the next chapter.

Consider a transformation, T , of the form (3.2) such that (2.28b) is transformed to approximate observer canonical coordinates. Utilizing (3.2) the filter equation (3.1) is transformed into

$$\dot{\hat{z}} = A\hat{z} + b(\hat{z}) + J(\hat{z})^{-1}K^*(\hat{z})L^{-1}(y - C\hat{z}),$$

where

$$J(\hat{z}) = \left. \frac{\partial T}{\partial z} \right|_{z=\hat{z}},$$

is the Jacobian of the transformation and L is the linear transformation of the output described in the previous paragraph. Since the measured variables are also state variables, the linear output transformation is imbedded in T . This is because the measured state variables are related to the transformed measured state variables through L , and hence it follows that the partial derivative of the measured state variables with respect to the transformed state variables is just L . Therefore, the elements of the matrix L are also elements of the matrix $J(\hat{z})$.

Define the time-varying, nonlinear gain

$$K(\hat{z}) := J(\hat{z})^{-1}K^*(\hat{z})L^T, \quad (3.3)$$

and the approximate observer canonical form estimation error

$$e_z := \hat{z} - z. \quad (3.4)$$

Then the estimation error (3.4) is described by the differential equation

$$\dot{e}_z = (A - K(\hat{z})C)e_z + b(\hat{z}) - b(z) + K(\hat{z})u_m - u_z. \quad (3.5)$$

Linearizing $b(z)$ about the estimated trajectory \hat{z} using a Taylor series expansion yields

$$b(z) = b(\hat{z}) - B(\hat{z})e_z - \bar{b}(z, \hat{z}), \quad (3.6)$$

where

$$B(\hat{z}) = \left. \frac{\partial b}{\partial z} \right|_{z=\hat{z}}.$$

Substituting (3.6) into (3.5) yields

$$\dot{e}_z = A^*(\hat{z})e_z + \bar{b}(z, \hat{z}) + K(\hat{z})u_m - u_z, \quad (3.7)$$

where

$$A^*(\hat{z}) = A - K(\hat{z})C + B(\hat{z}).$$

The goal of the GNF design is to compute $K(\hat{z})$ such that the estimation error described by (3.7) is stable. The computation of a transformation to approximate observer canonical form for the aircraft maneuver model is the topic of Chapter 4. The estimation error equation (3.7) is studied in detail in Chapters 5 and 6.

STEP 2: The second step is to compute $K(\hat{z})$ such that the desired eigenvalues of $A^*(\hat{z})$ are achieved for all $t \geq t_0$. It will be shown that it is possible, under certain conditions, to compute $K(\hat{z})$ such that

$$A^*(\hat{z}) = Q^{-1}(\hat{z})(A - K_1 C)Q(\hat{z}),$$

where K_1 is specified to achieve the desired eigenvalues. Clearly $A^*(\hat{z})$ and $A - K_1 C$ have the same eigenvalues. The con-

struction of such $K(\hat{z})$ is presented in Chapter 5. It is a characteristic of time-varying systems that asymptotic stability of the equilibrium point 0 of

$$\dot{e}_z = A^*(\hat{z})e_z$$

is not insured by the fact that all the eigenvalues of $A^*(\hat{z})$ have negative real parts. Therefore the time variation of $A^*(\hat{z})$ must be accounted for in the stability analysis. This is discussed in detail in Chapter 6.

STEP 3: This step involves the stability analysis. The gain $K(\hat{z})$ must be chosen so that the estimation error approaches zero asymptotically when the nonlinear term $\bar{b}(z, \hat{z})$ is accounted for. The sufficient conditions to guarantee asymptotic stability in the presence of nonzero $\bar{b}(z, \hat{z})$ are obtained through the application of Lyapunov's indirect method. The effect of the random disturbances u_m and u_z on the asymptotic stability must be quantified. This is accomplished using the stochastic Lyapunov function approach. The stability analysis is presented in Chapter 6.

STEP 4: The final step in the design process is to compute $K^*(\hat{z})$ via

$$K^*(\hat{z}) = J(\hat{z})K(\hat{z})L.$$

Stability of e_z implies stability of e_x . To see this consider the following theorem taken from Munkres [25],

THEOREM 3.1

The function $T:R^n \rightarrow R^n$ is continuous if and only if for every convergent sequence $z_n \rightarrow z$ in R^n , the sequence $T(z_n)$ converges to $T(z)$.

$T \in C^0$ is a continuous function. So,

$$z \rightarrow z \Rightarrow T(z) \rightarrow T(z) \Rightarrow \hat{x} \rightarrow x$$

since $\hat{x} = T(z)$ and $x = T(z)$. ■

These four design steps are discussed in detail in the following chapters.

Chapter 4

Approximate Observer Canonical Form

4.1 Introduction

The first step in the GNF design process is to find a (bijective C^∞) transformation $T: \mathbb{R}^n \rightarrow \mathbb{R}^n$ which transforms the state x to z :

$$x = T(z)$$

in such a way that the system

$$\dot{x} = f(x)$$

$$y = h(x)$$

is transformed into observer canonical form

$$\dot{z} = Az + b(Cz)$$

$$y = Cz.$$

The main characteristics of the observer canonical form are that the measurements are linear in the state and that the (nonlinear) output injection term depends only on states that are measured. In this case, the partial derivative matrix, or Jacobian, of the transformation can be expressed in terms of a single vector which is obtained directly from the observability matrix (see Appendix B). This result is due to Bestle and Zeitz [2]. Integrating the Jacobian matrix yields, in principle, the desired transformation T . The existence of solutions has been studied by Krener and Isidori [17], Krener and Respondek [19], and Hunt, et al. [11]. It appears that

the family of nonlinear systems which can be brought to observer canonical form through use of a nonlinear transformation with output injection is not large.

To enlarge the family of nonlinear systems to which this geometric method might be applied when a transformation as described above does not exist, two other canonical forms have been introduced: the modified observer canonical and the approximate observer canonical forms. Both canonical forms are given by

$$\dot{z} = Az + b(z) \quad (4.2)$$

$$y = Cz.$$

In this case the (nonlinear) output injection term $b(z)$ can be a function of states that cannot be measured. Since any nonlinear system of the form (4.1) can be transformed to the form (4.2), there is no advantage of the modified or approximate observer canonical form over the original nonlinear form unless $b(z)$ has certain properties. In the modified observer canonical form (Krener [16] and Frezza, et al. [7]) the output injection term is a function of states that are not measured but can be estimated quickly and accurately. For example, if the measured states are position and the output injection term contains states which are the time-derivative of the position (i.e. the velocity), then the transformation is useful. This was demonstrated in the one-dimensional tracking problem as reported in Bishop and Antoulas [3] and Frezza, et al. [7]. In the one-dimensional tracking problem, the states are position,

velocity and ballistic coefficient. The output injection term is a function of velocity which is the time-derivative of the position measurement. If the output injection term was a function of the ballistic coefficient (which is not a time-derivative of the measured position), then the tracking results would not be good, hence the transformation is not useful. In the approximate observer canonical form (Krener, et al. [18]), the output injection term contains states that deviate only slightly from nominal values. This form is useful when considering the problem of high-order approximations of nonlinear systems.

The aircraft maneuver model, presented in Chapter 2, cannot be transformed to observer canonical form. However, it can be transformed to approximate observer canonical form in which $b(z)$ is approximately zero for small turn rates.

The nonlinear transformations to modified and approximate observer canonical form are usually not unique. Recall that when a transformation to observer canonical form exists, it can be obtained, in principle, by integrating a Jacobian matrix which is itself a function of one vector obtained from the observability matrix. This is a straight forward calculation of the transformation. However, when a transformation to observer canonical form does not exist, the transformation to modified or approximate canonical form must be obtained by other methods. These methods depend on the given problem and no general theory is available. Krener et al. [18] have

reported results, applicable to the problem of high order approximations of nonlinear systems, which lead to a straight forward calculation of the transformation to approximate canonical form for certain nonlinear systems. Regardless of how the transformation is obtained, for the estimation problem the ultimate test of the chosen transformation is the tracking performance and stability characteristics.

As previously mentioned, the maneuvering aircraft model cannot be brought to observer canonical form. This follows directly from the fact the nonlinear system does not satisfy the necessary conditions for transformation of observer canonical form as stated in Theorem 4 (page 203) of Krener and Respondek [19]. More specifically, the mixed partial conditions of Remark 4.2 (page 204) are not satisfied. Therefore, the GNF design presented in this thesis will rely on a transformation to approximate observer canonical form. The particular transformation, T , used in the sequel is presented in the next section.

4.2 Transformation

For the aircraft maneuver model (2,28a), the transformation to approximate observer canonical form is not unique. The transformation, T , proposed here is based on the fact that the maneuver model describes planar trajectories. The nonlinear output injection term, $b(z)$, (described in detail later in this section) which results from the application of T is a function of the angle θ . Recall that θ is the angle in the maneuver

plane of the aircraft velocity vector and the maneuver plane reference frame (see Figure 2.1, Chapter 2). One important characteristic of $b(z)$ is that when $\theta=0$, $b(z)=0$ and (4.2) is exactly linear and in observer canonical form. For small turn rates, $\theta \approx 0$, it follows that $b(z) \approx 0$ and (4.2) is *approximately* in observer canonical form, hence the label *approximate observer canonical form*.

The nonlinear transformation which transforms the aircraft maneuver model to approximate observer canonical form is

$$x = T(z) \quad (4.3)$$

where

$$x_{4i-3} = n_{i1}z_1 + (n_{i2}\cos\phi + n_{i3}\sin\phi)z_5 + (-n_{i2}\sin\phi + n_{i3}\cos\phi)z_9$$

$$x_{4i-2} = n_{i1}z_2 + (n_{i2}\cos\phi + n_{i3}\sin\phi)z_6 + (-n_{i2}\sin\phi + n_{i3}\cos\phi)z_{10}$$

$$x_{4i-1} = \left(\frac{n_{i1}z_2 + n_{i3}(z_{10}\cos\phi + z_6\sin\phi)}{\sqrt{z_2^2 + (z_{10}\cos\phi + z_6\sin\phi)^2}} \right) (z_3 - g_1) + \\ \left(\frac{n_{i3}\sin\phi z_2 - n_{i1}\sin\phi(z_{10}\cos\phi + z_6\sin\phi)}{\sqrt{z_2^2 + (z_{10}\cos\phi + z_6\sin\phi)^2}} + n_{i2}\cos\phi \right) (z_7 - g_2) - \\ \left(\frac{n_{i3}\cos\phi z_2 - n_{i1}\cos\phi(z_{10}\cos\phi + z_6\sin\phi)}{\sqrt{z_2^2 + (z_{10}\cos\phi + z_6\sin\phi)^2}} + n_{i2}\sin\phi \right) (z_{11} - g_3)$$

$$x_{4i} = z_{4i}$$

where $i=1,2,3$ and ϕ is the aircraft roll angle (assumed constant in the maneuver model) and the constant terms n_{ij} 's are the (i,j) th elements of L_{EM} .

Remarks 1) The transformation (4.3) is a diffeomorphism.

- 2) The requirement that the aircraft velocity be non-zero implies that $\sqrt{z_2^2 + (z_{10}\cos\phi + z_6\sin\phi)^2}$ is non-zero.
- 3) $|x| = |z|$.

The transformation (4.3) takes the aircraft maneuver model to approximate observer canonical form

$$\begin{aligned}\dot{z} &= Az + b(z) \\ y &= Cz\end{aligned}\tag{4.4}$$

where A and C are block diagonal matrices $A = \text{diag}(A_{11}, A_{22}, A_{33})$ and $C = \text{diag}(C_{11}, C_{22}, C_{33})$ with

$$A_{ii} = \begin{bmatrix} 0 & 1 & 0 & 0 \\ 0 & 0 & 1 & 0 \\ 0 & 0 & 0 & 1 \\ 0 & 0 & 0 & -\alpha_i \end{bmatrix} \text{ and } C_{ii} = [1 \ 0 \ 0 \ 0] \text{ for } i = 1, 2, 3.$$

The non-zero elements of the output injection term are

$$\begin{aligned}b_2(z) &= (z_3 - g_1)(\cos\theta - 1) - ((z_7 - g_2)\sin\phi + (z_{11} - g_3)\cos\phi)\sin\theta, \\ b_6(z) &= (z_3 - g_1)\sin\phi\sin\theta + ((z_7 - g_2)\sin\phi + (z_{11} - g_3)\cos\phi)\sin\phi(\cos\theta - 1), \\ b_{10}(z) &= (z_3 - g_1)\cos\phi\sin\theta + ((z_7 - g_2)\sin\phi + (z_{11} - g_3)\cos\phi)\cos\phi(\cos\theta - 1),\end{aligned}$$

where

$$\cos\theta = \frac{z_2}{\sqrt{z_2^2 + (z_{10}\cos\phi + z_6\sin\phi)^2}}, \quad \sin\theta = \frac{-(z_{10}\cos\phi + z_6\sin\phi)}{\sqrt{z_2^2 + (z_{10}\cos\phi + z_6\sin\phi)^2}},$$

and

$$g_1 = n_{31}g, \quad g_2 = (n_{32}\cos\phi + n_{33}\sin\phi)g, \text{ and } g_3 = (n_{33}\cos\phi - n_{32}\sin\phi)g.$$

It is easy to see from $b(z)$ that when $\theta = 0$, $b(z) = 0$.

An important characteristic of the transformation (4.3) is with regard to the state uncertainties described in Section 2.5. As discussed in Section 4.2, state transformations transform the state noise and output transformations transform the measurement noise. The effect of the transformation (4.3) on the uncertainties is now considered.

Consider the measurement uncertainty first. The state variables (z_1, z_4, z_7) and (x_1, x_4, x_7) are related through the constant, orthogonal matrix

$$L = \begin{bmatrix} n_{11} & n_{21} & n_{31} \\ n_{12}\cos\phi + n_{13}\sin\phi & n_{22}\cos\phi + n_{23}\sin\phi & n_{32}\cos\phi + n_{33}\sin\phi \\ n_{13}\cos\phi - n_{12}\sin\phi & n_{23}\cos\phi - n_{22}\sin\phi & n_{33}\cos\phi - n_{32}\sin\phi \end{bmatrix}.$$

The covariance of the measurement noise u_m (as defined in Section 4.2) is

$$E(u_m(t)u_m^T(\tau))\delta(t-\tau) = \sigma_m^2 I\delta(t-\tau).$$

After applying the transformation, the covariance of the measurement noise is

$$E[(Lu_m(t))(Lu_m(\tau))^T] = E[Lu_m(t)u_m^T(\tau)L^T].$$

Since the matrix L is constant and non-random, it follows that

$$E[Lu_m(t)u_m^T(\tau)L^T] = L[\sigma_m I]L^T\delta(t-\tau) = \sigma_m I\delta(t-\tau). \quad (4.5)$$

Remarks 1) In general, even though orthogonal matrix L is constant, if it depends on stochastic variables then (4.5) is an approximation. It is however an approximation commonly used in tracking problems (in practice).

- 2) The GNF filter presented in the sequel does not require any explicit transformation of the measurements to the maneuver plane, as the state estimation is carried out in the original inertial reference frame. This is just a step implicit in the design of the gain K .

This demonstrates the fact that in the special case of a diagonal noise covariance matrix with equal values on the diagonal, transforming the output using a constant, orthogonal matrix does not affect the covariance matrix. Thus, the output transformation proposed here transforms the white, gaussian stochastic process to a white, gaussian stochastic process with equal covariance matrices.

The transformation (4.3) also transforms the state noise u_x in a desirable fashion. The transformed state noise is given by

$$u_z = \left[\frac{\partial T}{\partial z} \right]^{-1} u_x.$$

Using (2.28) and (4.3), it follows that

$$u_z = u_x.$$

Therefore, in approximate observer canonical form, the aircraft maneuver model is

$$\dot{z} = Az + b(z) + u_z \tag{4.6}$$

$$y = Cz + u_m$$

where A , $b(z)$, and C are defined in (4.4), and

$$E[\mathbf{u}_m(t)\mathbf{u}_m^T(\tau)] = \sigma_m^2 \mathbf{I} \delta(t - \tau), \text{ and}$$

$$E[\mathbf{u}_z(t)\mathbf{u}_z^T(\tau)] = E[\mathbf{u}_g(t)\mathbf{u}_g^T(\tau)] = \Sigma \delta(t - \tau),$$

where Σ is defined in (2.28a).

Chapter 5

GNF Gain Calculation

5.1 Introduction

In this section, a method for arbitrarily placing the poles of $A^*(z)$ in (3.7) is presented. This is of interest because in the deterministic case (i.e. $u_m(t) = u_z(t) = 0$) and when the higher-order terms in the Taylor series expansion of the estimation error equation are neglected (i.e. $\bar{b}(z, z) = 0$), the error equation (3.7) reduces to

$$\dot{e}_z = A^*(z)e_z. \quad (5.1)$$

In practice, the system disturbances and the higher-order terms cannot be neglected. However, the gain matrix derived by first considering (5.1) serves as the starting point. The effect of non-zero system disturbances and the higher-order terms in the Taylor series expansion on stability can then be investigated. This is the subject of the next chapter.

In this chapter, it will be shown that if a full rank condition of a certain observability like matrix is satisfied, the gain $K(z)$ can be computed so that

$$A^*(z) = A - K(z)C + B(z) = Q^{-1}(z)(A - K_1C)Q(z).$$

Therefore, the eigenvalues of $A^*(z)$ are equal to the eigenvalues of $A - K_1C$. The matrix K_1 is specified *a priori* so that $A - K_1C$ is stable, implying that $A^*(z)$ is stable. Since $A^*(z)$ is a

time-varying matrix, stability is not insured by the fact that all the eigenvalues of $A^*(\hat{z})$ have negative real parts. To insure asymptotic stability, an additional condition for the time-varying system (5.1) is that

$$\sup_{t \geq t_0} \left\| \frac{dA^*(\hat{z})}{dt} \right\|_i = \sup_{t \geq t_0} \left\| \frac{d}{dt} (Q^{-1}(\hat{z})(A - K_1 C)Q(\hat{z})) \right\|_i = \epsilon$$

is sufficiently small (see Vidyasagar [33]). Thus (5.1) must be a *slowly varying* system. Clearly, this puts conditions on $|Q(\hat{z})|$. If the time variation of $Q(\hat{z})$ corresponding to the given nonlinear transformation is not sufficiently small, then asymptotic stability cannot be guaranteed, hence the transformation will not be useful. The definition of "sufficiently small" is given in the next chapter where the impact of this characteristic of time-varying systems on the stability of the estimation error is analyzed.

A diagram of the proposed GNF gain calculation is shown in Figure 5.1. The input is the pre-computed nominal gain K_1 and the state estimate \hat{z} . The output is K^* . Figure 5.1 illustrates the fact that the computation of K^* depends on the state-dependent matrices $\bar{\Theta}(\hat{z})$, $Q_s(\hat{z})$, $B_1(\hat{z})$, $R(\hat{z})$, $J(\hat{z})$ and L . The matrices $J(\hat{z})$ and L were defined in the previous chapter. Recall that once $J(\hat{z})$ is computed, L follows directly without further computations. The remaining matrices will be defined subsequently. Figure 5.1 also illustrates the fact that the

computation of $\bar{\Theta}(\hat{z})$, $Q_a(\hat{z})$, $R(\hat{z})$, $B_1(\hat{z})$, and $J(\hat{z})$ is independent of each other and can be calculated simultaneously. Also, the computation of $\bar{\Theta}^{-1}(\hat{z})Q_a^{-1}(\hat{z})$ and $R(\hat{z})+K_1$ can be accomplished simultaneously. Thus, if parallel computational facilities are available, the calculation of $K(\hat{z})$ can be performed more efficiently.

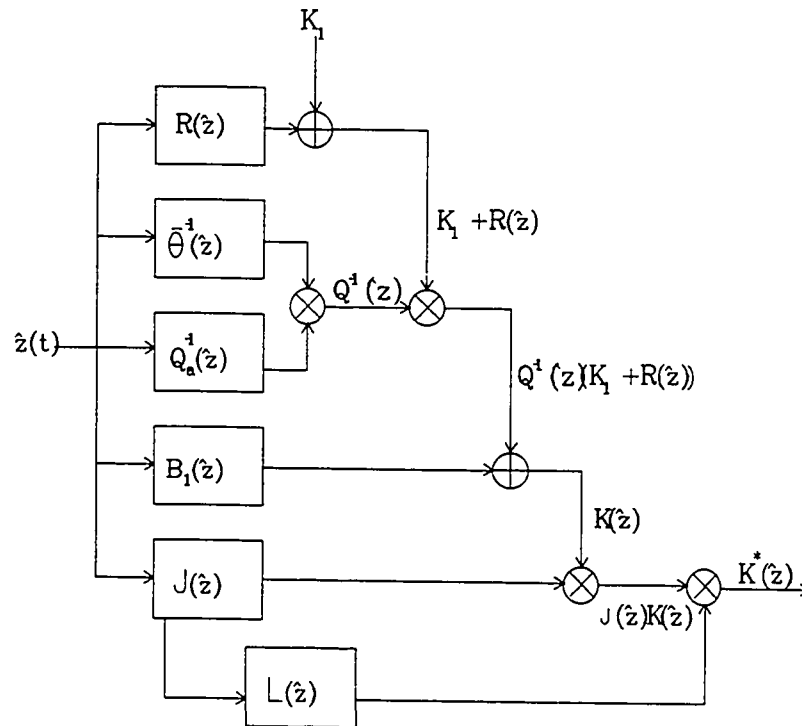


Figure 5.1. GNFS Gain Calculation

Notice that the on-line gains $K(\hat{z})$ vary as a function of the estimated state \hat{z} so that the eigenvalues of $A'(\hat{z})$ remain stable, and in fact, the eigenvalues can be made constant if K_1 is constant. The key to this approach is that while the GNFS gains are adaptive (i.e. they are a function of the estimated

state) like the EKF gains, they are computed without requiring the on-line integration of a matrix Riccati equation. The result is a substantial savings in computational (CPU) time for the GNF over the EKF. It will be shown in subsequent chapters that in addition to being faster computationally, the tracking performance and stability characteristics of the GNF are superior to the EKF.

5.2 Designing the Gain in the Scalar Output Case

The scalar output case is presented first for simplicity. The extension to the multi-output case is straight-forward. The multi-output version of all the formulas presented in this section are presented in Section 5.4 for the case where the number of states is twelve, the number of outputs is three, and the observability indices are $l_1 = l_2 = l_3 = 4$. This particular multi-output case is important in the maneuvering aircraft tracking problem.

As previously remarked, the construction of the stabilizing gain $K(\hat{z})$ depends on the matrices $\bar{\Theta}(\hat{z})$, $Q_s(\hat{z})$, $R(\hat{z})$, $B_1(\hat{z})$, $J(\hat{z})$ and L . Before stating the main theorem of this chapter, these matrices will be defined ($J(\hat{z})$ and L were defined in the previous chapter). The matrix $B_1(\hat{z})$ is defined as

$$B_1(\hat{z}) := B(\hat{z})C^T.$$

Then, associated with $B_1(\hat{z})$

is

$$B^*(\hat{z}) := B(\hat{z}) - B_1(\hat{z})C = B(\hat{z})(I - C^T C).$$

Utilizing the above definition of $B^*(z)$, the matrix $\bar{\Theta}(z)$ is defined as

$$\bar{\Theta}(z) := \begin{bmatrix} C \\ C(A+B^*(z)) \\ \vdots \\ C(A+B^*(z))^{n-1} \end{bmatrix} \quad (5.2a).$$

The main assumption used in the sequel is

$$\text{rank } \bar{\Theta}(z) = n, \quad \forall t \geq t_0. \quad (5.2b)$$

Since, by assumption, $\text{rank } \bar{\Theta}(z) = n, \forall t \geq t_0$, there exist real-valued functions $a_i(z)$ such that

$$\begin{aligned} C(A+B^*(z))^n &= a_0(z)C + a_1(z)[C(A+B^*(z))] + \cdots \\ &+ a_{n-1}(z)[C(A+B^*(z))^{n-1}]. \end{aligned} \quad (5.3)$$

Note that since $B^*(z(t))$ has zeroes in the first column it follows that $a_0(z(t)) = 0$. The matrices $Q_a(z)$ and $R(z)$, which are a function of the functions $a_i(z)$, are defined as

$$Q_a(z) := \begin{bmatrix} 1 & 0 & 0 & 0 & \cdots & 0 \\ -a_{n-1}(z) & 1 & 0 & 0 & \cdots & 0 \\ -a_{n-2}(z) & -a_{n-1}(z) & 1 & 0 & \cdots & 0 \\ \vdots & -a_{n-2}(z) & -a_{n-1}(z) & \vdots & \ddots & \vdots \\ \vdots & \vdots & \vdots & \vdots & 1 & 0 \\ -a_1(z) & -a_2(z) & -a_3(z) & \cdots & -a_{n-1}(z) & 1 \end{bmatrix}, \quad (5.4)$$

and

$$R(z) := \begin{pmatrix} a_{n-1}(z) \\ \vdots \\ \vdots \\ a_1(z) \\ 0 \end{pmatrix}. \quad (5.5)$$

Using the above definitions, the main theorem is stated as

Theorem 5.1 (Scalar Output): Suppose that the desired characteristic polynomial of $A^*(z)$ is

$$\rho_{des} = \rho_n + \rho_{n-1}S + \dots + \rho_1 S^{n-1} + S^n.$$

Associated with the desired characteristic polynomial, define the vector

$$K_1 = \begin{pmatrix} \rho_1 \\ \rho_2 \\ \vdots \\ \rho_n \end{pmatrix}.$$

Define

$$K(z) := B_1(z) + Q^{-1}(z)[K_1 + R(z)]$$

where

$$Q(z) = Q_s(z)\bar{\Theta}(z),$$

then it follows that

$$A^*(z) = A - K(z)C + B(z) = Q^{-1}(z)(A - K_1 C)Q(z)$$

and its characteristic polynomial is ρ_{des} .

proof: See Appendix C.

Remark: The existence of $Q^{-1}(z)$ is guaranteed by the assumption

$$\text{rank } \bar{\Theta}(z) = n, \forall t \geq t_0.$$

The following example, taken from Bishop and Antoulas [3], illustrates the above result.

Example This example is a simplified version of the one-dimensional tracking problem (see Figure 5.2) presented in Gelb [8]. The nonlinear system model is

$$\dot{x}_1 = x_2$$

$$\dot{x}_2 = -x_2 x_3^2$$

$$\dot{x}_3 = 0$$

$$y = x_1$$

where x_1, x_2 are the position and velocity, respectively, of the falling body and x_3 is the inverse of the ballistic coefficient scaled by the average atmospheric density. Utilizing the transformation

$$z_1 = x_1$$

$$z_2 = -\frac{x_2^2(0)}{x_2}$$

$$z_3 = -x_2^2(0)x_3$$

the nonlinear system model is transformed to the modified observer canonical form

$$\dot{z} = Az + b(z)$$

$$y = Cz$$

where the non-zero element of $b(z)$ is

$$b_1(z) = -(z_2 + z_2^2(0)/z_2),$$

and

$$A = \begin{bmatrix} 0 & 1 & 0 \\ 0 & 0 & 1 \\ 0 & 0 & 0 \end{bmatrix}, \quad C = (1 \ 0 \ 0), \quad \text{and} \quad B(z) = \begin{bmatrix} 0 & -1 + \frac{z_2^2(0)}{z_2^2} & 0 \\ 0 & 0 & 0 \\ 0 & 0 & 0 \end{bmatrix}.$$

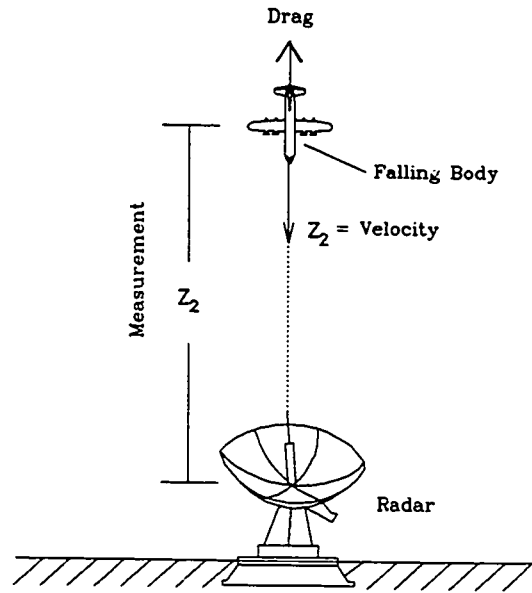


Figure 5.2. The One-Dimensional Tracking Problem

The matrix $B_1(z)$ is zero and the matrix $\bar{\Theta}(z)$ is

$$\bar{\Theta}(z) = \begin{bmatrix} 1 & 0 & 0 \\ 0 & \frac{z_2^2(0)}{z_2^2} & 0 \\ 0 & 0 & \frac{z_2^2(0)}{z_2^2} \end{bmatrix}.$$

To insure that the rank $\bar{\Theta}(z) = n$, it is required that $z_2 \neq 0, \forall t \geq t_0$.

Now,

$$C(A + B^*(z))^3 = 0.$$

This implies that $a_1(z) = a_2(z) = 0$. Thus,

$$Q(z) = \bar{\Theta}(z), \text{ and}$$

$$R(z) = 0.$$

Suppose that the desired characteristic polynomial is

$$\rho_{des} = \rho_3 + \rho_2 s + \rho_1 s^2 + s^3.$$

With

$$K_1 = \begin{pmatrix} \rho_1 \\ \rho_2 \\ \rho_3 \end{pmatrix},$$

it follows that the gain matrix is

$$K(\hat{z}) = Q^{-1}(\hat{z}) K_1 = \begin{pmatrix} \rho_1 \\ \frac{z_2^2}{z_2^2(0)} \rho_2 \\ \frac{z_2^2}{z_2^2(0)} \rho_3 \end{pmatrix}.$$

It can be checked that

$$\det(sI - A + K(\hat{z})C - B(\hat{z})) = \det \begin{pmatrix} s + \rho_1 & -\frac{z_2^2(0)}{z_2^2} & 0 \\ \frac{z_2^2}{z_2^2(0)} \rho_2 & s & -1 \\ \frac{z_2^2}{z_2^2(0)} \rho_3 & 0 & s \end{pmatrix} = \rho_{des},$$

as desired. ■

5.3 Special Cases of Theorem 5.1

In the previous section, the output injection term is, in general, a function of all the states. For the case when the output injection term is a function (linear or nonlinear) of only the measurement, the calculation of $K(\hat{z})$ reduces to a simple formula. The linear case is presented first since it is probably familiar to most readers. The nonlinear case follows. This case is a subset of the general case presented

in the previous section. It is also the case that is most often considered in the literature (see Bestle and Zeitz [2], for example).

Linear Case : Suppose that the output injection term is a linear function of the measurement (but not of any other states). Then

$$B(\hat{z}) = \left. \frac{\partial \mathbf{b}z}{\partial z} \right|_{z=\hat{z}} = \begin{pmatrix} b_1 \\ \vdots \\ b_n \end{pmatrix} C$$

where the b_i 's are constants and

$$C = (1 \ 0 \ \dots \ 0).$$

Clearly, $B(\hat{z})$ is a constant matrix. Thus,

$$\dot{\hat{e}}_z = (\tilde{A} - KC)e_z$$

where

$$\tilde{A} = \begin{bmatrix} b_1 & 1 & 0 & 0 & 0 & \dots & 0 \\ b_2 & 0 & 1 & 0 & 0 & \dots & 0 \\ \vdots & \vdots & \vdots & \vdots & \vdots & \vdots & \vdots \\ b_{n-1} & 0 & 0 & \dots & 0 & \cdot & 1 \\ b_n & 0 & 0 & 0 & \dots & 0 & 0 \end{bmatrix}.$$

Since (\tilde{A}, C) is observable, it follows that the eigenvalues of $\tilde{A} - KC$ can be arbitrarily placed, as desired. In this case, K is a constant matrix.

Nonlinear Case : Suppose that the output injection term is a nonlinear function of the measurement (but not of any other states). Then

$$B(\hat{z}) = \left. \frac{\partial \mathbf{b}(z)}{\partial z} \right|_{z=\hat{z}} = \begin{pmatrix} B_{11}(\hat{z}_1) \\ \vdots \\ B_{n1}(\hat{z}_1) \end{pmatrix} \mathbf{C}$$

where

$$\mathbf{C} = (1 \ 0 \ \dots \ 0).$$

Thus,

$$\dot{\mathbf{e}}_z = (\tilde{\mathbf{A}}(\hat{z}) - \mathbf{K}(\hat{z})\mathbf{C})\mathbf{e}_z$$

where

$$\tilde{\mathbf{A}} = \begin{bmatrix} B_{11}(\hat{z}_1) & 1 & 0 & 0 & 0 & \dots & 0 \\ B_{21}(\hat{z}_1) & 0 & 1 & 0 & 0 & \dots & 0 \\ \vdots & \vdots & \vdots & \vdots & \vdots & \vdots & \vdots \\ B_{n-11}(\hat{z}_1) & 0 & 0 & \dots & 0 & \cdot & 1 \\ B_{n1}(\hat{z}_1) & 0 & 0 & 0 & \dots & 0 & 0 \end{bmatrix}.$$

Define

$$\mathbf{K}(\hat{z}) = \begin{pmatrix} \rho_1 + B_1(\hat{z}_1) \\ \rho_2 + B_2(\hat{z}_1) \\ \vdots \\ \rho_n + B_n(\hat{z}_1) \end{pmatrix}, \quad (5.5)$$

where ρ_i are the coefficients of the desired characteristic polynomial defined in Theorem 5.1. Then the characteristic polynomial of $\tilde{\mathbf{A}} - \mathbf{K}(\hat{z})\mathbf{C}$ is ρ_{des} . Thus, the eigenvalues can be arbitrarily placed.

This has been proposed in the literature as a good filter design technique (see Bestle and Zeitz [2], for example). Of course, this special case relies on the fact that the output

injection term is a function of the measured state only, state and measurement noise are not considered, and the higher-order terms of the Taylor series expansion of the estimation error equation are neglected. This technique has been generalized in this thesis to include the case when the output injection term contains states that are not measured. Also, the effects of non-zero system disturbances and the higher-order terms on the estimation error are considered.

5.4 Designing the Gain in the Multi-Output Case

In this section, the specific multi-output situation that is considered has twelve states, three outputs, and the observability indices are $l_1 = l_2 = l_3 = 4$. This case is of importance to the maneuvering aircraft tracking problem and will illustrate the extension of Theorem 5.1 (single output) to the multi-output case. The extension to other multi-output situations follows the same patterns established in this section.

In the multi-output case the matrices A and C are in block Brunovsky form, which means $A = \text{diag} (A_{11}, A_{22}, A_{33})$ and $C = \text{diag} (C_{11}, C_{22}, C_{33})$ are block diagonal matrices where

$$A_{ii} = \begin{bmatrix} 0 & 1 & 0 & 0 \\ 0 & 0 & 1 & 0 \\ 0 & 0 & 0 & 1 \\ 0 & 0 & 0 & 0 \end{bmatrix}, \quad C_{ii} = [1 \quad 0 \quad 0 \quad 0].$$

The only two matrices out of the group $\bar{\Theta}(2)$, $Q_s(2)$, $R(\dot{z})$, $B_1(2)$, and $J(\dot{z})$ that must be changed for the multi-output case are $Q_s(2)$ and $R(\dot{z})$. These changes are a direct result of the fact that the multi-output version of (5.3) is

$$C(A+B^*(\hat{z}))^4 = [a_{1jk}(\hat{z})][C(A+B^*(\hat{z}))] + [a_{2jk}(\hat{z})][C(A+B^*(\hat{z}))^2] + [a_{3jk}(\hat{z})][C(A+B^*(\hat{z}))^3],$$

where $[a_{ijk}(\hat{z})]$ are 3×3 matrices, instead of scalars. Since, by assumption, the rank $\bar{\theta}(t) = n = 12, \forall t \geq t_0$, the matrices $[a_{ijk}(\hat{z})]$ exist. The multi-output version of $Q_s(\hat{z})$ is

$$Q_s(\hat{z}) := \begin{bmatrix} Q_{s11}(\hat{z}) & Q_{s12}(\hat{z}) & Q_{s13}(\hat{z}) \\ Q_{s21}(\hat{z}) & Q_{s22}(\hat{z}) & Q_{s23}(\hat{z}) \\ Q_{s31}(\hat{z}) & Q_{s32}(\hat{z}) & Q_{s33}(\hat{z}) \end{bmatrix},$$

where

$$Q_{sii}(\hat{z}) = \begin{bmatrix} 1 & 0 & 0 & 0 \\ -a_{ii3} & 1 & 0 & 0 \\ -a_{ii2} & -a_{ii3} & 1 & 0 \\ -a_{ii1} & -a_{ii2} & -a_{ii3} & 1 \end{bmatrix},$$

and

$$Q_{sij}(\hat{z}) = \begin{bmatrix} 0 & 0 & 0 & 0 \\ -a_{ji3} & 0 & 0 & 0 \\ -a_{ji2} & -a_{ji3} & 0 & 0 \\ -a_{ji1} & -a_{ji2} & -a_{ji3} & 0 \end{bmatrix} \quad \text{for } i \neq j.$$

The multi-output version of $R(\hat{z})$ is

$$R(\hat{z}) := \begin{bmatrix} R_{11}(\hat{z}) \\ R_{21}(\hat{z}) \\ R_{31}(\hat{z}) \end{bmatrix},$$

where

$$R_{i1}(\hat{z}) = \begin{bmatrix} -a_{1i3} & -a_{2i3} & -a_{3i3} \\ -a_{1i2} & -a_{2i2} & -a_{3i2} \\ -a_{1i1} & -a_{2i1} & -a_{3i1} \\ 0 & 0 & 0 \end{bmatrix}.$$

With the above definitions, the multi-output (3 outputs, 12 states, observability indices $l_1 = l_2 = l_3 = 4$) version of Theorem 5.1 is

Theorem 5.2 (Multi-Output): Suppose that the desired characteristic polynomial of $A^*(z)$ is

$$\rho_{des} = \prod (s^4 + \rho_{4i-3,i} s^3 + \rho_{4i-2,i} s^2 + \rho_{4i-1,i} s + \rho_{4i,i}) \quad \text{for } i=1,2,3.$$

Associated with the desired characteristic polynomial, define the block diagonal matrix $K_1 = \text{diag} (K_{11}, K_{22}, K_{33})$ with

$$K_{1ii} = \begin{pmatrix} \rho_{4i-3,i} \\ \rho_{4i-2,i} \\ \rho_{4i-1,i} \\ \rho_{4i,i} \end{pmatrix}.$$

If

$$K(z) = B_1(z) + Q^{-1}(z)[K_1 + R(z)]$$

where

$$Q(z) = Q_a(z)\bar{\Theta}(z),$$

then it follows that the characteristic polynomial of $A^*(z)$ is

ρ_{des} . Also,

$$A^*(z) = A - K(z)C + B(z) = Q^{-1}(z)(A - K_1 C)Q(z).$$

proof: Direct extension of the scalar case (See Appendix C).

5.5 The GNF Gain

The aircraft maneuver model in approximate observer canonical coordinates is given in (4.6). The matrices $A = \text{diag} (A_{11}, A_{22}, A_{33})$ and $C = \text{diag} (C_{11}, C_{22}, C_{33})$ are block diagonal matrices with

$$A_{ii} = \begin{bmatrix} 0 & 1 & 0 & 0 \\ 0 & 0 & 1 & 0 \\ 0 & 0 & 0 & 1 \\ 0 & 0 & 0 & -\alpha_i \end{bmatrix},$$

and

$$C_{ii} = [1 \ 0 \ 0 \ 0].$$

These are not quite in Brunovsky canonical form because of the presence of the α_i 's. This presents no difficulty as will be shown subsequently.

The nonlinear output injection term $b(z)$ is a function of the states $z_2, z_3, z_6, z_7, z_{10}$ and z_{11} . Hence $B(\hat{z})$ has the form

$$B(\hat{z}) = \begin{bmatrix} B_{11}(\hat{z}) & B_{12}(\hat{z}) & B_{13}(\hat{z}) \\ B_{21}(\hat{z}) & B_{22}(\hat{z}) & B_{23}(\hat{z}) \\ B_{31}(\hat{z}) & B_{32}(\hat{z}) & B_{33}(\hat{z}) \end{bmatrix},$$

where

$$B_{ij}(\hat{z}) = \begin{bmatrix} 0 & 0 & 0 & 0 \\ 0 & B_{4i-2,4j-2} & B_{4i-2,4j-1} & 0 \\ 0 & 0 & 0 & 0 \\ 0 & 0 & 0 & 0 \end{bmatrix}.$$

Note that since $B(\hat{z})$ has zeroes in the first, fifth and ninth columns, it follows that $B'(\hat{z}) = B(\hat{z})$, hence $B_1(\hat{z}) = 0$. The non-zero elements of $B(\hat{z})$ can be explicitly computed and are given in Appendix D.

The matrix $\bar{\Theta}(\hat{z})$ has the form

$$\bar{\Theta}(\hat{z}) = \begin{bmatrix} \bar{\Theta}_{11}(\hat{z}) & \bar{\Theta}_{12}(\hat{z}) & \bar{\Theta}_{13}(\hat{z}) \\ \bar{\Theta}_{21}(\hat{z}) & \bar{\Theta}_{22}(\hat{z}) & \bar{\Theta}_{23}(\hat{z}) \\ \bar{\Theta}_{31}(\hat{z}) & \bar{\Theta}_{32}(\hat{z}) & \bar{\Theta}_{33}(\hat{z}) \end{bmatrix},$$

where

$$\bar{\Theta}_{ii}(\hat{z}) = \begin{bmatrix} 1 & 0 & 0 & 0 \\ 0 & 1 & 0 & 0 \\ 0 & \bar{\Theta}_{4i-1,4i-2} & \bar{\Theta}_{4i-1,4i-1} & 0 \\ 0 & \bar{\Theta}_{4i,4i-2} & \bar{\Theta}_{4i,4i-1} & \bar{\Theta}_{4i,4i} \end{bmatrix},$$

and

$$\bar{\Theta}_{ij}(\hat{z}) = \begin{bmatrix} 0 & 0 & 0 & 0 \\ 0 & 0 & 0 & 0 \\ 0 & \bar{\Theta}_{4i-1,4j-2} & \bar{\Theta}_{4i-1,4j-1} & 0 \\ 0 & \bar{\Theta}_{4i,4j-2} & \bar{\Theta}_{4i,4j-1} & \bar{\Theta}_{4i,4j} \end{bmatrix} \text{ for } i \neq j.$$

The non-zero elements of $\bar{\Theta}(\hat{z})$ are given in Appendix D. It follows that

$$\det \bar{\Theta}(\hat{z}) = 1$$

i.e.

$$\text{rank } \bar{\Theta}(\hat{z}) = 12, \forall t \geq t_0.$$

Since the rank condition is satisfied, there exists matrices $[a_{ijk}(\hat{z})]$ such that

$$\begin{aligned} C(A+B^*(\hat{z}))^4 &= [a_{1jk}(\hat{z})][C(A+B^*(\hat{z}))] + [a_{2jk}(\hat{z})][C(A+B^*(\hat{z}))^2] + \\ &\quad [a_{3jk}(\hat{z})][C(A+B^*(\hat{z}))^3]. \end{aligned}$$

The non-zero elements of the matrices $[a_{ijk}(\hat{z})]$ can be computed explicitly and are given in Appendix D.

For the aircraft tracking problem, the A matrix is not in Brunovsky canonical form because of the presence of the non-zero α_i 's. Theorem 5.1 utilized the special Brunovsky canonical form in the proof. However, the theorem is valid for any A as long as the rank condition

$$\text{rank } \bar{\Theta}(z) = \text{rank} \begin{bmatrix} C \\ C(A+B^*(z)) \\ \vdots \\ C(A+B^*(z))^{n-1} \end{bmatrix} = n$$

is satisfied when A contains non-zero α_i 's. The non-zero α_i are accounted for in

Proposition 5.1: Assume that the rank condition

$$\text{rank } \bar{\Theta}(z) = n$$

is satisfied. Define

$$[\bar{a}_{ijk}(z)] = [a_{ijk}(z)] \begin{bmatrix} 1 & 0 & 0 \\ -\alpha_i & 1 & 0 \\ 0 & \alpha_i^2 & 1 \end{bmatrix} + \begin{bmatrix} 0 & \alpha_i^3 & 0 \\ 0 & 0 & 0 \\ 0 & 0 & 0 \end{bmatrix},$$

and define the elements of the block matrix $Q_a(z)$ as

$$Q_{a,ii}(z) = \begin{bmatrix} 1 & 0 & 0 & 0 \\ -\bar{a}_{ii3} & 1 & 0 & 0 \\ -\bar{a}_{ii2} & -\bar{a}_{ii3} & 1 & 0 \\ -\bar{a}_{ii1} & -\bar{a}_{ii2} & -\bar{a}_{ii3} & 1 \end{bmatrix},$$

and

$$Q_{a,ij}(z) = \begin{bmatrix} 0 & 0 & 0 & 0 \\ -\bar{a}_{ji3} & 0 & 0 & 0 \\ -\bar{a}_{ji2} & -\bar{a}_{ji3} & 0 & 0 \\ -\bar{a}_{ji1} & -\bar{a}_{ji2} & -\bar{a}_{ji3} & 0 \end{bmatrix} \quad \text{for } i \neq j,$$

and the elements of the block matrix $R(z)$ as

$$R_{ij}(z) = \begin{bmatrix} -\bar{a}_{1i3} & -\bar{a}_{2i3} & -\bar{a}_{3i3} \\ -\bar{a}_{1i2} & -\bar{a}_{2i2} & -\bar{a}_{3i2} \\ -\bar{a}_{1i1} & -\bar{a}_{2i1} & -\bar{a}_{3i1} \\ \alpha_i \bar{a}_{1i1} & \alpha_i \bar{a}_{2i1} & \alpha_i \bar{a}_{3i1} \end{bmatrix}.$$

Then, if

$$K(z) = B_1(z) + Q^{-1}(z)[K_1 + R(z)]$$

where

$$Q(z) = Q_1(z)\bar{\theta}(z),$$

then it follows that the characteristic polynomial of $A^*(z)$ is

ρ_{des} . Also,

$$A^*(z) = A - K(z)C + B(z) = Q^{-1}(z)(A - K_1C)Q(z).$$

proof: Direct extension of the scalar case (See Appendix D).

The implementation of the gain calculation in Proposition 5.1 in the actual filter computer program will not include any matrix inverses. These inverses can be computed symbolically (via a symbolic manipulation program such as Mathematica or Macsyma) beforehand.

Chapter 6

Sufficient Stability Conditions

6.1 Introduction

A procedure for computing the filter gains such that $A^*(z)$ is stable was presented in the previous chapter. In this chapter it will be shown that these stabilizing gains provide a basis for constructing a stable filter, i.e. the solution to the error equation

$$\dot{e}_z = A^*(\hat{z})e_z + \bar{b}(z, \hat{z}) + K(\hat{z})u_m - u_z, \quad (6.1)$$

is asymptotically stable in the deterministic case (i.e. $u_m = 0$ and $u_z = 0$) and the moments (i.e. $E[e_z^T e_z]$) are bounded in the stochastic case.

The stability analysis will include a definition of the domain of attraction for the aircraft tracking problem. If the initial estimation error is within this domain then (deterministic) stability of the estimation error is insured. Because of the stochastic nature of the problem it turns out that the estimation error will not go to zero but will instead oscillate in a random manner about zero. It will, however, oscillate in a bounded region which will be defined.

In the sequel, the norm of the vector $v \in R^n$ is defined to be

$$|v| = \sqrt{v^T v}$$

and the norm of the matrix $M \in \mathbb{R}^{n \times n}$ is defined to be

$$|M| = \sqrt{\sigma_{\max}},$$

where σ_{\max} is the largest eigenvalue value of $M^T M$ and the largest singular value of M . σ_{\min} denotes the minimum eigenvalue value of $M^T M$.

The deterministic stability analysis is presented first, followed by the stochastic stability analysis.

6.2 Deterministic Stability

In the deterministic case (i.e. $u_m = 0$ and $u_z = 0$) the estimation error is given by

$$\dot{e}_z = A^*(\hat{z})e_z + \bar{b}(z, \hat{z}), \quad (6.2)$$

where

$$A^*(\hat{z}) = A - K(\hat{z})C + B(\hat{z}) = Q^{-1}(\hat{z})(A - K_1)Q(\hat{z})$$

is a stable matrix. Conditions for stability of the estimation error (6.2) are given in

Theorem 6.1 (Deterministic Stability)

Suppose (6.2) is given. Assume that

$$|\bar{b}(\hat{z}, z)| \leq \beta(e_z)|e_z| \quad \forall t \geq t_0, \quad (6.3)$$

and define

$$(i) \quad \epsilon(\hat{z}) := |\dot{Q}(\hat{z})|$$

$$(ii) \quad q(\hat{z}) := |Q(\hat{z})|$$

$$(iii) \quad \lambda_Q(\hat{z}) := \sigma_{\min}(Q)$$

$$(iv) \quad Q^*(\hat{z}) := Q^T(\hat{z})Q(\hat{z}) - \dot{Q}^T(\hat{z})P_0Q(\hat{z}) - Q^T(\hat{z})P_0\dot{Q}(\hat{z})$$

(v) $\lambda_q(\hat{z}) := \text{minimum eigenvalue of } Q^*(\hat{z})$

where P_0 is the symmetric, positive definite solution to the matrix Lyapunov equation

$$(A - K_1 C)^T P_0 + P_0 (A - K_1 C) = -I.$$

Then the estimation error is asymptotically stable if

$$\lambda_q(\hat{z}) > 2q(\hat{z}) |P_0| [\epsilon(\hat{z}) + q(\hat{z}) \beta(e_z)] \quad , \text{ or} \quad (6.4a)$$

$$\lambda_q(\hat{z}) > 2\beta(e_z) |P_0| q^2(\hat{z}). \quad (6.4b)$$

Remarks (1) Since $Q(\hat{z})$ is nonsingular $\lambda_q(\hat{z}) > 0$. $\lambda_q(\hat{z})$ is the smallest singular value of $Q(\hat{z})$.

(2) Condition (6.4b) is a tighter bound than (6.4a).

In other words, (6.4b) implies (6.4a). ■

The proof of Theorem 6.1 is based on the Lyapunov stability theorem:

THEOREM 6.2 (Kalman and Bertram [13])

For an autonomous system, asymptotic stability is assured by the existence of a scalar function $V(e_z)$ with continuous first partial derivatives with respect to e_z , such that $V(0) = 0$ and

- (i) $V(e_z) > 0 \quad \forall e_z \neq 0$;
- (ii) $\dot{V}(e_z) < 0 \quad \forall e_z \neq 0$; and
- (iii) $V(e_z) \rightarrow \infty$ with $|e_z| \rightarrow \infty$.

proof: see Kalman and Bertram [13].

The Lyapunov approach consists primarily of defining a function which satisfies the conditions in Theorem 6.2. This function is called a Lyapunov function and its existence implies stability. There is no theory which provides a general method for computing a Lyapunov function for any given nonlinear system. Therefore, the procedure that is usually followed is to first obtain a *candidate* function $V(e_z)$ by whatever method best suits the given problem. It must then be verified that $V(e_z)$ satisfies the conditions stated in Theorem 6.2. If this is the case, then the candidate function is in fact a (deterministic) Lyapunov function and the estimation error is asymptotically stable. For the aircraft tracking problem, the Lyapunov function used in the proof of Theorem 6.1 is

$$V(e_z) = e_z^T P(\hat{z}) e_z, \quad (6.5)$$

where $P(\hat{z})$ (defined subsequently in Lemma 6.1) is a real, symmetric positive definite matrix.

One further result needed in the proof of Theorem 6.1 is
Lemma 6.1: There exists a pair $(P(\hat{z}), \tilde{Q}(\hat{z}))$ such that

$$A^{*T}(\hat{z})P(\hat{z}) + P(\hat{z})A^*(\hat{z}) = -\tilde{Q}(\hat{z}) \quad \forall t \geq t_0 \quad (6.6)$$

where $P(\hat{z})$ and $\tilde{Q}(\hat{z})$ are symmetric and positive definite.

proof: Recall that

$$A^*(\hat{z}) = A - K(\hat{z})C + B(\hat{z}) = Q^{-1}(\hat{z})(A - K_1 C)Q(\hat{z}) \quad (6.7)$$

where the eigenvalues of the matrix $A - K_1 C$ have all negative real parts. It is well known that the matrix Lyapunov equation

$$(A - K_1 C)^T P_0 + P_0 (A - K_1 C) = -I \quad (6.8)$$

has a unique symmetric and positive definite solution P_0 . Define

$$P(\hat{z}) := Q^T(\hat{z}) P_0 Q(\hat{z}) \text{ and } \tilde{Q}(\hat{z}) := Q^T(\hat{z}) \dot{Q}(\hat{z}).$$

Note that $\tilde{Q}(\hat{z})$ is symmetric and positive definite since $Q^{-1}(t)$ exists. Pre- and post- multiplying (6.8) by $Q^T(\hat{z})$ and $Q(\hat{z})$, respectively, using the above definitions of $P(\hat{z})$ and $\tilde{Q}(\hat{z})$ and (6.7), (6.6) follows. ■

proof of Theorem 6.1: Using the Lyapunov function in (6.5), it follows that $V(0) = 0$ and that $V(e_z)$ has continuous first partial derivatives with respect to e_z . Also, $V(e_z) > 0 \forall e_z \neq 0$ and $V(e_z) \rightarrow \infty$ with $|e_z| \rightarrow \infty$. Thus, conditions (i) and (iii) of Theorem 6.2 are satisfied.

To check condition (ii) of Theorem 6.2, first take the time-derivative of $V(e_z)$ yielding

$$\dot{V}(e_z) = e_z^T [A^{*T}(\hat{z}) P(\hat{z}) + P(\hat{z}) A^*(\hat{z})] e_z + e_z^T \dot{P}(\hat{z}) e_z + 2\tilde{b}^T(z, \hat{z}) P(\hat{z}) e_z.$$

Using (6.6) from Lemma 6.1, it follows that

$$\dot{V}(e_z) = -e_z^T \tilde{Q} \hat{z} e_z + e_z^T \dot{P}(\hat{z}) e_z + 2\tilde{b}^T(z, \hat{z}) P(\hat{z}) e_z. \quad (6.9)$$

Taking the time derivative of $P(\hat{z})$ (defined in Lemma 6.1) yields

$$\dot{P}(\hat{z}) = \dot{Q}^T(\hat{z}) P_0 Q(\hat{z}) + Q^T(\hat{z}) P_0 \dot{Q}(\hat{z}),$$

hence

$$|\dot{P}(\hat{z})| \leq 2\epsilon(\hat{z}) q(\hat{z}) |P_0|, \quad (6.10)$$

and

$$|P(\hat{z})| \leq q^2(\hat{z}) |P_0|. \quad (6.11)$$

Substituting (6.3), (6.10) and (6.11) into (6.9) yields

$$\dot{V}(e_z) \leq [-\lambda_Q(\hat{z}) + 2q(\hat{z})|P_0|(\epsilon(\hat{z}) + q(\hat{z})\beta(e_z))] |e_z|^2.$$

Therefore,

$$\lambda_Q(\hat{z}) > 2q(\hat{z})|P_0|[\epsilon(\hat{z}) + q(\hat{z})\beta(e_z)] \Rightarrow \dot{V}(e_z) < 0, e_z \neq 0, \forall t \geq t_0.$$

To prove (6.4b), rewrite (6.9) as

$$\dot{V}(e_z) = -e_z^T [Q^T(\hat{z})Q(\hat{z}) - \dot{Q}^T(\hat{z})P_0Q(\hat{z}) - Q^T(\hat{z})P_0\dot{Q}(\hat{z})]e_z + 2\bar{b}_0(z, \hat{z})P(\hat{z})e_z.$$

Using definitions (ii), (iv), (6.3) and (6.11), it follows that

$$\dot{V}(e_z) \leq [-\lambda_{Q^*}(\hat{z}) + 2\beta(e_z)|P_0|]q^2(\hat{z})|e|^2.$$

Therefore,

$$\lambda_{Q^*}(\hat{z}) > 2\beta(e_z)q^2(\hat{z})|P_0| \Rightarrow \dot{V}(e_z) < 0, e_z \neq 0 \quad \forall t \geq t_0. \quad \blacksquare$$

Satisfying either stability condition above implies that condition (ii) of Theorem 6.2 is met, and consequently asymptotic stability is guaranteed.

Remarks (1) The effect of the time variation of $A^*(\hat{z})$ on the stability appears directly in the stability condition (6.4a) via $\epsilon(\hat{z})$. Recall that $\epsilon(\hat{z})$ measures the time rate of change of $Q(\hat{z})$. For the aircraft tracking problem, the effect of $\epsilon(\hat{z})$ on the stability is negligible (i.e. the planar maneuver coordinated turn model is slowly time varying). In the literature (see Vidyasagar [33], for example), the

time-varying effects do not explicitly appear in the stability conditions. The stability conditions generally take the form of (6.4b).

- (2) The effect of the term $\bar{b}(z, \hat{z})$ on the stability appears directly via $\beta(e_z)$.
- (3) If $\epsilon(\hat{z}) = 0$ and $\beta(e_z) = 0$, then the stability conditions reduce to $\lambda_{q^*}(\hat{z}) = \lambda_q(\hat{z}) > 0$ which is equivalent to requiring that $Q^{-1}(\hat{z})$ exist, which is always the case by design.
- (4) If, for some fixed $|P_0|$, condition (6.4) is satisfied for all e_z , then the estimation error is globally asymptotically stable. If condition (6.4) is satisfied for $|e_z| < \delta$, for some δ , then δ defines the *domain of attraction* within which stability is guaranteed. It is desirable, in addition to stability, to guarantee that

$$-\lambda_{q^*}(\hat{z}) + 2q^2(\hat{z})|P_0|\beta(e) < -\delta^* \quad .$$

Specifying non-zero δ^* affects the domain of attraction by reducing the size. In the stochastic stability analysis (section 6.4) a non-zero value of δ^* is assumed. The domain of attraction can be enlarged by decreasing $|P_0|$. This is accomplished by selecting K , properly (i.e. redefining the desired characteristic polynomial). Recall that

P_0 is related to K_1 through the matrix Lyapunov equation (6.8). Of course, in all cases $A - K_1 C$ must be stable. ■

6.3 Deterministic Stability Computations

It was assumed (in Theorem 6.1) that the bound on the nonlinear term $\bar{b}(z, \hat{z})$ has the form

$$|\bar{b}(z, \hat{z})| \leq \beta(e_z) |e_z|.$$

In fact, for the aircraft tracking problem, $\beta(e_z)$ can be bounded by

$$\beta(e_z) \leq c_0(\hat{z}) |\bar{e}_z|$$

where $c_0(\hat{z})$ is a bounded scalar and $|\bar{e}_z|$ is the magnitude of the velocity and acceleration estimation errors.

So, the bound on $\bar{b}(z, \hat{z})$ can also be written as

$$\lim_{|e_z| \rightarrow 0} \frac{|\bar{b}|}{|e_z|} \rightarrow 0.$$

This is the form of the bound on the nonlinear terms sometimes found in stability proofs (see Vidyasagar [33], page 188 for example).

The scalar $c_0(\hat{z})$ is calculated by taking successive higher-order partial derivatives of \bar{b} and computing the norm. For the particular $\bar{b}(z, \hat{z})$ in the aircraft tracking problem, the higher order derivatives are divided by successively higher powers of \hat{v} (i.e. $\hat{v}^2, \hat{v}^3, \dots$), where \hat{v} is the estimated magnitude of the aircraft velocity. For the velocities of interest the

series converges rapidly. When the ratio of the magnitude of the aerodynamic acceleration, \hat{a} , to the magnitude of the aircraft velocity, \hat{v} , is small then

$$\beta(e_z) \leq \frac{1}{\hat{v}} \left(1 + \frac{\hat{a}}{\hat{v}} \right) |\bar{e}_z|$$

where $|\bar{e}_z|$ is the magnitude of the velocity and acceleration estimation error. A reasonable upper bound on $\hat{a}/\hat{v} \leq 0.2$. These values will be used in Chapter 8 to compute an explicit formula for the domain of attraction (i.e. the stability region).

6.4 Stochastic Stability

In the stochastic case, the estimation error equation is

$$\dot{e}_z = A^*(\hat{z})e_z + \bar{b}(z, \hat{z}) + K(\hat{z})u_m - u_z.$$

This can be written in the form

$$\dot{e}_z = A^*(\hat{z})e_z + \bar{b}(z, \hat{z}) + G(\hat{z})u, \quad (6.12)$$

where

$$G(\hat{z}) := [K(\hat{z}) \quad -I]$$

and

$$u := \begin{pmatrix} u_m \\ u_z \end{pmatrix}$$

is a white gaussian noise process of zero mean and covariance

$$E(u(t)u^T(\tau)) = U\delta(t-\tau) = \begin{pmatrix} \sigma_m I & 0 \\ 0 & \Sigma \end{pmatrix} \delta(t-\tau).$$

Remark The sample paths of the stochastic process, e_z , may not be defined for all time. In other words, there is a nonzero probability that e_z may escape to infinity

at some finite time. An assumption, used in the sequel, is that e_z does not have a finite escape time (with probability one) to infinity. ■

Let $V(e_z)$ be a Lyapunov function. Then $V(e_z)$ satisfies the stochastic differential equation

$$\dot{V}(e_z) = \tilde{A}V(e_z) + \frac{\partial V(e_z)}{\partial e_z} C(z)u \quad (6.13)$$

where

$$\tilde{A}V(e_z) = \frac{\partial V(e_z)}{\partial t} + \left[\frac{\partial V(e_z)}{\partial e_z} \right]^T (A^*(z)e_z + \tilde{b}(z, z)) + \frac{1}{2} \text{tr} \left\{ G(z)UG^T(z) \frac{\partial^2 V(e_z)}{\partial e_z^2} \right\}$$

and tr designates trace. $\tilde{A}V(e_z)$ is known as the *differential generator* of the process and is interpreted as the *average time rate of change* of $V(e_z)$. $\tilde{A}V(e_z)$ is the stochastic analog of the deterministic derivative. Note that the *Itô differential rule* has been used in calculating (6.13). The stability results of Kushner [20], on which the stochastic stability results in this section are based, utilize the Itô calculus.

As in the deterministic case, the stochastic stability analysis is performed utilizing the Lyapunov function approach. In fact, the (deterministic) Lyapunov function (6.5) is used to compute stochastic stability. The stochastic stability theorem is

THEOREM 6.3 (Stochastic Stability)

Suppose (6.12) is given. Assume that the deterministic part of (6.12), namely

$$\dot{e}_z = A^*(\hat{z})e_z + \tilde{b}(z, \hat{z})$$

is asymptotically stable. In other words, the (deterministic) stability condition of Theorem 6.1

$$\lambda_q(\hat{z}) - 2q(\hat{z})|P_0|[\epsilon(\hat{z}) + q(\hat{z})\beta(e_z)] > \delta^*, \delta^* > 0$$

is satisfied (see also Remark 4, page 68) inside the domain of attraction. Also, assume that there exist $c < \infty$ such that

$$\frac{1}{2} \text{tr}[(K(\hat{z})K^T(\hat{z})\sigma_m + \Sigma)P(\hat{z})] \leq c^2, \quad \forall t \geq t_0.$$

Let the Lyapunov function (same as (6.5)) be

$$V(e_z) = e_z^T P(\hat{z}) e_z.$$

Then

$$\tilde{A} V(e_z) \leq -k(e_z) + c^2,$$

where

$$k(e_z) := \delta^* |e_z|^2$$

is strictly positive.

proof: Computing $\tilde{A} V(e_z)$ yields

$$\tilde{A} V(e_z) = e_z^T \dot{P}(\hat{z}) e_z - e_z^T \tilde{Q}(\hat{z}) e_z + 2e_z^T P(\hat{z}) \tilde{b}(z, \hat{z}) + \frac{1}{2} \text{tr}[(K(\hat{z})K^T(\hat{z})\sigma_m + \Sigma)P(\hat{z})]$$

where use is made of the fact that

$$A^{*T}(\hat{z})P(\hat{z}) + P(\hat{z})A^*(\hat{z}) = -\tilde{Q}(\hat{z})$$

and the fact that

$$G(\hat{z})UG^T(\hat{z}) = K(\hat{z})K^T(\hat{z})\sigma_m + \Sigma.$$

Assuming that the deterministic stability condition is satisfied, it follows that

$$\tilde{A}V(e_z) \leq -\delta^* |e_z|^2 + c^2.$$

Remark Generally, when e_z is large (but still within the domain of attraction), $\tilde{A}V(e_z)$ is negative hence, $V(e_z)$ decreases on the average along the trajectories of the process. When e_z is small, $\tilde{A}V(e_z)$ is positive, hence $\tilde{A}V(e_z)$ increases on the average. Near t_0 , when the estimation error, e_z , is usually large, $\tilde{A}V(e_z)$ is decreasing on the average, as desired. Unlike the deterministic case, the estimation error does not continue to converge to zero because once e_z is small enough that $k(e_z) < c^2$, then $V(e_z)$ begins increasing on the average. Therefore, the estimation error oscillates in a random fashion. ■

This is made more precise in the following theorem.

Theorem 6.4

Suppose the nonnegative scalar function $V(e_z)$, satisfying $V(0) = 0$, and $V(e_z) > 0$ when $e_z \neq 0$, is continuous and has continuous first and second order partial derivatives with respect to e_z . Also, suppose that $V(e_z)$ is bounded for finite e_z , and that e_z does not have a finite escape time (with probability one) to infinity. Let

$$\tilde{A}V(e_z) \leq -k(e_z) + c^2,$$

where $k(e_z) \geq 0$ and $0 < c < \infty$. Then,

$$\lim_{t \rightarrow \infty} \frac{1}{t} \int_0^t \frac{E_e[k(e_z(\tau))]d\tau}{c^2} \leq 1.$$

proof: see Kushner [20] (page 50)

Using the result of Theorem 6.3, it follows from Theorem 6.4 that

$$E(e_z^T e_z) \leq \frac{c^2}{\delta^*} \quad \text{as } t \rightarrow \infty. \quad (6.14)$$

Therefore the bounds on $E(e_z^T e_z)$ can be computed explicitly using the formula in Theorem 6.4. The constant c in (6.14) goes to zero as the state and measurement noise goes to zero, and gets correspondingly larger as the noise gets larger. This says that for noiseless systems the estimation error goes to zero while for increasingly noisy systems the estimation error oscillates in a random fashion in an increasingly larger region about zero. It will be shown in Chapter 8 that for the aircraft tracking problem (6.14) provides an accurate bound on the magnitude of the estimation errors. This fact is verified by many simulations.

Remark It can be seen from (6.14) that as the system tends toward instability (i.e. $\delta^* \rightarrow 0$) the bound on $E(e_z^T e_z)$ gets very large. The bound (6.14) is valid only when the error is within the domain of attraction. ■

Chapter 7

The Extended Kalman Filter

7.1 Introduction

The EKF design used for comparison with the GNF is presented here. The derivation of the EKF equations is not given but can be found in many standard references, including Jazwinski [12], Maybeck [21], and Gelb [8]. The EKF is applicable to nonlinear systems of the form

$$\dot{x} = f(x) + u_x \quad (7.1)$$

$$y = h(x) + u_m$$

where $f(x)$ is a nonlinear function of the state and u_x and u_m are zero mean white gaussian noise processes of covariance Σ and $\sigma_m^2 I$, respectively. The form of the filter is equivalent to the GNF form given in (3.1), namely,

$$\dot{\hat{x}} = f(\hat{x}) + K^*(y - h(\hat{x})). \quad (7.2)$$

The gain K^* is computed via

$$K^* = P(\hat{x})H^T(\hat{x})R^{-1}, \text{ and} \quad (7.3)$$

where

$$\dot{P}(\hat{x}) = F(\hat{x})P(\hat{x}) + P(\hat{x})F^T(\hat{x}) + Q - P(\hat{x})H^T(\hat{x})R^{-1}H(\hat{x})P(\hat{x}), \text{ and}$$

$$F(\hat{x}) = \left. \frac{\partial f(x)}{\partial x} \right|_{x=\hat{x}}, \text{ and}$$

$$H(\hat{x}) = \left. \frac{\partial h(x)}{\partial x} \right|_{x=\hat{x}}.$$

$P(\hat{x})$ is the estimation error covariance matrix where the estimation error is defined as

$$e := \hat{x} - x.$$

The differential equation for $P(\hat{x})$ given in (7.3), is only an approximate expression for propagating the true error covariance matrix. The fundamental step in the derivation of the EKF is a standard Taylor series linearization of $f(x)$ about the current estimate \hat{x} . All but the first term of the series are dropped, leading to the approximate error covariance propagation equation. Since the matrix $P(\hat{x})$ is only an approximation to the true covariance matrix, actual filter performance must be verified by monte carlo simulation. There is no guarantee that the actual estimate obtained using (7.2) and (7.3) will be close to the truly optimal estimate (Gelb [8]). There is, in fact, no guarantee that the filter estimate even converges to the true state. This also must be verified by monte carlo simulation.

An important characteristic of the EKF is that the gain K^* requires an on-line computation of a state-dependent matrix Riccati equation. This follows since $P(\hat{x})$ depends on \hat{x} through the terms $F(\hat{x})$ and $H(\hat{x})$, and \hat{x} is not known *a priori*.

7.2 Aircraft Maneuver Model EKF

The aircraft maneuver model is given in (2.28a). The first step in designing the EKF is to compute the state-dependent matrices $F(\hat{x})$ and $H(\hat{x})$. The matrix $F(\hat{x})$, defined above, has the form

$$F(\hat{x}) = \begin{bmatrix} F_{1,1} & F_{1,2} & F_{1,3} \\ F_{2,1} & F_{2,2} & F_{2,3} \\ F_{3,1} & F_{3,2} & F_{3,3} \end{bmatrix}$$

where

$$F_{ii} = \begin{bmatrix} 0 & 1 & 0 & 0 \\ 0 & 0 & 1 & 0 \\ 0 & F_{4i-1,4i-2} & F_{4i-1,4i-1} & F_{4i-1,4i} \\ 0 & 0 & 0 & -\alpha_i \end{bmatrix}, \text{ and}$$

$$F_{ij} = \begin{bmatrix} 0 & 0 & 0 & 0 \\ 0 & 0 & 0 & 0 \\ 0 & F_{4i-1,4j-2} & F_{4i-1,4j-1} & F_{4i-1,4j} \\ 0 & 0 & 0 & 0 \end{bmatrix}.$$

The terms needed to calculate F_{ij} are given in Appendix E. The matrix $H(\hat{x})$ is given by

$$H(\hat{x}) = \begin{bmatrix} 1 & 0 & 0 & 0 & 0 & 0 & 0 & 0 & 0 & 0 & 0 & 0 \\ 0 & 0 & 0 & 0 & 1 & 0 & 0 & 0 & 0 & 0 & 0 & 0 \\ 0 & 0 & 0 & 0 & 0 & 0 & 0 & 0 & 1 & 0 & 0 & 0 \end{bmatrix}.$$

$H(\hat{x})$ is not state-dependent since the measurements are linear combinations of the states.

The values chosen for simulation purposes (see results in Chapter 8) are $\alpha_i = 5.0$ and $\sigma_m = 1.0$. The initial error covariance matrix is $P(0) = \text{diag}(P_{11}(0), P_{22}(0), P_{33}(0))$ where

$$P_{ii}(0) = \begin{pmatrix} 10.0 & , & 0.0 & , & 0.0 & , & 0.0 \\ 0.0 & , & 100.0 & , & 0.0 & , & 0.0 \\ 0.0 & , & 0.0 & , & 1000.0 & , & 0.0 \\ 0.0 & , & 0.0 & , & 0.0 & , & 1000.0 \end{pmatrix}.$$

The state noise covariance matrix is $\Sigma = \text{diag}(\Sigma_{11}, \Sigma_{22}, \Sigma_{33})$ where

$$\Sigma_{ii} = \begin{pmatrix} 0.0 & , & 0.0 & , & 0.0 & , & 0.0 \\ 0.0 & , & 0.0 & , & 0.0 & , & 0.0 \\ 0.0 & , & 0.0 & , & 0.0 & , & 0.0 \\ 0.0 & , & 0.0 & , & 0.0 & , & 10.0 \end{pmatrix}.$$

When the EKF is used to track the actual aircraft trajectories in the next chapter, the initial state estimate is obtained by using the first three measurements in the formulas

$$\hat{x}_{4i-3}(0) = y_i(t_2)$$

$$\hat{x}_{4i-2}(0) = \frac{y_i(t_0) - 4y_i(t_1) + 3y_i(t_2)}{2\Delta T}$$

$$\hat{x}_{4i-1}(0) = \frac{y_i(t_0) - 2y_i(t_1) + y_i(t_2)}{\Delta T^2}$$

$$\hat{x}_{4i}(0) = 0$$

where $\Delta T = t_1 - t_0 = t_2 - t_1$. $y(t_1), y(t_2), y(t_3)$ are the first, second and third radar measurements. This is the same procedure used for initializing the GNF state estimates when tracking the actual trajectories. For the cases when the simulated aircraft trajectories are used, these formulas are not used for either the EKF or GNF.

Chapter 8

Aircraft Tracking Results

8.1 Introduction

The GNF design proposed in the previous chapters is tested here. The tests are based on two types of measurement data. The first type of measurement data is generated by simulation of the aircraft maneuver model (2.28). A more detailed analysis of the filter is possible since all parameters of the problem (i.e. initial state errors, state and measurement noise values) can be controlled. The second type of measurement data is actual aircraft maneuver data (see Appendix F) provided by Contraves [35]. Using actual radar measurements, the tracking performance of the GNF in a real-world environment can be verified.

A comparison of the GNF and the EKF is also presented. A detailed analysis, based on simulated aircraft trajectories, compares the stability characteristics of both filters as well as the behavior of both filters in the presence of nominal and near-nominal measurement noise. It will be shown that in some situations the GNF is stable and provides good tracking performance when, in the same situations, the EKF is unstable (i.e. cannot provide any tracking). Both filters work well

in the presence of nominal and near-nominal measurement noise with the GNF performance always at least as good as the EKF performance.

Using the radar measurements associated with the actual aircraft trajectories, the tracking performance of the GNF and the EKF is compared. It will be shown that the performance for limited number of available trajectories (i.e. 26) is nearly identical.

In all cases, the computational burden (i.e. CPU time) of the GNF is an order of magnitude less than the EKF. CPU time is of prime importance when considering implementing a filter in a commercial fire control computer.

In the sequel, the measure of tracking performance is the magnitude of the position error predicted one second ahead. The estimation state errors as well as the modelling inaccuracies of the state predictor affect this measure. Therefore, this measure is related to the hit probability (i.e. the smaller the predicted error, the greater the hit probability). The hit probability is the probability that a missile (fired from the vicinity of the radar) actually hits the maneuvering aircraft. Computing the hit probability is beyond the scope of this thesis. However, to compute a more realistic measure of filter performance, the data from the first five seconds of each run is not included in the final analysis since there is no chance of the missile reaching the target in that time, hence no chance of a hit.

8.2 Comparison Based on Simulated Aircraft Trajectories

The effects on the tracking performance of the GNF and the EKF resulting from two sources of errors, namely initial state errors and measurement noise, are investigated here.

The stability of each filter in the presence of nominal and off-nominal initial state errors is tested. It will be shown that there exists cases wherein the GNF is stable and provides good tracking performance, while the EKF is unstable.

The tracking performance of each filter in the presence of nominal and near-nominal measurement noise is also tested. Here it is shown that the GNF performs as least as well as the EKF in all cases.

The results of this section are based on the nominal trajectory in Figure 8.1. This trajectory was generated using the coordinated turn model (2.28) with the initial conditions

$$\begin{aligned} \mathbf{r}(0) &= (-3800.0, -3700.0, 1000.0) \text{ m} \\ \mathbf{v}(0) &= (300.0, 0.0, 0.0) \text{ m/sec} \\ \mathbf{a}(0) &= (0.0, 19.612, 0.0) \text{ m/sec}^2. \end{aligned} \tag{8.1}$$

There is nothing special about this particular trajectory other than it is representative of the type of trajectories of interest and it is similar to previously published trajectories (see Berg [1], for example).

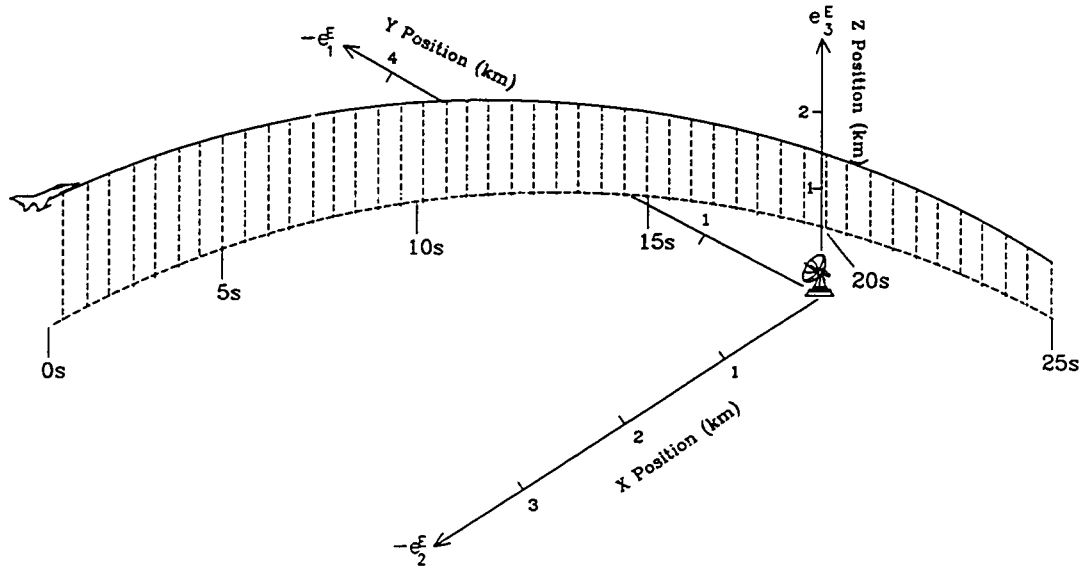


Figure 8.1. The Simulated Nominal Trajectory

8.2.1 Stability Analysis

It was shown in Theorem 6.1 that a sufficient condition for stability of the GNF estimation error is

$$\lambda_Q(\dot{z}) - 2q(\dot{z})|P_0|[\epsilon(\dot{z}) + q(\dot{z})\beta(e_z)] > \delta, \text{ where } \delta \geq 0.$$

The practical implication of this condition is now investigated. The first step is to choose the gains K_1 to guarantee stability. Recall that (see Chapter 4) the transformation T given in (4.3) takes the aircraft maneuver model to approximate observer canonical form. So, when the aircraft turn rate in the maneuver plane is zero (i.e. $\theta=0$), $b(z)=0$ and the transformed system (4.4) is the linear system

$$\dot{z} = Az \tag{8.2}$$

$$y = Cz$$

where A and C are block diagonal matrices $A = \text{diag} (A_{11}, A_{22}, A_{33})$ and $C = \text{diag} (C_{11}, C_{22}, C_{33})$ with

$$A_{ii} = \begin{bmatrix} 0 & 1 & 0 & 0 \\ 0 & 0 & 1 & 0 \\ 0 & 0 & 0 & 1 \\ 0 & 0 & 0 & -\alpha_i \end{bmatrix} \text{ and } C_{ii} = [1 \ 0 \ 0 \ 0] \text{ for } i=1,2,3.$$

With the linear system (8.2) it is possible to compute the optimal Kalman gains off-line via

$$K_i = PC^T \sigma_m^{-1}$$

where P is the solution of the matrix Riccati equation

$$\dot{P} = A^T P + P A + \Sigma - \sigma_m^{-1} P C^T C P.$$

The values for input into the above Riccati equation are $\alpha_i = 5.0$, $\sigma_m = 1.0$. The initial error covariance matrix is $P(0) = \text{diag} (P_{11}(0), P_{22}(0), P_{33}(0))$ where

$$P_{ii}(0) = \begin{pmatrix} 10.0 & , & 0.0 & , & 0.0 & , & 0.0 \\ 0.0 & , & 100.0 & , & 0.0 & , & 0.0 \\ 0.0 & , & 0.0 & , & 1000.0 & , & 0.0 \\ 0.0 & , & 0.0 & , & 0.0 & , & 1000.0 \end{pmatrix}.$$

The state noise covariance matrix is $\Sigma = \text{diag} (\Sigma_{11}, \Sigma_{22}, \Sigma_{33})$ where

$$\Sigma_{ii} = \begin{pmatrix} 0.0 & , & 0.0 & , & 0.0 & , & 0.0 \\ 0.0 & , & 0.0 & , & 0.0 & , & 0.0 \\ 0.0 & , & 0.0 & , & 0.0 & , & 0.0 \\ 0.0 & , & 0.0 & , & 0.0 & , & 10.0 \end{pmatrix}.$$

The steady-state solution of the above Riccati equation is then modified slightly (i.e. tuned) to obtain the block diagonal matrix $K_i = \text{diag}(K_{11}, K_{22}, K_{33})$ where

$$K_{ii} = \begin{pmatrix} 1.6 \\ 1.6 \\ 0.5 \\ 0.001 \end{pmatrix}. \quad (8.3)$$

This approach to computing K_1 leads to GNF gains that are optimal when the aircraft is on a straight line path. In maneuvering situations these gains provide stability of the estimation error but are not optimal. They also provide a good trade-off between the desire to speed up the convergence of the estimation error by using large gains and the desire to eliminate the effects of the measurement and state noise by using small gains.

Another approach to computing the GNF gains is to find K_1 such that the matrix Lyapunov equation

$$(A - K_1 C)^T P_0 + P_0 (A - K_1 C) = -I \quad (8.4)$$

is satisfied and $|P_0|$ is minimized. Then $\dot{V}(e_z)$ is maximized, hence convergence of the estimation error is maximized. This does not imply that optimal estimates (maximum likelihood or minimum variance) will be obtained. It does, however, imply stability. This approach follows that suggested by Pearson [28].

The gains K_1 in (8.3) lead to the desired characteristic polynomial

$$\rho_{des} = (s^4 + 6.6s^3 + 9.6s^2 + 8.5s + 2.5)^3$$

with multiple zeroes at $s = -0.5664 \pm 0.866i$, $s = -0.4672$, and $s = -5.0$. By construction (as described in Chapter 5) the matrix $A^*(2)$ will have this same (constant) characteristic polynomial.

Since A and C are block diagonal matrices it follows that $P_0 = \text{diag}(P_{11}, P_{22}, P_{33})$. The solution to the matrix Lyapunov equation (8.4) corresponding to the above choice of K_1 in (8.3) is

$$P_0 = \begin{pmatrix} +1.265 & -0.500 & -1.447 & -0.259 \\ -0.500 & +1.447 & -0.500 & -0.152 \\ -1.447 & -0.500 & +5.228 & +1.015 \\ -0.259 & -0.152 & +1.015 & +0.303 \end{pmatrix}$$

where

$$|P_0| = 5.9.$$

$|P_0|$ is one of the terms needed in the stability condition.

It was stated in the previous chapter that the term $\beta(e_z)$ satisfies

$$\beta(e_z) \leq c_0(\hat{z}) |\bar{e}_z|.$$

When the ratio of the magnitude of the aerodynamic acceleration, \hat{a} , to the magnitude of the aircraft velocity, \hat{v} , is small then

$$\beta(e_z) \leq \frac{1}{\hat{v}} \left(1 + \frac{\hat{a}}{\hat{v}} \right) |\bar{e}_z|$$

where $|\bar{e}_z|$ is the magnitude of the velocity and acceleration estimation error and \hat{v} is the estimated velocity magnitude. For the trajectory illustrated in Figure 8.1, $a/v \approx 0.07$. When this ratio is small the value of $|\bar{e}_z|$ is approximately equal

to the velocity estimation error $|e_v|$ (in other words, the majority of the velocity plus the acceleration estimation error is due to the velocity error).

The remaining terms in the stability conditions are related to the matrix $Q(\hat{z})$. For the $Q(\hat{z})$ matrix given in (5.6), $\lambda_Q(\hat{z}) \approx q(\hat{z}) \approx 1$. This implies that $\kappa_Q := q^2(\hat{z})/\lambda_Q(\hat{z}) \approx 1$. κ_Q is the condition number of $Q(\hat{z})$. The fact that $\kappa_Q \approx 1$ verifies the fact that $Q(\hat{z})$ is invertible.

Combining the above calculations (specific to this aircraft tracking problem) it follows that stability is guaranteed when the initial velocity estimation error satisfies the inequality

$$|e_v| \leq \frac{\hat{v}}{12.8}(1 - \delta^*). \quad (8.5)$$

The above inequality defines a domain of attraction which states that if the initial estimate of the aircraft velocity and the actual aircraft velocity differ by less than $\hat{v}/12.8$ (for $\delta^* = 0$) then stability of the estimation error is guaranteed. (Note: The inequality (8.6) is valid when \hat{a}/\hat{v} is small, $\epsilon(\hat{z})$ is negligible, and the condition number of $Q(\hat{z})$ satisfies $\kappa_Q \approx 1$).

There are no stability results for the EKF. The stability of the EKF must be verified by monte carlo analysis (i.e. simulations).

Consider the nominal trajectory in Figure 8.1. The true initial conditions are given in (8.1). Suppose the filters are initialized with

$$\begin{aligned}
 \mathbf{f}(0) &= (-4400.0, -3690.0, 1030.0)\text{m} \\
 \dot{\mathbf{v}}(0) &= (275.0, 0.0, -1.0)\text{m/sec} \\
 \ddot{\mathbf{a}}(0) &= (0.0, 9.806, 0.0)\text{m/sec}^2.
 \end{aligned}
 \tag{8.6}$$

Then the resulting tracking is shown in Figure 8.2. It is obvious that the EKF is unstable, while the GNF is not only stable, but the tracking performance is good. The GNF is expected to be stable since the stability condition (6.4a) is satisfied.

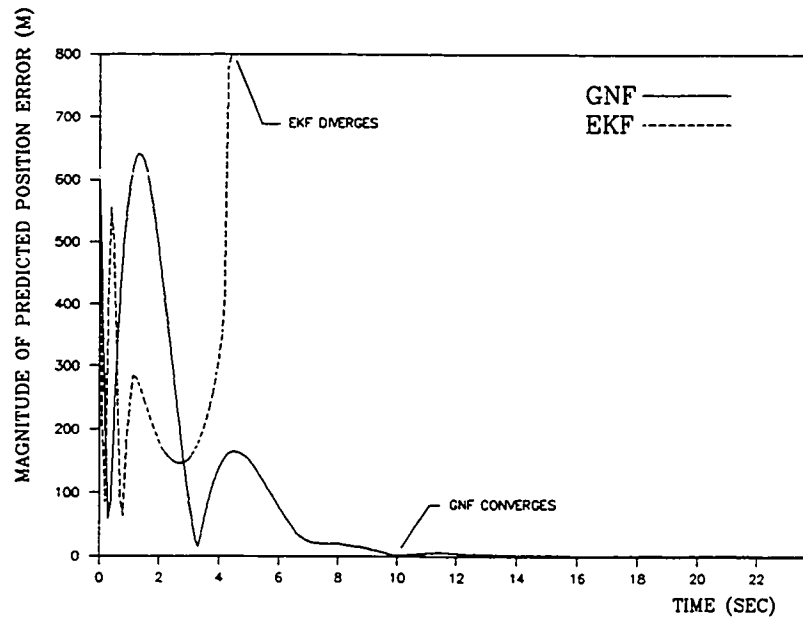


Figure 8.2. A Stress Case Tracking Result

The initial state errors (computed from (8.1) and (8.6)) represent a realistic but stressful situation for both filters. The main result that this case illustrates is that the GNF with its explicit stability conditions is stable in a situation where the EKF is not. Simulation results show that the GNF

will converge with any realistic initial state error. On the other hand, other unstable initial conditions for the EKF can be easily generated.

To investigate the stability characteristics of the filters initialized with nominal and near-nominal initial state errors, one-hundred state errors were generated from the covariance matrix $P(0) = \text{diag}(P_{11}, P_{22}, P_{33})$, where

$$P_{ii} = \begin{bmatrix} 10 & 0 & 0 & 0 \\ 0 & 100 & 0 & 0 \\ 0 & 0 & 1000 & 0 \\ 0 & 0 & 0 & 1000 \end{bmatrix}.$$

This is the same $P(0)$ used in the EKF initialization. The square root of the i th diagonal element of $P(0)$, denoted by σ_i , represents the so-called 1σ value of the initial state error. Thus, it is expected that the actual initial state error is less than or equal to $\pm\sigma_i$ sixty-eight percent of the time. These 1σ initial state errors are the *nominal* initial state errors. Utilizing these 1σ values, one-hundred initial state errors were generated from which one-hundred trajectories were generated. Both filters, initialized with the values in (8.1), tracked these trajectories successfully.

The same procedure was conducted for the *near-nominal* cases which are defined to be the 2σ and 3σ initial state errors. It is expected that the actual initial state error is less than or equal to $\pm 2\sigma_i$ ninety-five percent of the time and less than or equal to $\pm 3\sigma_i$ ninety-eight percent of the time.

The results of this part of the study showed that both filters converged nicely. This shows that when the EKF is initialized with initial state errors at or near its design values, it will converge. The GNF will converge in these cases in addition to most other stress cases that the EKF cannot handle.

In summary, in the nominal and near-nominal cases, both filters have good convergence properties. However, there exist stress cases in which the GNF will converge nicely, while the EKF is unstable.

8.2.2 Measurement Noise

The effect of state measurement noise on the GNF and the EKF is investigated here. Since stability is not the issue, an initial 1σ state error is selected so that both filters will converge. As before, the nominal trajectory is shown in Figure 8.1.

The effects of varying levels of measurement noise on the tracking performance is investigated by considering the 1σ , 2σ , and 3σ values of the measurement noise covariance, where the 1σ value is 1.0 meter. In all the simulation runs, the 1σ value of the state noise was used. For each level of measurement noise, one-hundred runs were made with each run corresponding to a different trial of the state and measurement noise processes. This is accomplished by varying the random number generator initial seed values. This process was repeated for the 2σ and 3σ cases for both the GNF and the EKF.

Before proceeding to the simulation results, it is useful to utilize the stochastic stability results of Chapter 6 to obtain an upper bound on the expected errors. The values of the state and measurement noise covariances are

$$\sigma_m = 1.0, \quad \text{and} \quad (8.7)$$

$$\Sigma_{ii} = \begin{cases} 10.0 & i = 4, 8, 12 \\ 0 & \text{otherwise} \end{cases}.$$

Using the values previously defined for K_1 and P_0 it can be computed that

$$\frac{1}{2} \text{tr}[(K(\hat{z})K^T(\hat{z})\sigma_m + \Sigma)P(\hat{z})] \leq 1.75, \quad \forall t \geq t_0.$$

For the aircraft tracking case under investigation here, it follows that

$$E(e_z^T e_z) \rightarrow \frac{1.75}{\delta^*}. \quad (8.8)$$

This bound on $E(e_z^T e_z)$ is valid only when the estimation error is within the domain of attraction.

The average magnitude of the errors for the 100 runs made at the nominal noise level of 1 meter are shown in Figure 8.3. It can be seen in Figure 8.3 that this computed upper bound does in fact bound the errors after about 7.7 seconds. It should be remembered that (8.8) bounds the error magnitude as time gets large and does not provide a bound for all time. The fact that this computed bound is reasonable (i.e. small)

gives us confidence that (under the stated conditions of the simulations) the GNF filter will provide good predicted position estimates.

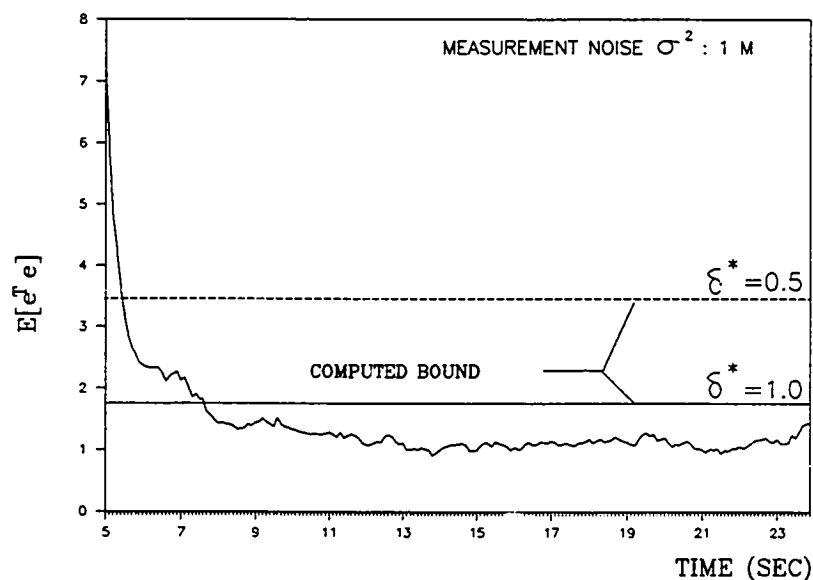


Figure 8.3. Estimation Errors with Nominal Measurement Noise

As previously stated, the measure of tracking performance is the predicted position errors one second ahead of current time. The scalar measure that is used here is the percentage of time that the projected position error was less than five meters and ten meters. This was calculated and averaged over the one-hundred runs. A higher percentage implies better performance (i.e. higher hit probability). The results are shown in Figure 8.4. They show that both filters perform quite well and the results are quite similar. The performance degrades as the noise level increases, as expected. The trends indicate that the GNF performs as well or better than the EKF

near the design point ($\sigma_m^2 = 1, 4$) but tends to drop off faster than the EKF as the noise increases ($\sigma_m^2 = 9$). So, for very large measurement noises, the EKF will perform better.

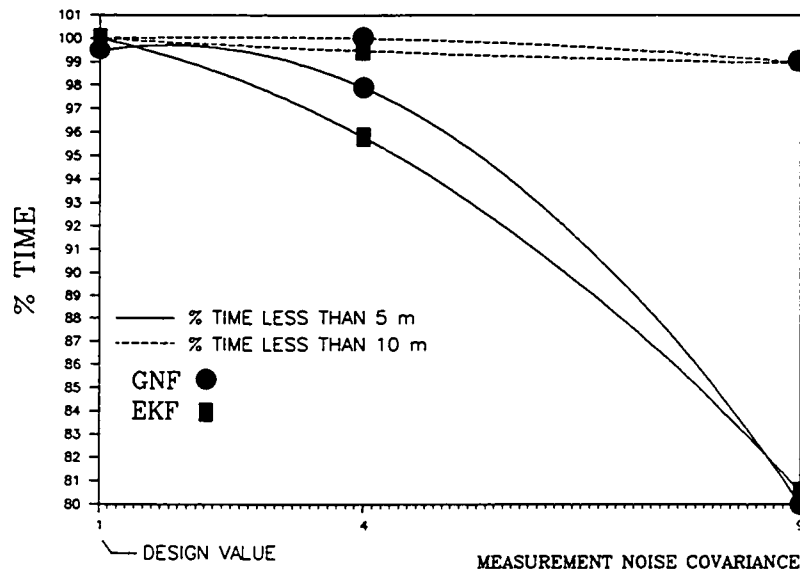


Figure 8.4. Performance in the Presence of Measurement Noise

The conclusion is that the tracking performance of the EKF and the GNF is similar, yet the GNF takes about ten times less CPU time. Therefore, the GNF is a better solution to this nonlinear tracking problem than the EKF from both a stability point-of-view (see previous section) as well as a CPU performance point-of-view. The GNF takes about ten times more CPU than a constant gain filter (i.e. no on-line gain computation) and the EKF takes about one-hundred times more CPU.

From a tracking performance (i.e. hit probability) point-of-view, both filters have approximately the same performance for different expected levels of measurement noise.

8.3 Comparison Based on Actual Aircraft Trajectories

Up to this point, all the analysis was done using simulated aircraft trajectories. The performance of the two filters in a "real-world" environment is investigated by processing actual radar measurement data in both the GNF and the EKF. The measurement data was provided by Contraves [35, see Appendix F]. An example of an actual aircraft trajectory is shown in Figure 8.5. This is Traj A. In each of the trajectories, as in Traj A, the aircraft is approaching the radar. In general, the maneuvering is done in the $e_1^E - e_2^E$ plane with only small altitude (e_3^E direction) changes. The main characteristic of the trajectories is that they are planar maneuvers separated by a discrete number of plane changes. These plane changes are accomplished by a rapid roll maneuver. Traj A contains four such roll maneuvers, occurring approximately at two, fifteen, twenty-four and thirty-six seconds. An experienced pilot will perform the roll maneuver very quickly.

Between the discrete roll maneuvers, the trajectories are described very accurately by the coordinated turn model, thus justifying the proposed aircraft maneuver model of Chapter 2. The rapid roll maneuvers and accompanying plane changes are not modeled explicitly in the maneuver model. They are treated as perturbations to the model through the roll rate uncertainty. This uncertainty is modelled as a markov stochastic process

(see Chapter 2) with the associated time constant and variance chosen to give good tracking performance during and immediately after the roll maneuver. This

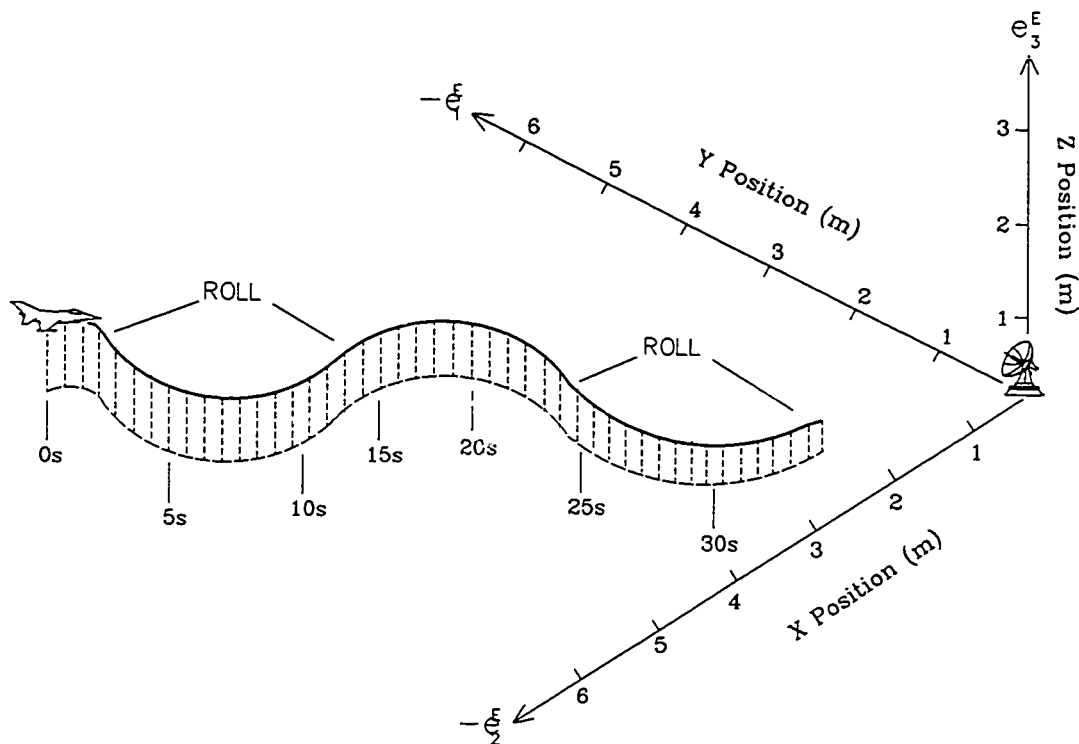


Figure 8.5. An Example Aircraft Trajectory - Traj A is part of the so-called "filter-tuning" process. Some "tuning" was done here for the purposes of comparing the GNF and EKF, however, a more complete "tuning" is necessary before either filter can be utilized commercially.

Since actual aircraft trajectories were used for the comparisons, the true state (i.e position, velocity and acceleration) are not known. All that is known is the measured position (which serve as the measurements for the filters) in the inertial reference frame. Therefore, to compare the two

filters, the estimated state was used to predict the aircraft position ahead for 0.96 seconds. The prediction scheme was identical for both filters and consists of the coordinated turn maneuver model. The error is then defined to be the predicted position minus the measured position at that future time. Since the measurements are noisy, this noise shows up in the error plots.

The tracking performance for Traj A is shown in Figure 8.6. The first noticeable characteristic is that the GNF and EKF performance is similar in all three inertial directions. This also turns out to be the case for the remaining twenty-five trajectories (see Figure 8.6b-z).

The roll maneuvers show up as increased errors. In Figure 8.6a, it can be seen that the two roll maneuvers result in increased errors in the e_1^E direction and the remaining two roll maneuvers result in increased errors in the e_2^E direction. Between the roll maneuvers the errors are less than fifteen meters (remember that these are errors predicted ahead 0.96 seconds and that they include measurement noise directly as well as estimation errors). The errors in the e_3^E direction are small and uneventful since the aircraft is exhibiting very little motion in that direction.

To compare the GNF and EKF a performance index, π , is defined as the average (over all twenty-six trajectories) of the predicted position error squared. The results show that

$$\pi(\text{GNF}) = 376.3$$

$$\pi(\text{EKF}) = 412.7.$$

Thus, for these particular test cases, the GNF performed better.

The performance of both filters would be improved by application of a roll maneuver detection scheme. This is not investigated in this thesis but is a good topic for future research.

The conclusion drawn from these actual aircraft tracking results is that the GNF looks promising. A more exhaustive "tuning" followed by further detailed engineering analysis (i.e monte carlo analysis) is warranted. The GNF performance compares favorably with the EKF tracking performance but at a substantial reduction in CPU time. These facts make the GNF the more desirable solution.

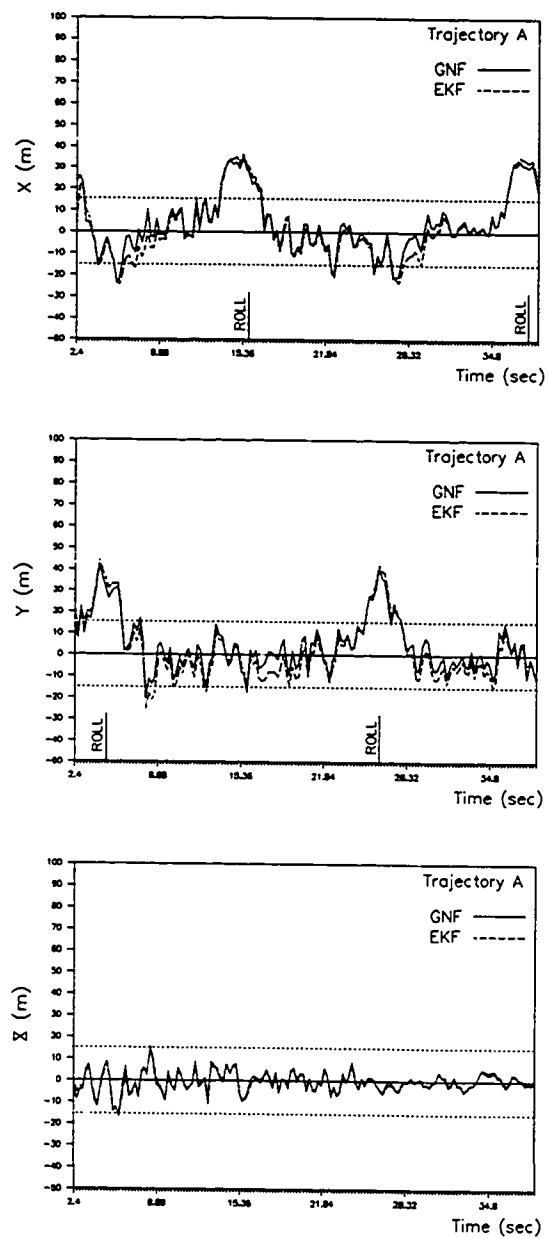


Figure 8.6a. Traj A Tracking Performance Comparison

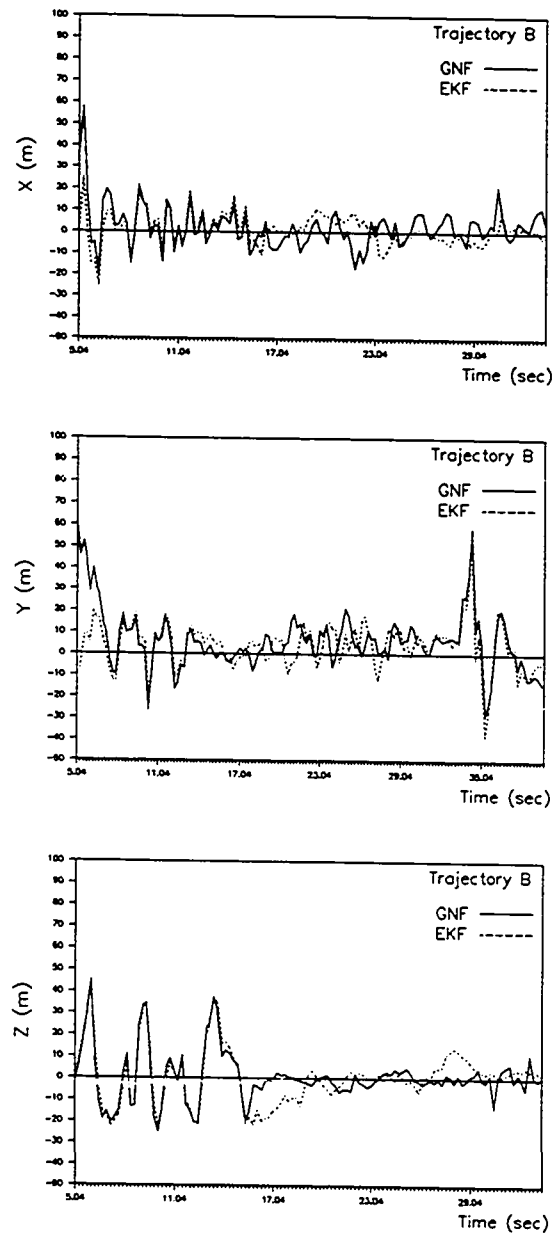


Figure 8.6b. Traj B Tracking Performance Comparison

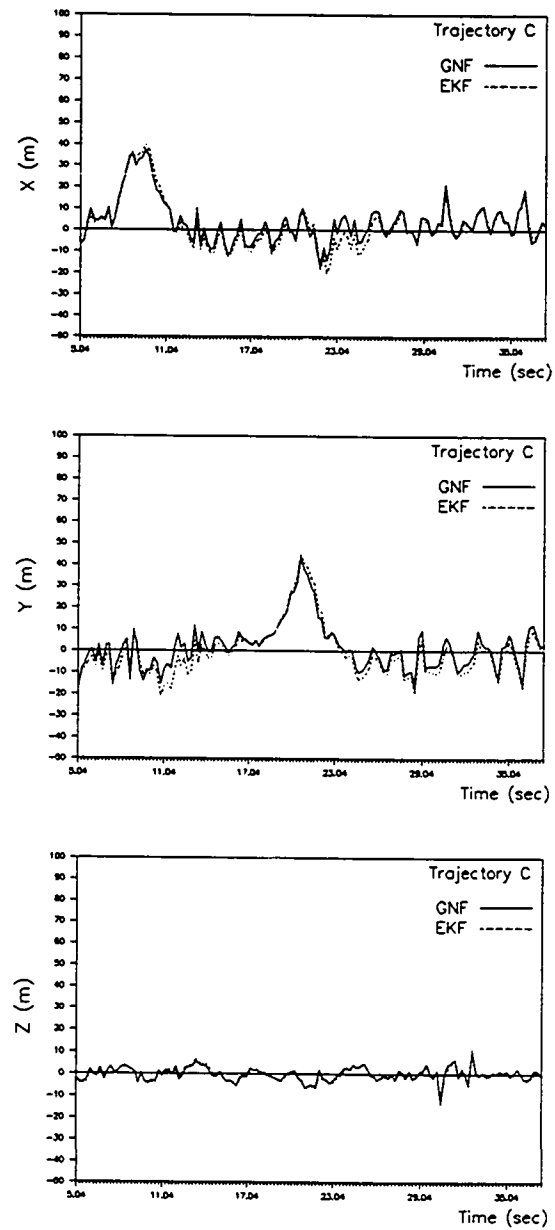


Figure 8.6c. Traj C Tracking Performance Comparison

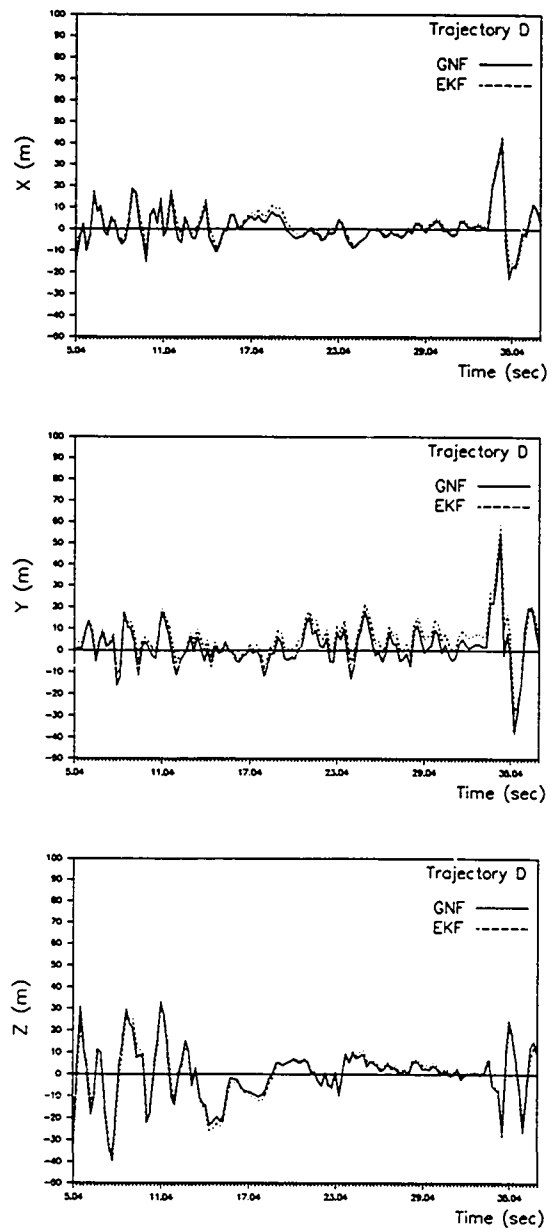


Figure 8.6d. Traj D Tracking Performance Comparison

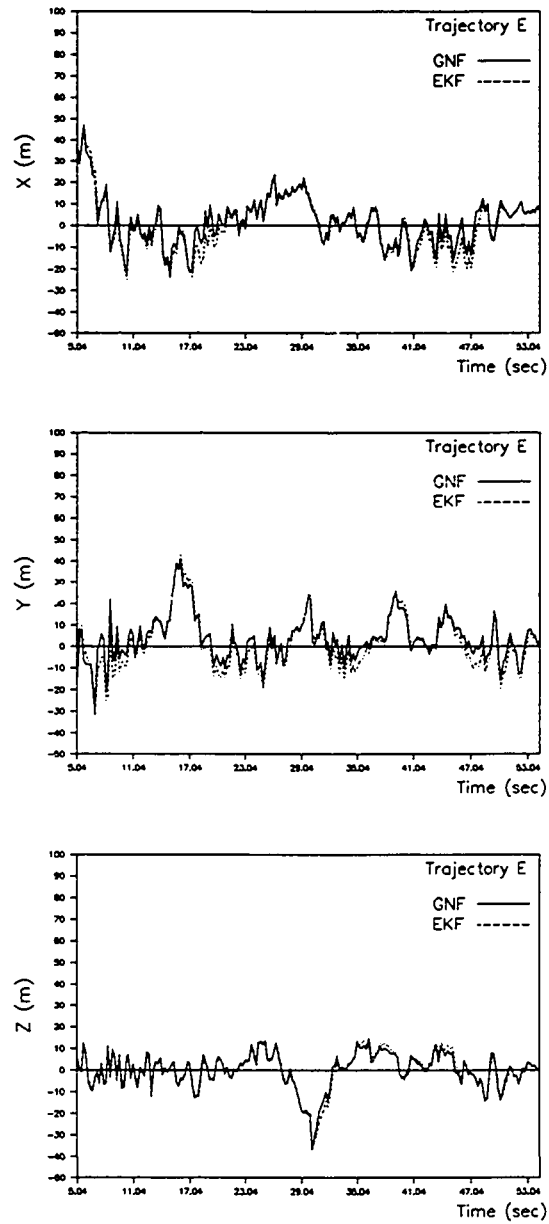


Figure 8.6e. Traj E Tracking Performance Comparison

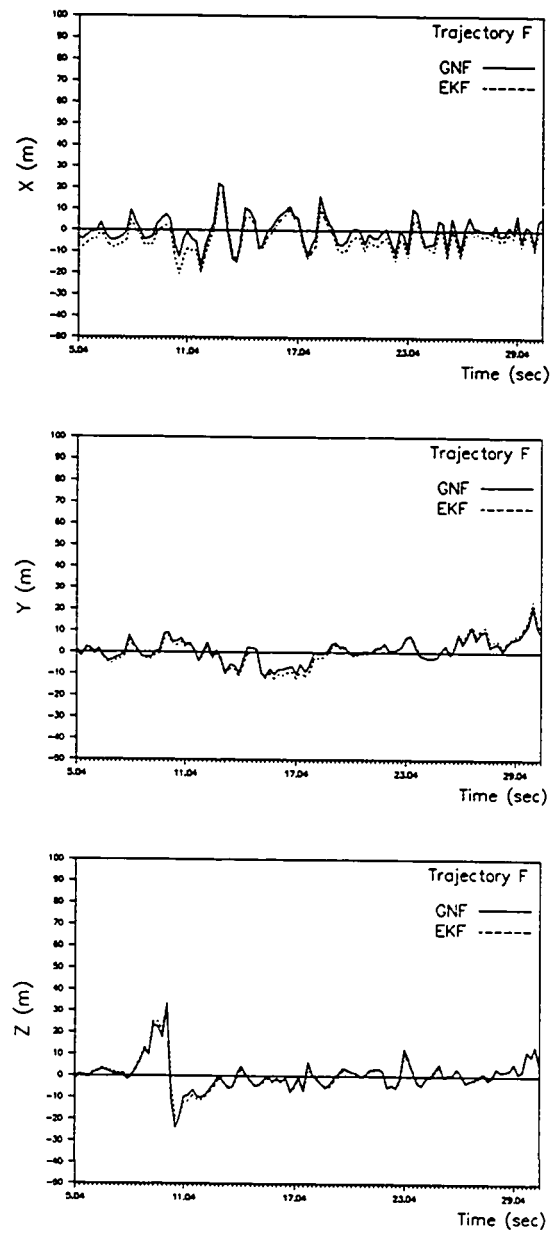


Figure 8.6f. Traj F Tracking Performance Comparison

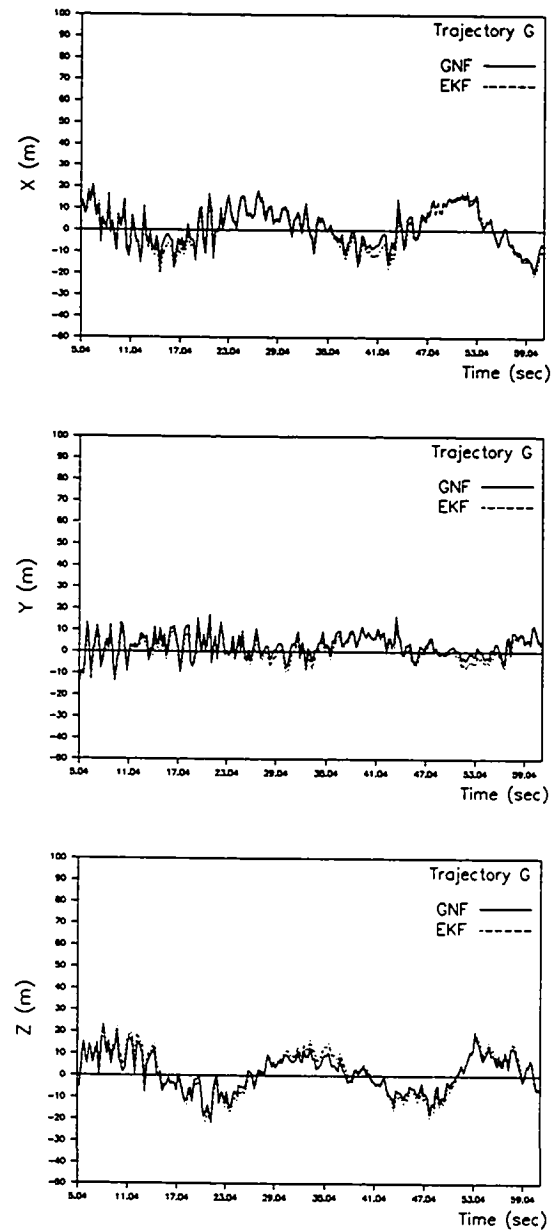


Figure 8.6g. Traj G Tracking Performance Comparison

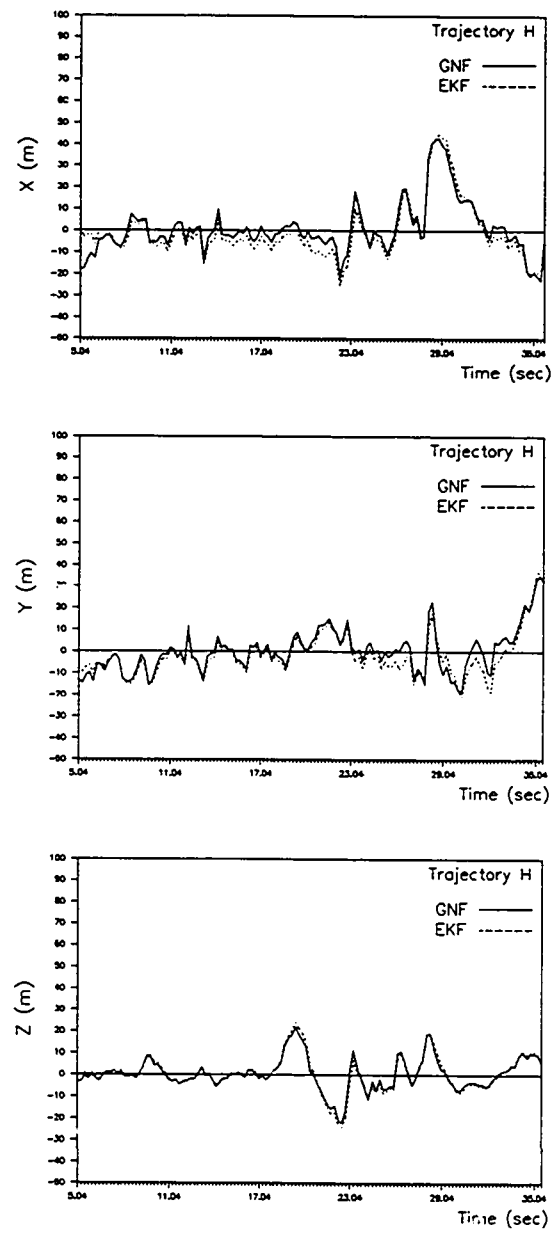


Figure 8.6h. Traj H Tracking Performance Comparison

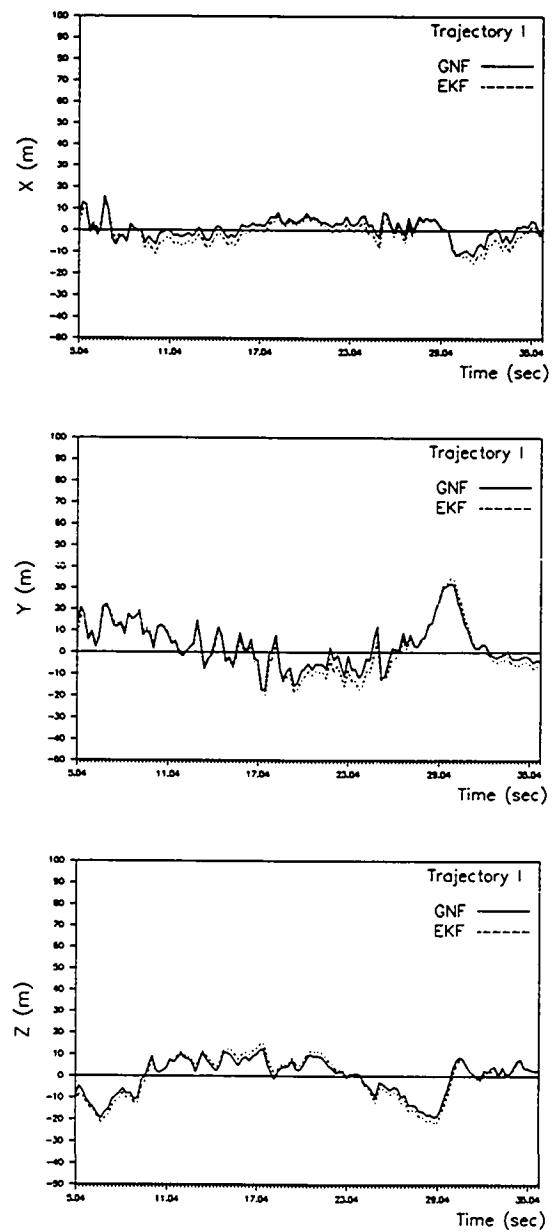


Figure 8.6i. Traj I Tracking Performance Comparison

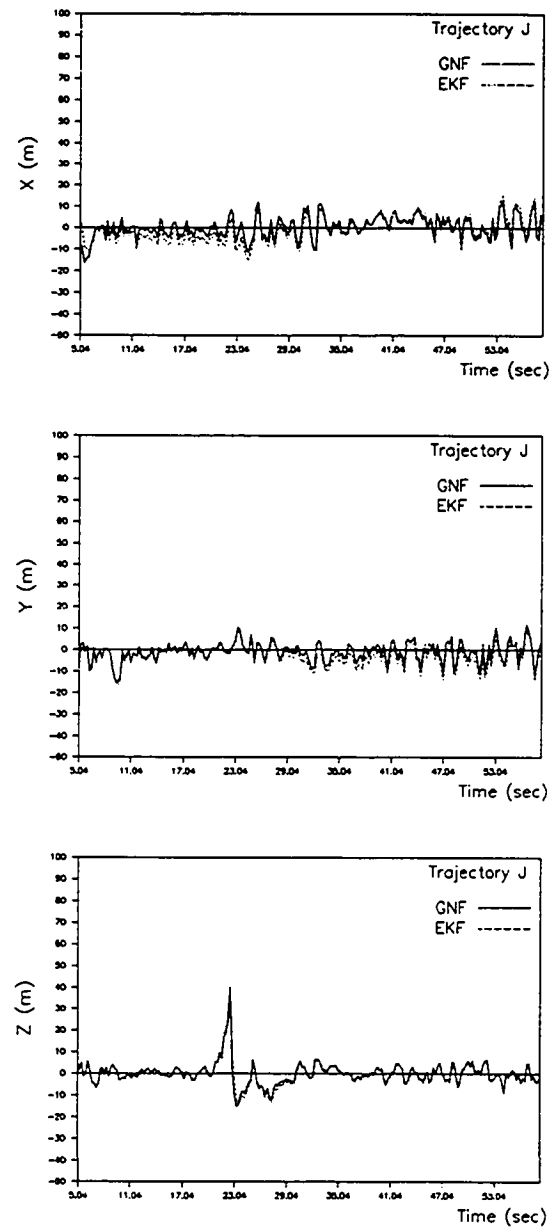


Figure 9.6j. Traj J Tracking Performance Comparison

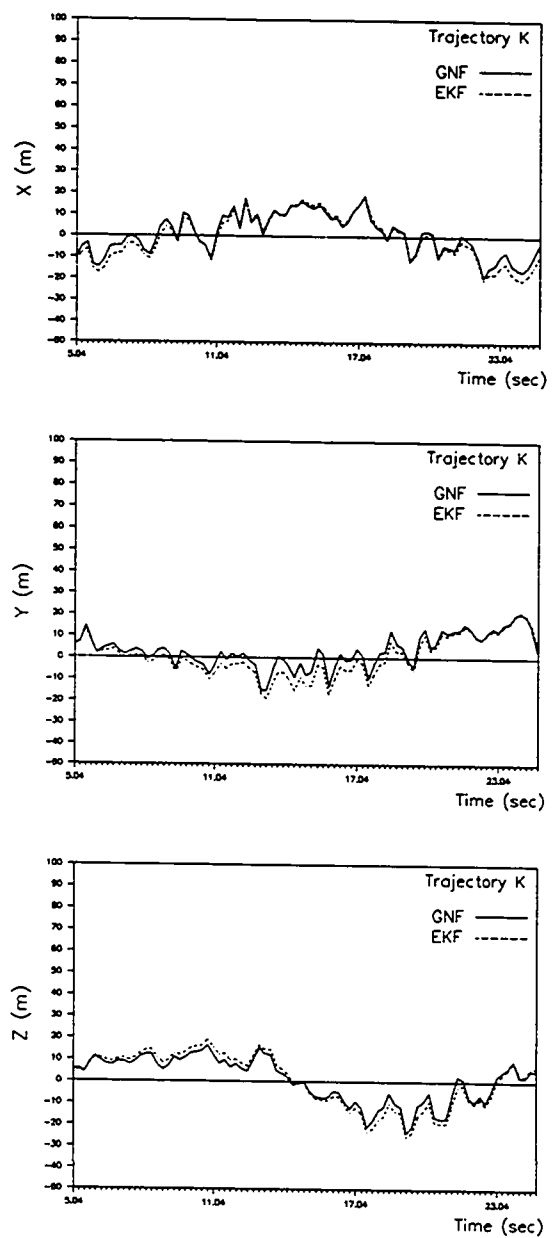


Figure 8.6k. Traj K Tracking Performance Comparison

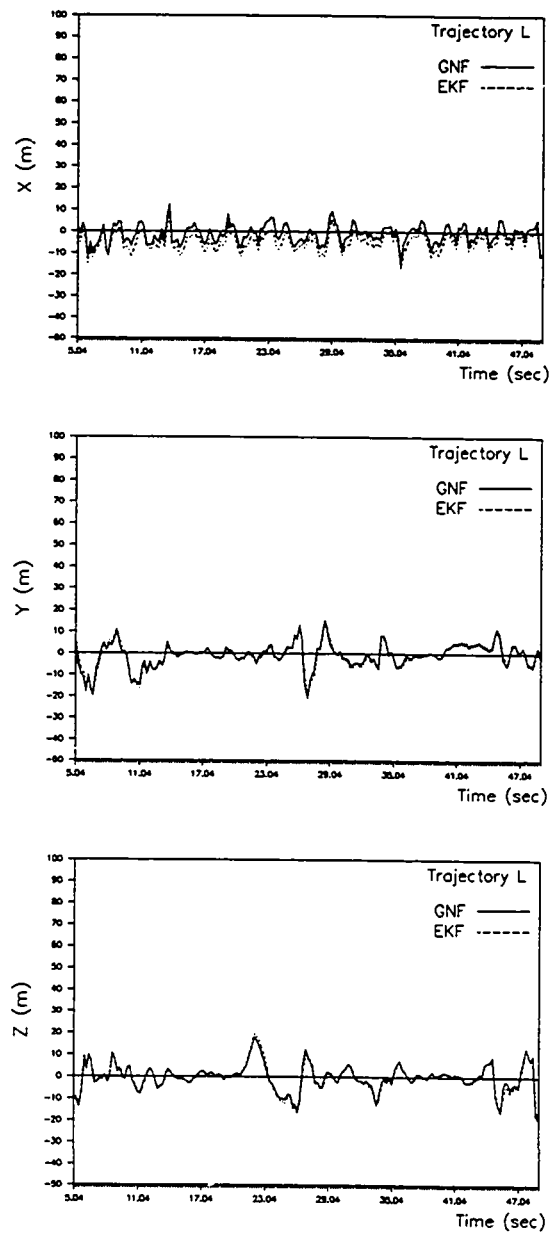


Figure 8.61. Traj L Tracking Performance Comparison

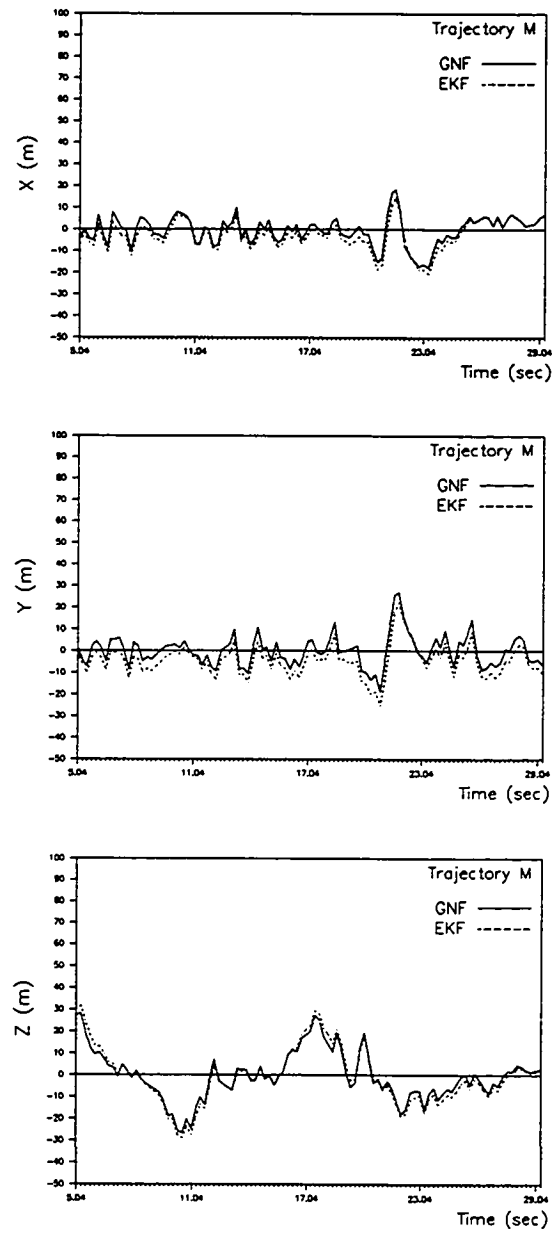


Figure 8.6m. Traj M Tracking Performance Comparison

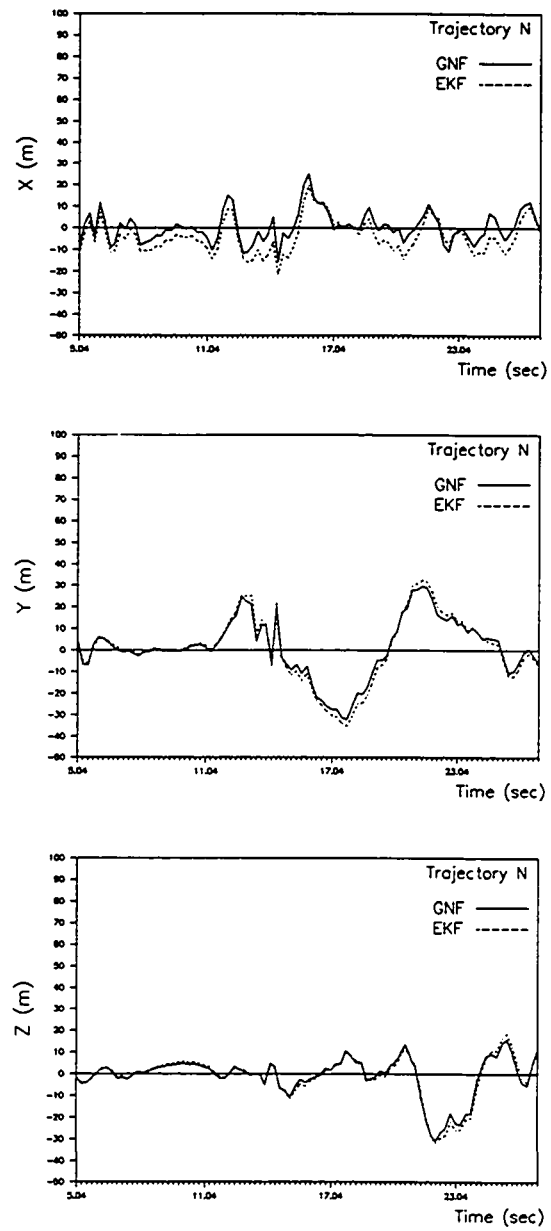


Figure 8.6n. Traj N Tracking Performance Comparison

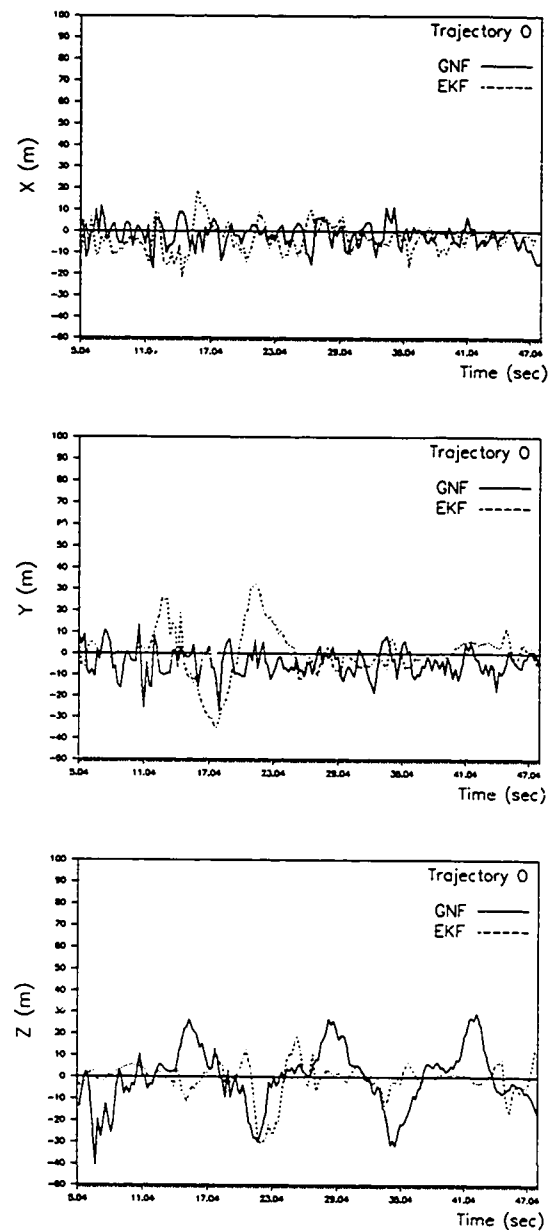


Figure 8.6o. Traj 0 Tracking Performance Comparison

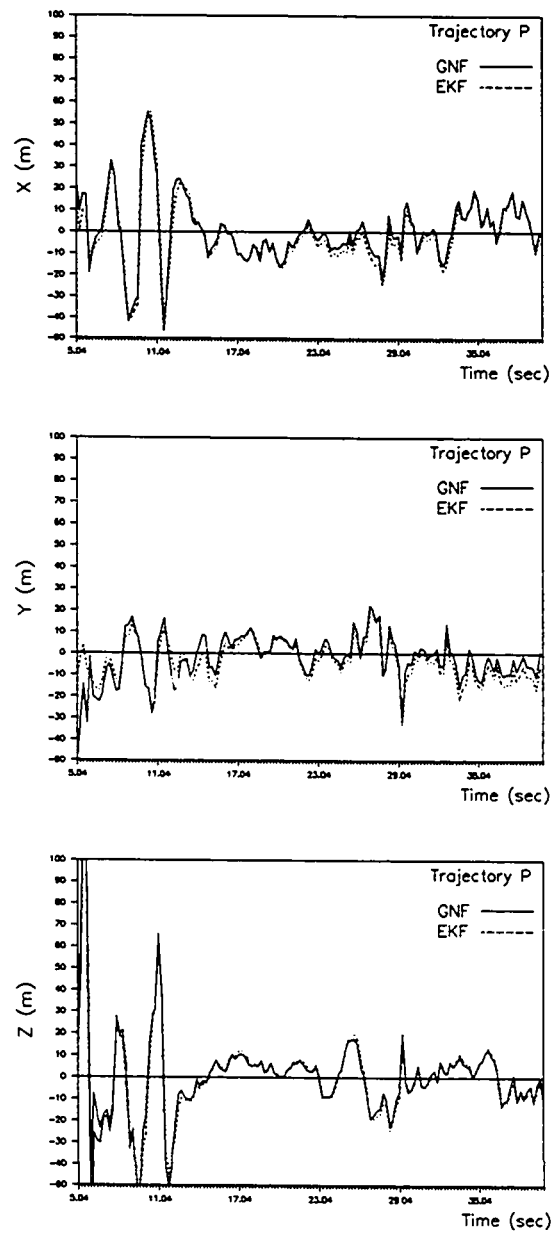


Figure 8.6p. Traj P Tracking Performance Comparison

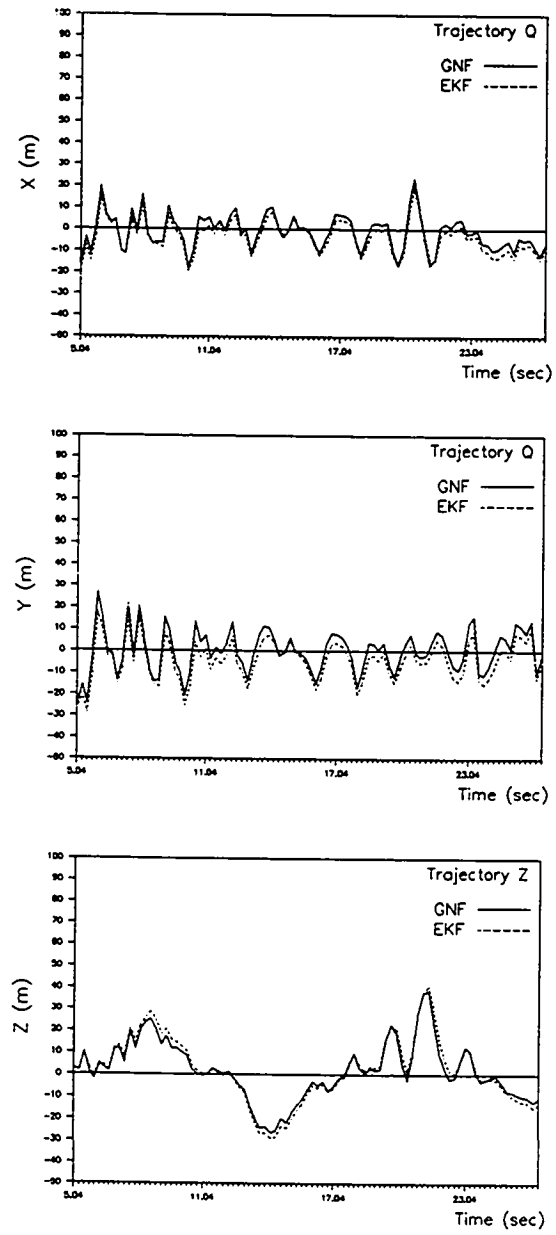


Figure 8.6q. Traj Q Tracking Performance Comparison

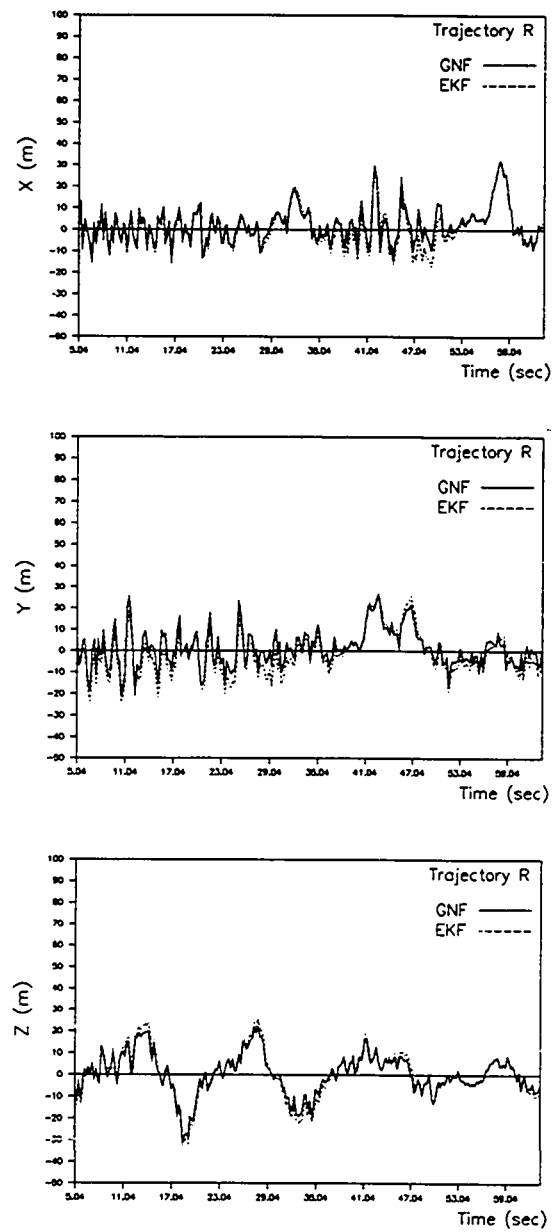


Figure 8.6r. Traj R Tracking Performance Comparison

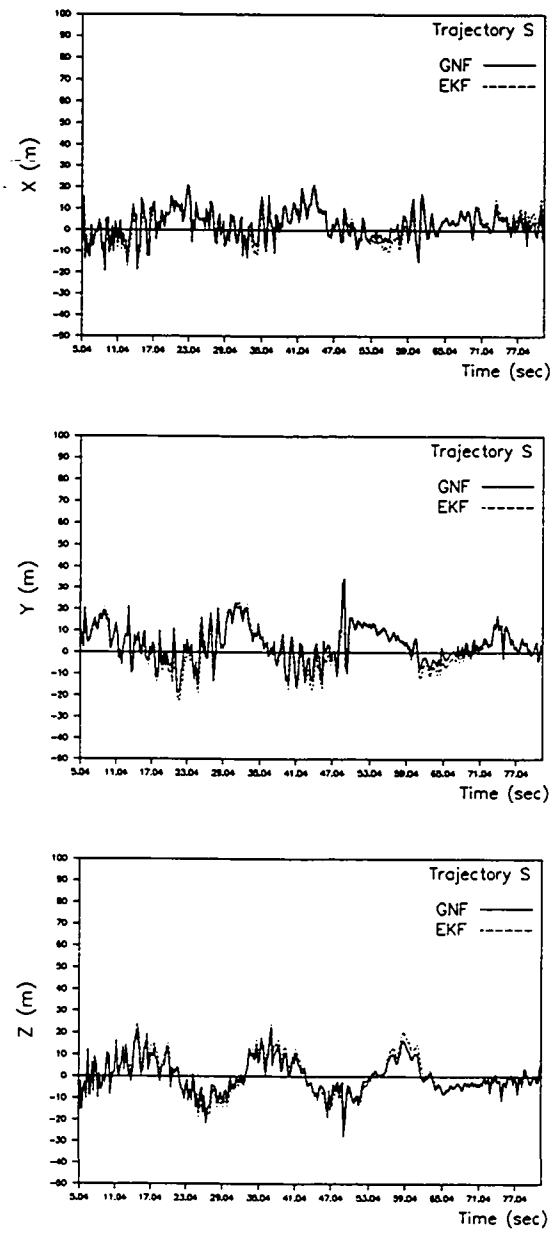


Figure 8.6s. Traj S Tracking Performance Comparison

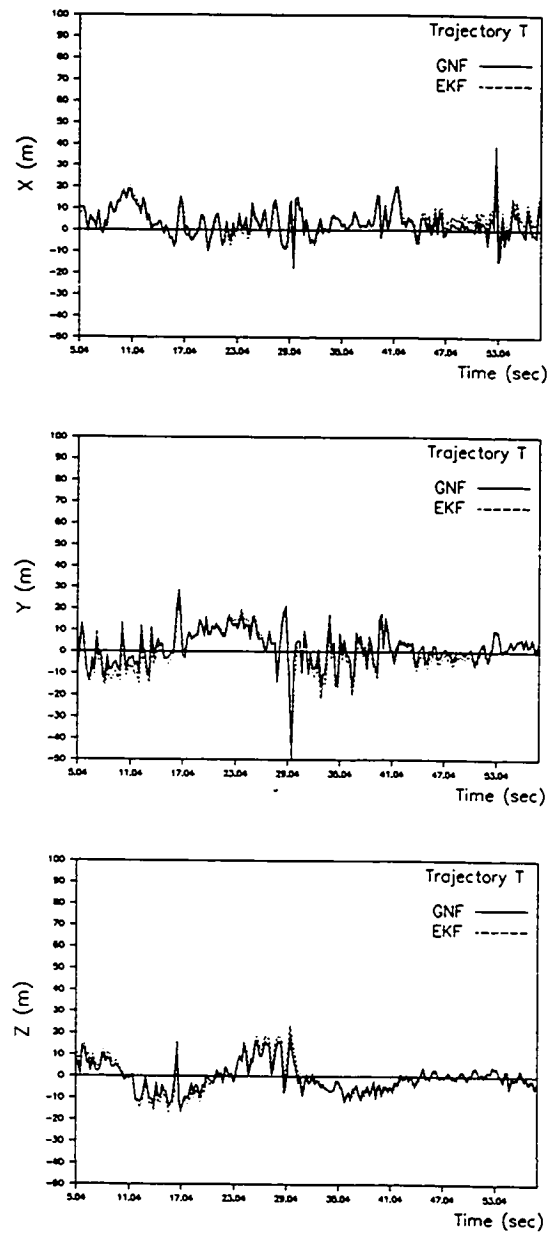


Figure 8.6t. Traj T Tracking Performance Comparison

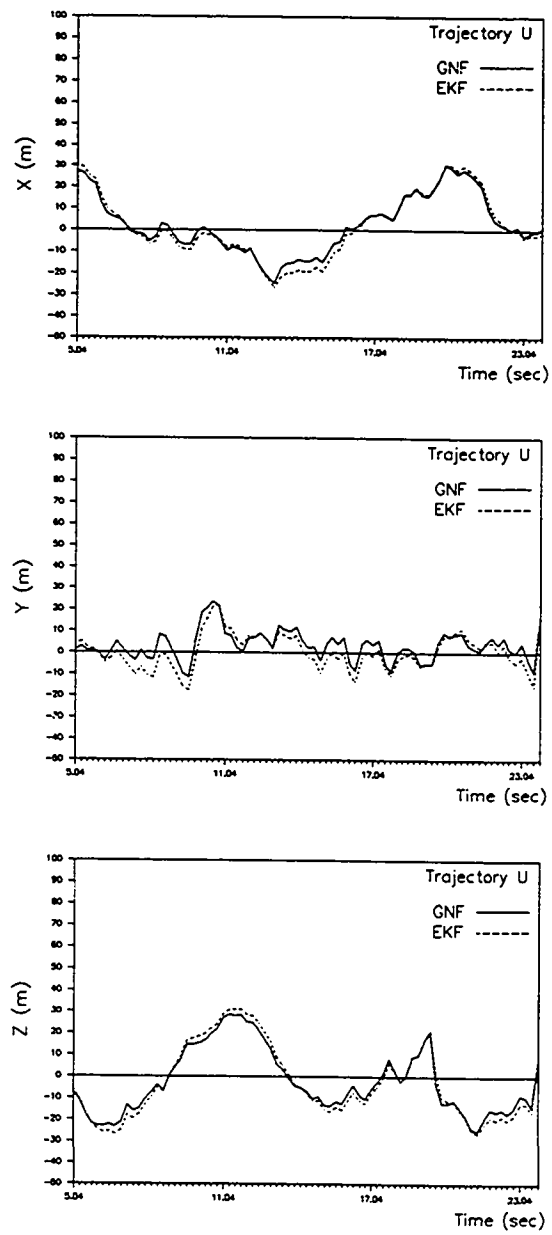


Figure 8.6u. Traj U Tracking Performance Comparison

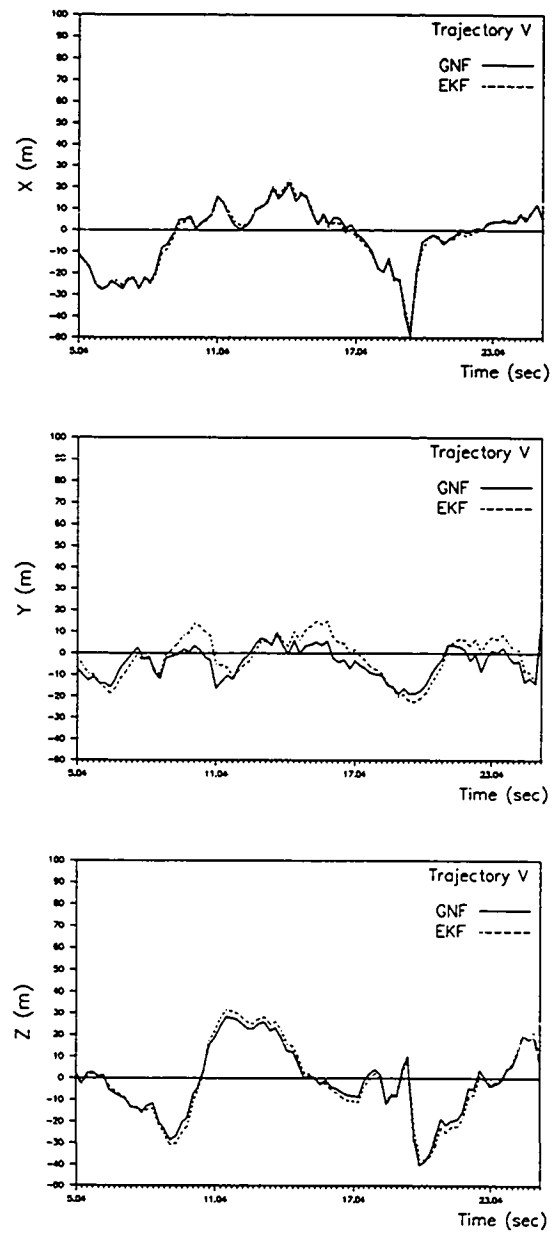


Figure 8.6v. Traj V Tracking Performance Comparison

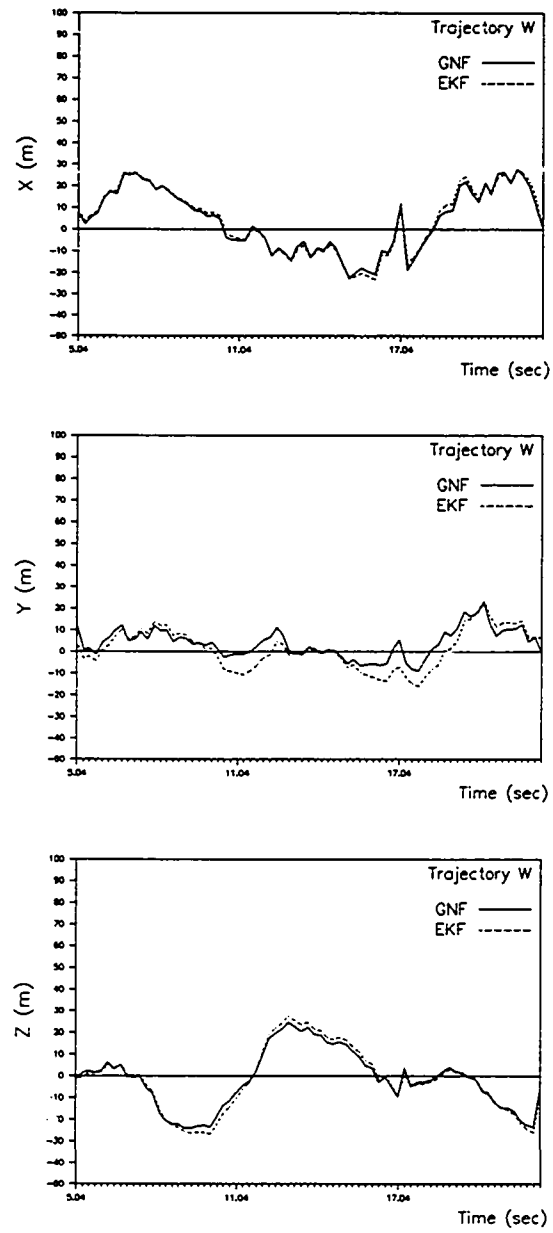


Figure 8.6w. Traj W Tracking Performance Comparison

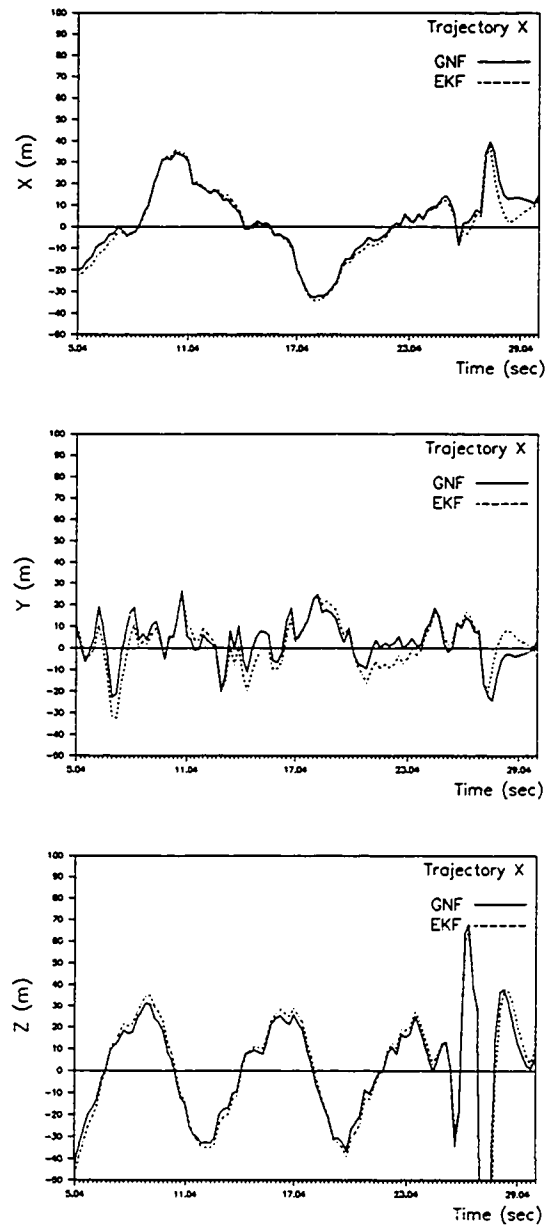


Figure 3.6x. Traj X Tracking Performance Comparison

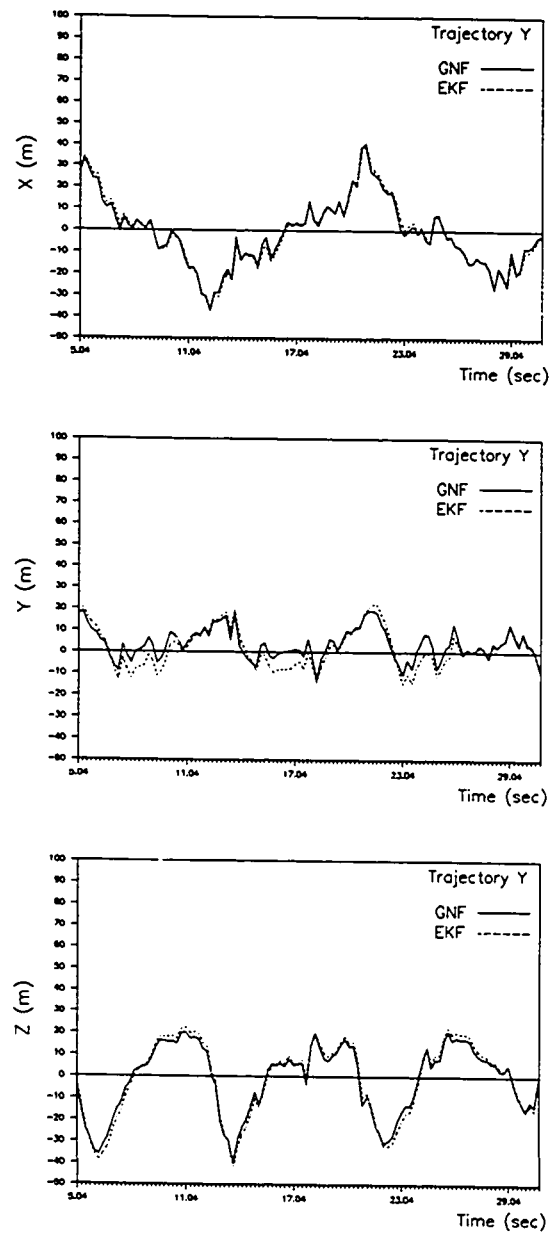


Figure 8.6y. Traj Y Tracking Performance Comparison

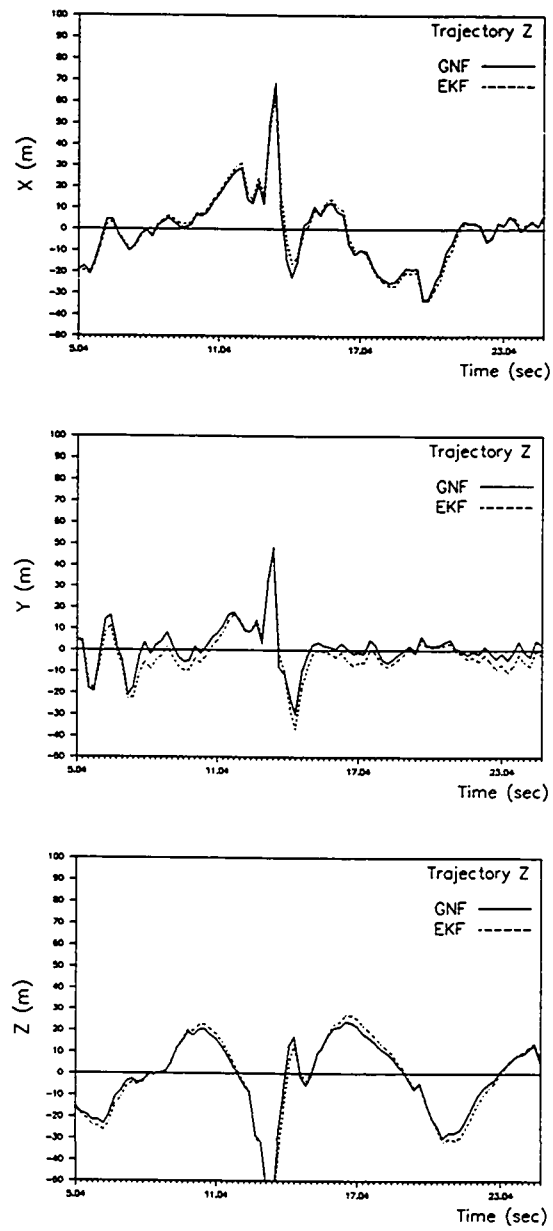


Figure 8.62. Traj Z Tracking Performance Comparison

Chapter 9

Conclusions

The geometric nonlinear filtering theory has been successfully applied to the problem of tracking a maneuvering aircraft.

The coordinated turn model developed in Chapter 2 is a more realistic model for describing the trajectories of a maneuvering aircraft than the constant velocity models currently in use. It is a highly coupled, nonlinear model which describes planar trajectories. The suitability of the coordinated turn model for use in a nonlinear filter (GNF and/or EKF) has been demonstrated.

The coordinated turn model cannot be transformed to observer canonical form. However, it can be transformed to a (useful) approximate observer canonical form as shown in Chapter 4, thus making the geometric nonlinear filtering theory applicable.

A procedure for calculating the GNF gains that insure stability of the estimation error is given in Chapter 5. The GNF gain, $K(\hat{z})$, is computed such that

$$A^*(\hat{z}) = A - K(\hat{z})C + B(\hat{z}) = Q^{-1}(\hat{z})(A - K_1C)Q(\hat{z}),$$

where $A - K_1C$ is stable. The time-variation of $A^*(\hat{z})$ is equivalent to the time-variation of $Q(\hat{z})$. This decomposition of $A^*(\hat{z})$

into a stable (and constant) part and a time-varying part leads to precise conditions for stability of the estimation error. The sufficient conditions for stability of the GNF is given in Chapter 6. Utilizing these conditions, an explicit calculation of domain of attraction for the aircraft tracking problem is given in Chapter 8. The EKF theory has no explicit conditions for stability.

The GNF gains are state-dependent but do not require the on-line integration of a Riccati equation as does the EKF. This translates into a substantial savings in computation time. The GNF runs about ten times faster than the EKF.

It was shown that the GNF and the EKF are stable for initial state errors at or near the nominal values. However, the GNF is shown to be stable for cases which may exist in practice where the EKF is not. It is difficult to find realistic cases in which the GNF will not converge. The EKF, on the other hand, did not converge for many of the cases in which the GNF converged nicely.

The tracking performance of both filters is comparable at the 1σ level of measurement noise. As expected, the performance of both filters drops as the noise increases. The GNF performance is better than the EKF performance at the 2σ level. The GNF performance drops off faster than the EKF performance so that at the 3σ level the EKF performs better.

The GNF is a practical solution to the problem of tracking a maneuvering aircraft utilizing a nonlinear filter. It has been shown to be effective in a "real-world" situation by successfully tracking the aircraft trajectories provided by Contraves [35].

Topics for future research include the development of *optimal* gains for the GNF and the incorporation of a roll maneuver detection scheme into the GNF.

Appendix A

Reference Frames

Inertial Reference Frame

In any dynamics problem there exists an inertial reference frame in which Newton's second law, describing the motion of a particle, is valid. The term inertial refers to the fact that the frame is fixed or in uniform rectilinear motion with respect to the distant stars. For aircraft tracking problems an earth-fixed frame, denoted by F_E , can be used as the inertial frame even though it is not inertially fixed, under the assumption that the maximum aircraft velocity is limited. To see this consider two reference frames, one earth-fixed and denoted by F_E and one earth centered, inertially fixed and denoted by F_I . Let $r = r_0 + s$ be the position vector of the aircraft center of mass (CM). Let the subscripts I, E denote a vector with respect to F_I , F_E and let L_{EI} denote the rotation matrix transforming an F_I -vector to an F_E -vector. The velocity and acceleration of CM with respect to F_I are $v_I = \dot{r}_I = \dot{r}_{0I} + \dot{s}_I$ and $a_I = \ddot{r}_{0I} + \ddot{s}_I$, respectively. So, the velocity of CM with respect to F_E is

$$v_E = L_{EI} \dot{r}_I = v_{0E} + \dot{s}_E + \omega_E^E \times s_E$$

where ω^E is the angular velocity of F_E relative to F_I ; thus ω^E denotes the earth's rotation. The term $\omega_E^E \times s_E$ is the transport velocity. The acceleration of CM is given by

$$a_E = L_{EI} a_I = a_{OE} + \ddot{s}_E + \dot{\omega}_E^E \times s_E + 2\omega_E^E \times \dot{s}_E + \omega_E^E \times (\omega_E^E \times s_E). \quad (A1)$$

The term a_{OE} is the acceleration of the origin of F_E ; the term \ddot{s}_E represents the acceleration of CM relative to the origin of F_E ; the term $\dot{\omega}_E^E \times s_E$ is the tangential acceleration due to the rotational acceleration of F_E ; the term $2\omega_E^E \times \dot{s}_E$ is the Coriolis acceleration and $\omega_E^E \times (\omega_E^E \times s_E)$ is the centripetal acceleration. The earth's rotation, ω^E , consists of the superposition of the earth's rotation on its axes, precession and nutation of its axes, rotation in its orbit about the sun, etc.. For atmospheric flight all are negligible except possibly for the rotation of the earth on its axis. However, for the velocity range corresponding to about Mach < 3 (approximately 800 m/sec depending on altitude) the rotation of the earth and the curvature of the earth can be neglected (Etkin [6], Chapter 5). Therefore, the following assumptions are made:

- (1) the earth's rotation is negligible
(i.e. $\omega^E = \dot{\omega}^E = 0$) ,
- (2) the earth's curvature is negligible , and
- (3) the maximum aircraft velocity is 800 m/sec.

Assumption (1) is applied to equation (A1) and yields

$$a_E = \ddot{s}_E. \quad (A2)$$

In other words, under assumption (1) the earth-fixed frame F_E is in fact an inertially fixed frame. Assumption (2), also known as the flat-earth assumption, is utilized in the description of the gravity acceleration acting on the aircraft. Thus, in the inertial reference frame the earth's gravity vector is

$$\mathbf{g}_E = -g \mathbf{e}_3^E, \text{ where } g = 9.805 \text{ m/sec}^2. \quad (\text{A3})$$

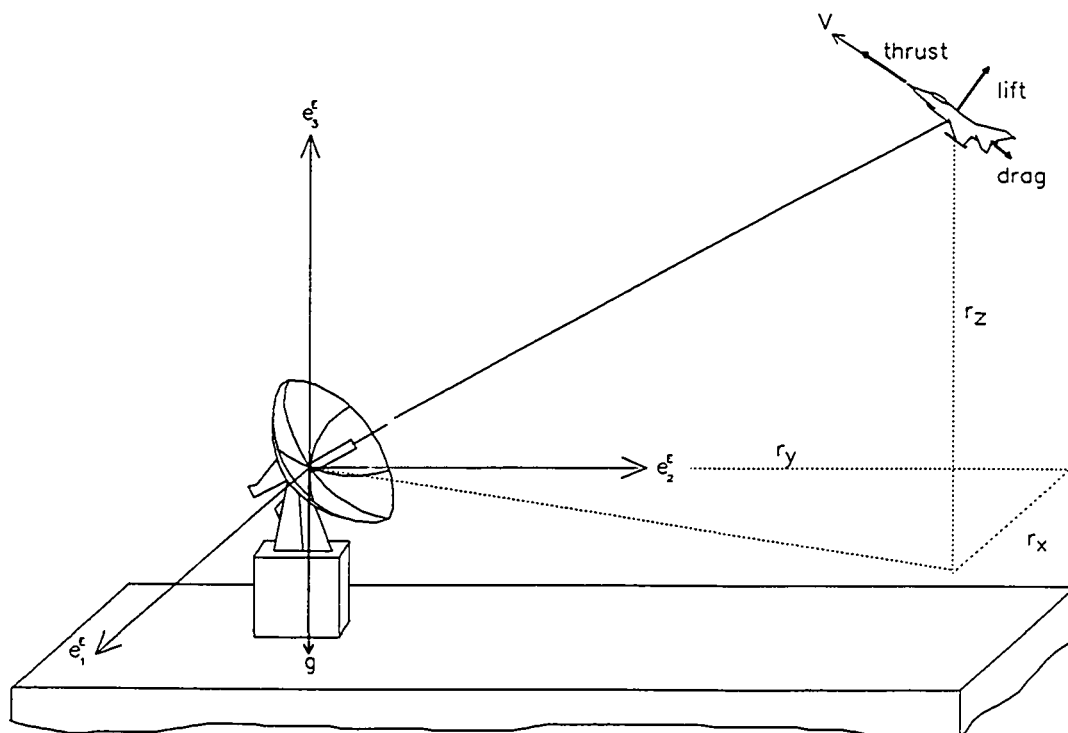


Figure A1. Inertial Reference Frame

A natural location for F_E is to affix it to the radar with the z-axis positive up (see Figure A1).

Body Reference Frame

The body axes frame, denoted by F_B , has its origin at the aircraft center of mass (CM) (see Figure A2). Thus e_1^B is along the aircraft longitudinal axis, positive in the direction of the velocity vector. The unit vector e_3^B is in the aircraft plane of symmetry and positive up, and the unit vector e_2^B completes the right-handed coordinate system. The angular velocity of F_B relative to F_E is $\omega^B = (p, q, r)$. The triple (e_1^B, e_2^B, e_3^B) will denote unit vectors along the body x, y and z axes, respectively.

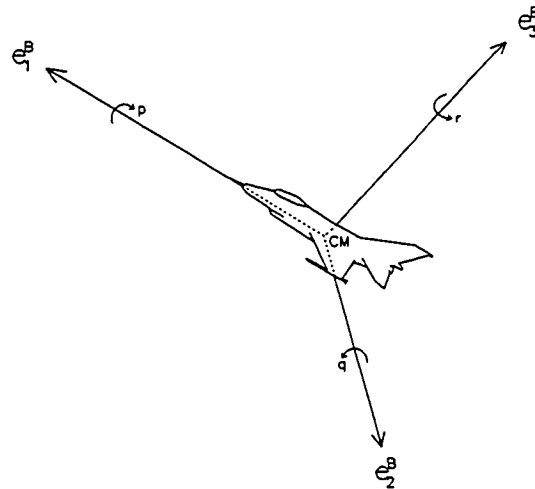


Figure A2. Body Reference Frame

Wind Reference Frame

The wind axes frame, denoted by F_W , has its origin at the aircraft center of mass (CM) (see Figure A3). Let (e_1^W, e_2^W, e_3^W) denote unit vectors along the wind x, y and z axes, respectively, where e_1^W is defined to be along the velocity vector of the

aircraft relative to the atmosphere. The velocity of the aircraft center of mass relative to the local atmosphere plays an important role in atmospheric flight, however, a common assumption (and one that is made here) is that the atmosphere is at rest. This assumption implies that the relative velocity is simply the aircraft velocity and changes in the aerodynamic accelerations (which are functions of the relative velocity) are not caused by atmospheric changes. Thus e_1^W is along the aircraft velocity vector, the unit vector e_3^W is in the aircraft plane of symmetry and positive up, and the unit vector e_2^W completes the right-handed coordinate system.

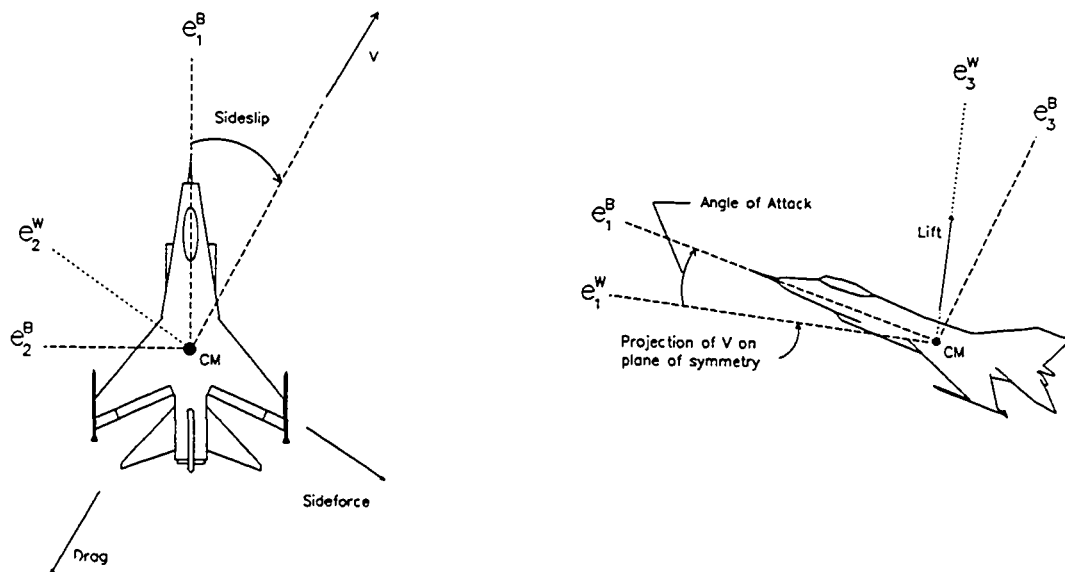


Figure A3. Wind Reference Frame

Appendix B

Theory of Nonlinear Geometric Estimation

The theory of nonlinear geometric estimation depends on the existence of a transformation of the given nonlinear system

$$\dot{x} = f(x)$$

$$y = h(x)$$

to observer canonical form

$$\dot{z} = Az + b(Cz)$$

$$y = Cz$$

where A and C are in Brunovsky canonical form. The existence of transformations has been studied by Krener and Isidori [17], Krener and Respondek [19], and Hunt, et al. [11]. The nonlinear geometric estimator design theory that follows assumes that a transformation exists. It appears that the family of nonlinear systems which can be linearized through use of a nonlinear transformation with output injection is not large. The aircraft maneuver model (2.28) cannot be transformed to observer canonical form. Therefore, other canonical forms (related to the observer canonical form) must be used in the design process. The GNF design presented in Chapters 4, 5, and 6 for the aircraft tracking problem is based on an approximate observer canonical form.

The design of a stable estimator for the nonlinear system is simplified by utilizing the observer canonical form. The design procedure that follows is valid for the scalar output case (extending readily to the multi-output case) and does not include output transformations. Krener and Respondek [19] consider output transformations.

B1. Lie Algebraic Notation

Consider the vector-valued functions $f:R^n \rightarrow R^n$ and $g:R^n \rightarrow R^n$ where f and g are vector fields in C^∞ . A vector field f on R^n is a function that assigns to each point p of R^n a tangent vector $f(p)$ to R^n at p . The Lie bracket of f and g is defined by

$$[f, g] := \frac{\partial f}{\partial x} g - \frac{\partial g}{\partial x} f \quad (B1)$$

where $\partial f / \partial x$ and $\partial g / \partial x$ are the Jacobian matrices of f and g , respectively. The notation for successive Lie brackets is

$$\begin{aligned} (ad^0 f, g) &= g \\ (ad^1 f, g) &= [f, g] \\ (ad^2 f, g) &= [f, [f, g]] \\ &\vdots \\ (ad^k f, g) &= [f, (ad^{k-1} f, g)]. \end{aligned} \quad (B2)$$

Consider a C^∞ function $h:R^n \rightarrow R$ with gradient dh . The Lie derivative of h with respect to the vector field f is defined by

$$L_f h := L_f(h) := \langle dh, f \rangle \quad (B3)$$

where $\langle \cdot, \cdot \rangle$ denotes the standard inner product in R^n . The notation for successive Lie derivatives is

$$\begin{aligned} L_f^0 h &= h \\ L_f^1 h &= L_f h \\ &\vdots \\ L_f^k h &= L_f(L_f^{k-1} h). \end{aligned} \tag{B4}$$

The Lie derivative of h with respect to the vector field $[f, g]$ is

$$L_{[f, g]} h = \langle dh, [f, g] \rangle = L_g L_f h - L_f L_g h. \tag{B5}$$

This is the Leibnitz formula. Furthermore, the Lie derivative of dh with respect to the vector field f is

$$L_f(dh) = dL_f h. \tag{B6}$$

B2. Transformation to Observer Canonical Form

Let the nonlinear system

$$\begin{aligned} \dot{x} &= f(x) \\ y &= h(x) \end{aligned} \tag{B7}$$

be given. We are looking for a bijective C^∞ transformation $T: R^n \rightarrow R^n$ such that (B7) is transformed into observer canonical form

$$\begin{aligned} \dot{z} &= Az + b(Cz) \\ y &= Cz \end{aligned} \tag{B8}$$

where A and C are in Brunovsky canonical form.

The first step is the computation of the partial derivative matrix, or Jacobian, of the transformation. Consider the scalar output case without output transformations. It is

possible to express the columns of the Jacobian matrix in terms of a single vector (Bestle and Zeitz [2]). To arrive at this result the time-derivative of

$$\mathbf{x} = \mathbf{T}(\mathbf{z}) \quad (\text{B9})$$

is substituted in (B7) to obtain

$$\dot{\mathbf{x}} = \mathbf{f}(\mathbf{x}) = \frac{\partial \mathbf{T}}{\partial \mathbf{z}} (\mathbf{A}\mathbf{z} + \mathbf{b}(\mathbf{C}\mathbf{z})) \quad (\text{B10})$$

where

$$\frac{\partial \mathbf{T}}{\partial \mathbf{z}} = \left(\frac{\partial \mathbf{T}}{\partial z_1} \quad \dots \quad \frac{\partial \mathbf{T}}{\partial z_n} \right)^T.$$

The partial derivative of (B10) with respect to z_k yields

$$\frac{\partial \mathbf{f}(\mathbf{x})}{\partial z_k} = \frac{\partial \frac{\partial \mathbf{T}}{\partial \mathbf{z}}}{\partial z_k} (\mathbf{A}\mathbf{z} + \mathbf{b}(\mathbf{C}\mathbf{z})) + \frac{\partial \mathbf{T}}{\partial \mathbf{z}} \frac{\partial}{\partial z_k} (\mathbf{A}\mathbf{z} + \mathbf{b}(\mathbf{C}\mathbf{z})). \quad (\text{B11})$$

From the left-hand side of (B11), using (B9) we obtain

$$\frac{\partial \mathbf{f}(\mathbf{x})}{\partial z_k} = \frac{\partial \mathbf{f}(\mathbf{T}(\mathbf{z}))}{\partial z_k} = \frac{\partial \mathbf{f}(\mathbf{x})}{\partial \mathbf{x}} \frac{\partial \mathbf{T}(\mathbf{z})}{\partial z_k}. \quad (\text{B12})$$

Similarly, for the first term on the right-hand side of (B11) it follows that

$$\frac{\partial \frac{\partial \mathbf{T}}{\partial \mathbf{z}}}{\partial z_k} (\mathbf{A}\mathbf{z} + \mathbf{b}(\mathbf{C}\mathbf{z})) = \frac{\partial \frac{\partial \mathbf{T}}{\partial z_k}}{\partial \mathbf{x}} \frac{\partial \mathbf{T}}{\partial \mathbf{z}} (\mathbf{A}\mathbf{z} + \mathbf{b}(\mathbf{C}\mathbf{z})) = \frac{\partial \frac{\partial \mathbf{T}}{\partial z_k}}{\partial \mathbf{x}} \mathbf{f}(\mathbf{x}). \quad (\text{B13})$$

Using the fact that \mathbf{A} and \mathbf{C} are matrices of the Brunovsky canonical form, the second term on the right-hand side of (B11) is

$$\frac{\partial \mathbf{T}}{\partial \mathbf{z}} \frac{\partial}{\partial z_k} (\mathbf{A}\mathbf{z} + \mathbf{b}(\mathbf{C}\mathbf{z})) = \begin{cases} \frac{\partial \mathbf{T}}{\partial \mathbf{z}} \frac{\partial \mathbf{b}(z_1)}{\partial z_1} & k = 1 \\ \frac{\partial \mathbf{T}}{\partial z_{k-1}} & k = 2, \dots, n. \end{cases} \quad (\text{B14})$$

Substituting (B12), (B13), and (B14) into (B11) yields

$$\frac{\partial T}{\partial z} \frac{\partial b(z_1)}{\partial z_1} = \frac{\partial f}{\partial x} \frac{\partial T}{\partial z_1} - \frac{\partial^2 T}{\partial z_1^2} f(x) \quad (B15)$$

and

$$\frac{\partial T}{\partial z_{k-1}} = \frac{\partial f}{\partial x} \frac{\partial T}{\partial z_k} - \frac{\partial^2 T}{\partial z_k^2} f(x) \quad k = 2, \dots, n. \quad (B16)$$

Utilizing the Lie notation introduced in Section B1, (B15) can be rewritten as

$$\frac{\partial T}{\partial z} \frac{\partial b(z_1)}{\partial z_1} = \left[f, \frac{\partial T}{\partial z_1} \right], \quad (B17)$$

and (B16) as

$$\frac{\partial T}{\partial z_{k-1}} = \left[f, \frac{\partial T}{\partial z_k} \right], \quad k = 2, \dots, n. \quad (B18)$$

Hence, it follows that

$$\frac{\partial T}{\partial z_{n-1}} = \left[f, \frac{\partial T}{\partial z_n} \right] = \left(ad^1 f, \frac{\partial T}{\partial z_n} \right),$$

and

$$\frac{\partial T}{\partial z_{n-2}} = \left[f, \frac{\partial T}{\partial z_{n-1}} \right] = \left[f, \left[f, \frac{\partial T}{\partial z_n} \right] \right] = \left(ad^2 f, \frac{\partial T}{\partial z_n} \right).$$

Therefore, in general

$$\frac{\partial T}{\partial z_{n-k+1}} = \left(ad^{k-1} f, \frac{\partial T}{\partial z_n} \right) \quad k = 2, \dots, n.$$

Thus, the Jacobian of the transformation is given by

$$\frac{\partial T}{\partial z} = \left[\left(ad^{n-1} f, \frac{\partial T}{\partial z_n} \right), \dots, \left(ad^2 f, \frac{\partial T}{\partial z_n} \right), \left(ad^1 f, \frac{\partial T}{\partial z_n} \right), \left(ad^0 f, \frac{\partial T}{\partial z_n} \right) \right], \quad (B19)$$

which shows that the Jacobian matrix can be generated using the single vector $\partial T / \partial z_n$. To obtain a formula for this vector, the partial derivative of the output, $y = h(x)$, with respect to z is computed:

$$\frac{\partial y}{\partial z} = \frac{\partial h}{\partial x} \frac{\partial T}{\partial z} = (1 \ 0 \ \dots \ 0). \quad (B20)$$

The last component of (B20) can be written as

$$\frac{\partial h}{\partial x} \frac{\partial T}{\partial z_n} = \langle dh, \frac{\partial T}{\partial z_n} \rangle = L_f^0(dh) \frac{\partial T}{\partial z_n} = 0. \quad (B21)$$

Using Leibnitz's formula, the second to last component of (B20) is

$$\begin{aligned} \frac{\partial h}{\partial x} \frac{\partial T}{\partial z_{n-1}} &= \langle dh, \left[f, \frac{\partial T}{\partial z_n} \right] \rangle = \langle d \langle dh, f \rangle, \frac{\partial T}{\partial z_n} \rangle - \langle d \langle dh, \frac{\partial T}{\partial z_n} \rangle, f \rangle \\ &= \langle d \langle dh, f \rangle, \frac{\partial T}{\partial z_n} \rangle = L_f^1(dh) \frac{\partial T}{\partial z_n} = 0. \end{aligned} \quad (B22)$$

Repeated use of Leibnitz's formula yields:

$$\begin{pmatrix} L_f^0(dh) \\ L_f^1(dh) \\ \vdots \\ L_f^{n-1}(dh) \end{pmatrix} \frac{\partial T}{\partial z_n} = \begin{pmatrix} 0 \\ \vdots \\ 0 \\ 1 \end{pmatrix}, \quad (B23)$$

where the matrix

$$\Theta(x) = \begin{pmatrix} L_f^0(dh)(x) \\ L_f^1(dh)(x) \\ \vdots \\ L_f^{n-1}(dh)(x) \end{pmatrix}$$

is the observability matrix. Thus, $\partial T / \partial z_n$ is the last column of the inverse of the observability matrix. The Jacobian matrix of the transformation (B19) can now be computed using (B23). Integrating (B19) yields, in principle, the desired transformation T.

B3. Stable Estimator Design

Consider the nonlinear estimator (Kou et. al. [14] and Thau [31])

$$\dot{\hat{x}} = f(\hat{x}) + K^*(\hat{x})(y - h(\hat{x})) \quad (\text{B24})$$

associated with the nonlinear system (B7). The measurement is $y = x_1$. The objective is to design the gains, $K^*(\hat{x})$, so that the estimation error approaches zero asymptotically. The method presented here is based on Bestle and Zietz [2]. This method guarantees asymptotic stability of the estimation error without regard to state and measurement noises. The interesting characteristic of the method is that the transformation to observer canonical form is never actually computed although its existence is assumed.

Consider the relationship

$$\hat{x} = T(\hat{z})$$

which transforms (B24) into

$$\dot{\hat{z}} = A\hat{z} + b(C\hat{z}) + \frac{\partial T^{-1}}{\partial \hat{z}} K^*(\hat{z})(y - \hat{z}_1).$$

Define the nonlinear gain

$$K(\hat{z}) = \frac{\partial T^{-1}}{\partial \hat{z}} K^*(\hat{z}).$$

Then with the estimation error defined by

$$e := \hat{z} - z,$$

the differential equation describing the estimation error is

$$\dot{e} = (A - K(\hat{z})C)e + b(C\hat{z}) - b(Cz). \quad (\text{B25})$$

If the output injection term in (B25) is linearized about the reconstructed trajectory using a Taylor series expansion, (B25) can be written as

$$\dot{e} = (A - K(\hat{z})C)e + \left. \frac{\partial b}{\partial z_1} \right|_{z_1} Ce + \dots$$

Choosing

$$K(\hat{z}) = p + \frac{\partial b}{\partial \hat{z}_1} \quad (B26)$$

and assuming that the output injection term has a 'small' second derivative leads to the approximate estimation error equation

$$\dot{e} = (A - pC)e. \quad (B27)$$

The vector p is composed of the coefficients of the desired characteristic polynomial. Thus if the desired characteristic polynomial is

$$p_{\text{desired}} = p_0 + p_1 s + p_2 s^2 + \dots + p_{n-1} s^{n-1} + s^n,$$

$$p = \begin{pmatrix} p_{n-1} \\ p_{n-2} \\ \vdots \\ \vdots \\ p_2 \\ p_1 \\ p_0 \end{pmatrix}.$$

The estimator gains, $K'(\hat{z})$, of the estimator (B24) are

$$K'(\hat{z}) = \frac{\partial T}{\partial \hat{z}} \left(p + \frac{\partial b}{\partial \hat{z}_1} \right). \quad (B28)$$

Using (B15) and (B19), the gains (B28) are computed:

$$K^*(\hat{x}) = K^*(x)|_{\hat{x}} = \left(\frac{\partial T}{\partial z} p + \frac{\partial f}{\partial x} \frac{\partial T}{\partial z_1} - \frac{\partial \frac{\partial T}{\partial z_1}}{\partial x f(x)} \right) |_{\hat{x}}. \quad (B29)$$

All the terms in the above gains calculation can be computed without explicit knowledge of the transformation T .

Appendix C

Proof of Theorem 5.1

Theorem 5.1 (Scalar Output): Suppose that the desired characteristic polynomial of $A^*(z)$ is

$$\rho_{des} = \rho_n + \rho_{n-1}S + \dots + \rho_1 S^{n-1} + S^n.$$

Associated with the desired characteristic polynomial, define the vector

$$K_1 = \begin{pmatrix} \rho_1 \\ \rho_2 \\ \vdots \\ \rho_n \end{pmatrix}.$$

Define

$$K(z) := B_1(z) + Q^{-1}(z)[K_1 + R(z)] \quad (C1)$$

where

$$Q(z) = Q_a(z)\bar{\theta}(z),$$

then it follows that

$$(A^*(z) = A - K(z)C + B(z) = Q^{-1}(z)(A - K_1 C)Q(z))$$

and its characteristic polynomial is ρ_{des} .

proof:

Suppose that the conditions

$$CQ^{-1}(z) = C, \text{ and} \quad (C2)$$

$$Q(z)(A + B^*(z))Q^{-1}(z) - R(z)C = A, \quad (C3)$$

are true. Substituting (C1) into $A^*(z) = A - K(z)C + B(z)$ and utilizing the conditions (C2) and (C3) yields

$$A - K(z)C + B(z) = Q^{-1}(z)(A - K_1 C)Q(z).$$

It follows that the characteristic polynomial of $A - K(z)C + B(z)$ is equal to the characteristic polynomial of $A - K_1 C$, as desired. So, all that needs to be shown is that conditions (C2) and (C3) are true.

Condition (C2):

Since

$$CQ_1(z) = [1 \ 0 \ \dots \ 0] \begin{bmatrix} 1 & 0 & 0 & 0 & \dots & 0 \\ -a_{n-1}(z) & 1 & 0 & 0 & \dots & 0 \\ -a_{n-2}(z) & -a_{n-1}(z) & \cdot & 0 & \dots & 0 \\ \cdot & -a_{n-2}(z) & -a_{n-1}(z) & \cdot & & \cdot \\ \cdot & \cdot & \cdot & & \cdot & 0 \\ -a_1(z) & -a_2(z) & -a_3(z) & \dots & -a_{n-1}(z) & 1 \end{bmatrix} = [1 \ 0 \ \dots \ 0] = C$$

it follows that

$$CQ(z) = C\bar{\Theta}(z) = [1 \ 0 \ \dots \ 0] \begin{bmatrix} C \\ C(A + B^*(z)) \\ \cdot \\ \cdot \\ \cdot \\ \cdot \\ C(A + B^*(z))^{n-1} \end{bmatrix} = C.$$

Therefore,

$$CQ(z) = C \Rightarrow CQ^{-1}(z) = C.$$

Condition (C3):

Condition (C3) can be rewritten as

$$Q(z)(A + B^*(z)) + R(z)C = A Q(z).$$

Direct calculation of $Q(z)(A + B^*(z)) + R(z)C$ yields,

$$\begin{bmatrix} 1 & 0 & 0 & 0 & \dots & 0 \\ -a_{n-1}(z) & 1 & 0 & 0 & \dots & 0 \\ -a_{n-2}(z) & -a_{n-1}(z) & \cdot & 0 & \dots & 0 \\ \cdot & -a_{n-2}(z) & -a_{n-1}(z) & \cdot & \cdot & \cdot \\ \cdot & \cdot & \cdot & \cdot & \cdot & 0 \\ -a_1(z) & -a_2(z) & -a_3(z) & \dots & -a_{n-1}(z) & 1 \end{bmatrix} \begin{bmatrix} C(A+B^*(z)) \\ C(A+B^*(z))^2 \\ \cdot \\ \cdot \\ \cdot \\ C(A+B^*(z))^n \end{bmatrix} + \begin{bmatrix} -a_{n-1}(z) & 0 & \dots & 0 \\ -a_{n-2}(z) & 0 & \dots & 0 \\ \cdot & \cdot & \cdot & \cdot \\ \cdot & \cdot & \cdot & \cdot \\ \cdot & \cdot & \cdot & \cdot \\ -a_1(z) & 0 & \dots & 0 \\ 0 & 0 & \dots & 0 \end{bmatrix}$$

$$= \begin{bmatrix} C(A+B^*(z)) - a_{n-1}(z)C \\ -a_{n-1}(z)C(A+B^*(z)) + C(A+B^*(z))^2 - a_{n-2}(z)C \\ \cdot \\ \cdot \\ -a_2(z)C(A+B^*(z)) - \dots - a_{n-1}(z)C(A+B^*(z))^{n-2} + C(A+B^*(z))^{n-1} - a_1(z)C \\ -a_1(z)C(A+B^*(z)) - \dots - a_n(z)C(A+B^*(z))^{n-1} + C(A+B^*(z))^n \end{bmatrix}$$

$$= \begin{bmatrix} C(A+B^*(z)) - a_{n-1}(z)C \\ -a_{n-1}(z)C(A+B^*(z)) + C(A+B^*(z))^2 - a_{n-2}(z)C \\ \cdot \\ \cdot \\ -a_2(z)C(A+B^*(z)) - \dots - a_{n-1}(z)C(A+B^*(z))^{n-2} + C(A+B^*(z))^{n-1} - a_1(z)C \\ 0 \end{bmatrix}$$

$$= \begin{bmatrix} 0 & 1 & 0 & 0 & \dots & 0 \\ 0 & 0 & 1 & 0 & \dots & 0 \\ \cdot & \cdot & \cdot & \cdot & \cdot & \cdot \\ \cdot & \cdot & \cdot & \cdot & \cdot & 0 \\ \cdot & \cdot & \cdot & \cdot & \cdot & 1 \\ 0 & 0 & 0 & 0 & 0 & 0 \end{bmatrix} \begin{bmatrix} 1 & 0 & 0 & 0 & \dots & 0 \\ -a_{n-1}(z) & 1 & 0 & 0 & \dots & 0 \\ -a_{n-2}(z) & -a_{n-1}(z) & \cdot & 0 & \dots & 0 \\ \cdot & -a_{n-2}(z) & -a_{n-1}(z) & \cdot & \cdot & \cdot \\ \cdot & \cdot & \cdot & \cdot & \cdot & 0 \\ -a_1(z) & -a_2(z) & -a_3(z) & \dots & -a_{n-1}(z) & 1 \end{bmatrix} \begin{bmatrix} C \\ C(A+B^*(z)) \\ \cdot \\ \cdot \\ \cdot \\ C(A+B^*(z))^{n-1} \end{bmatrix}$$

$$= A Q_a(z) \bar{\Theta}(z) = A Q(z).$$

In the above development, use is made of the fact that since, by assumption, $\text{rank } \bar{\Theta}(z) = n, \forall t \geq t_0$, there exist real-valued functions $a_i(z)$ such that

$$C(A+B^*(z))^n = a_1(z)[C(A+B^*(z))] + a_{n-1}(z)[C(A+B^*(z))^{n-1}].$$

Appendix D

GNF Gain Calculations

The various terms needed to calculate the GNF gains are presented here. For reference, see Figure 5.1. Define the functions

$$a_x(\hat{z}) = \hat{z}_3 - g_1,$$

$$a_{yz}(\hat{z}) = (\hat{z}_7 - g_2)\sin\hat{\phi} + (\hat{z}_{11} - g_3)\cos\hat{\phi},$$

$$\xi_1(\hat{z}) = (\cos\theta(\hat{z})a_x(\hat{z}) + \sin\theta(\hat{z})a_{yz}(\hat{z}))/v(\hat{z}),$$

$$\xi_2(\hat{z}) = (\sin\theta(\hat{z})a_x(\hat{z}) - \cos\theta(\hat{z})a_{yz}(\hat{z}))/v(\hat{z}),$$

$$\xi_3(\hat{z}) = (\xi_1(\hat{z})\cos\theta(\hat{z}) + \xi_2(\hat{z})\sin\theta(\hat{z}))/v(\hat{z}) = a_x(\hat{z})/v^2(\hat{z}),$$

$$\xi_4(\hat{z}) = (\xi_1(\hat{z})\sin\theta(\hat{z}) - \xi_2(\hat{z})\cos\theta(\hat{z}))/v(\hat{z}) = a_{yz}(\hat{z})/v^2(\hat{z}),$$

where

$\hat{\phi}$ is the estimated aircraft roll angle,

$$v^2(\hat{z}) = \hat{z}_2^2 + (\hat{z}_6\sin\hat{\phi} + \hat{z}_{10}(t)\cos\hat{\phi})^2,$$

$$\cos\theta(\hat{z}) = \hat{z}_2/v(\hat{z}), \text{ and}$$

$$\sin\theta(\hat{z}) = -(\hat{z}_6(t)\sin\hat{\phi} + \hat{z}_{10}\cos\hat{\phi})/v(\hat{z}).$$

The nonzero elements of $B(\hat{z})$ are

$$B_{2,2}(\hat{z}) = \sin\theta(\hat{z})\xi_2(\hat{z})$$

$$B_{2,3}(\hat{z}) = \cos\theta(\hat{z}) - 1$$

$$B_{2,6}(\hat{z}) = \cos\theta(\hat{z})\sin\hat{\phi}\xi_2(\hat{z})$$

$$B_{2,7}(\hat{z}) = \sin\hat{\phi}\sin\theta(\hat{z})$$

$$B_{2,10}(\hat{z}) = \cos\theta(\hat{z})\cos\hat{\phi}\xi_2(\hat{z})$$

$$B_{2,11}(\hat{z}) = \cos\hat{\phi}\sin\theta(\hat{z})$$

$$B_{6,2}(\hat{z}) = \sin\theta(\hat{z})\sin\hat{\phi}\xi_1(\hat{z})$$

$$B_{6,3}(\hat{z}) = -\sin\hat{\phi}\sin\theta(\hat{z})$$

$$B_{6,6}(\hat{z}) = \cos\theta(\hat{z})\sin^2\hat{\phi}\xi_1(\hat{z})$$

$$B_{6,7}(\hat{z}) = \sin^2\hat{\phi}(\cos\theta(\hat{z}) - 1)$$

$$B_{6,10}(\hat{z}) = \cos\theta(\hat{z})\cos\hat{\phi}\sin\hat{\phi}\xi_1(\hat{z})$$

$$B_{6,11}(\hat{z}) = \cos\hat{\phi}\sin\hat{\phi}(\cos\theta(\hat{z}) - 1)$$

$$B_{10,2}(\hat{z}) = \sin\theta(\hat{z})\cos\hat{\phi}\xi_1(\hat{z})$$

$$B_{10,3}(\hat{z}) = -\cos\hat{\phi}\sin\theta(\hat{z})$$

$$B_{10,6}(\hat{z}) = \cos\theta(\hat{z})\cos\hat{\phi}\sin\hat{\phi}\xi_1(\hat{z})$$

$$B_{10,7}(\hat{z}) = \cos\hat{\phi}\sin\hat{\phi}(\cos\theta(\hat{z}) - 1)$$

$$B_{10,10}(\hat{z}) = \cos\theta(\hat{z})\cos^2\hat{\phi}\xi_1(\hat{z})$$

$$B_{10,11}(\hat{z}) = \cos^2\hat{\phi}(\cos\theta(\hat{z}) - 1).$$

The nonzero elements of $\bar{\Theta}(\hat{z})$ are

$$\bar{\Theta}_{3,2}(\hat{z}) = \sin\theta(\hat{z})\xi_2(\hat{z})$$

$$\bar{\Theta}_{3,3}(\hat{z}) = \bar{\Theta}_{4,4}(\hat{z}) = \cos\theta(\hat{z})$$

$$\bar{\Theta}_{3,6}(\hat{z}) = \bar{\Theta}_{4,8}(\hat{z}) = \cos\theta(\hat{z})\sin\hat{\phi}\xi_2(\hat{z})$$

$$\bar{\Theta}_{3,7}(\hat{z}) = -\bar{\Theta}_{7,3}(\hat{z}) = -\bar{\Theta}_{8,4}(\hat{z}) = \sin\theta(\hat{z})\sin\hat{\phi}$$

$$\bar{\Theta}_{3,10}(\hat{z}) = \cos\theta(\hat{z})\cos\hat{\phi}\xi_2(\hat{z})$$

$$\bar{\Theta}_{3,11}(\hat{z}) = \bar{\Theta}_{4,12}(\hat{z}) = -\bar{\Theta}_{11,3}(\hat{z}) = -\bar{\Theta}_{12,4}(\hat{z}) = \sin\theta(\hat{z})\cos\hat{\phi}$$

$$\bar{\Theta}_{4,2}(\hat{z}) = \sin\theta(\hat{z})\xi_2(\hat{z})\xi_3(\hat{z})$$

$$\bar{\Theta}_{4,6}(\hat{z}) = \cos\theta(\hat{z})\sin\hat{\phi}\xi_2(\hat{z})\xi_3(\hat{z})$$

$$\bar{\Theta}_{4,7}(\hat{z}) = \sin\hat{\phi}\xi_2(\hat{z})$$

$$\bar{\Theta}_{4,10}(\hat{z}) = \cos\theta(\hat{z})\cos\hat{\phi}\xi_2(\hat{z})\xi_3(\hat{z})$$

$$\bar{\Theta}_{4,11}(\hat{z}) = \cos\hat{\phi}\xi_2(\hat{z})$$

$$\bar{\Theta}_{7,2}(\hat{z}) = \sin\theta(\hat{z})\sin\hat{\phi}\xi_1(\hat{z})$$

$$\bar{\Theta}_{7,6}(\hat{z}) = \cos\theta(\hat{z})\sin^2\hat{\phi}\xi_1(\hat{z})$$

$$\bar{\Theta}_{7,7}(\hat{z}) = \bar{\Theta}_{8,8}(\hat{z}) = 1 + \sin^2\hat{\phi}(\cos\theta(\hat{z}) - 1)$$

$$\bar{\Theta}_{7,10}(\hat{z}) = \bar{\Theta}_{11,6}(\hat{z}) = \cos\theta(\hat{z})\cos\hat{\phi}\sin\hat{\phi}\xi_1(\hat{z})$$

$$\bar{\Theta}_{7,11}(\hat{z}) = \bar{\Theta}_{8,12}(\hat{z}) = \bar{\Theta}_{11,7}(\hat{z}) = \bar{\Theta}_{12,8}(\hat{z}) = \cos\hat{\phi}\sin\hat{\phi}(\cos\theta(\hat{z}) - 1)$$

$$\bar{\Theta}_{8,2}(\hat{z}) = \sin\theta(\hat{z})\sin\hat{\phi}\xi_1(\hat{z})\xi_3(\hat{z})$$

$$\bar{\Theta}_{8,6}(\hat{z}) = \cos\theta(\hat{z})\sin^2\hat{\phi}\xi_1(\hat{z})\xi_3(\hat{z})$$

$$\bar{\Theta}_{8,7}(\hat{z}) = \sin^2\hat{\phi}\xi_1(\hat{z})$$

$$\bar{\Theta}_{8,10}(\hat{z}) = \bar{\Theta}_{12,6}(\hat{z}) = \cos\theta(\hat{z})\cos\hat{\phi}\sin\hat{\phi}\xi_1(\hat{z})\xi_3(\hat{z})$$

$$\bar{\Theta}_{8,11}(\hat{z}) = \bar{\Theta}_{12,7}(\hat{z}) = \cos\hat{\phi}\sin\hat{\phi}\xi_1(\hat{z})$$

$$\bar{\Theta}_{11,2}(\hat{z}) = \sin\theta(\hat{z})\cos\hat{\phi}\xi_1(\hat{z})$$

$$\bar{\Theta}_{11,10}(\hat{z}) = \cos\theta(\hat{z})\cos^2\hat{\phi}\xi_1(\hat{z})$$

$$\bar{\Theta}_{11,12}(\hat{z}) = \bar{\Theta}_{12,12}(\hat{z}) = 1 + \cos^2\hat{\phi}(\cos\theta(\hat{z}) - 1)$$

$$\bar{\Theta}_{12,2}(\hat{z}) = \sin\theta(\hat{z})\cos\hat{\phi}\xi_1(\hat{z})\xi_3(\hat{z})$$

$$\bar{\Theta}_{12,10}(\hat{z}) = \cos\theta(\hat{z})\cos^2\hat{\phi}\xi_1(\hat{z})\xi_3(\hat{z})$$

$$\bar{\Theta}_{12,11}(\hat{z}) = \cos^2\hat{\phi}\xi_1(\hat{z}).$$

The terms needed to calculate $R(\hat{z})$ and $Q_{\hat{z}}(\hat{z})$ are

$$a_{112}(\hat{z}) = \sin\theta(\hat{z})(-\alpha_1 \cos\theta(\hat{z})\xi_4(\hat{z}) + \sin\theta(\hat{z})(\alpha_3 \cos^2\hat{\phi} + \alpha_2 \sin^2\hat{\phi})\xi_3(\hat{z}))$$

$$a_{113}(\hat{z}) = \sin\theta(\hat{z})\xi_2(\hat{z}) - \alpha_1 \cos^2\theta(\hat{z}) - \sin^2\theta(\hat{z})(\alpha_3 \cos^2\hat{\phi} + \alpha_2 \sin^2\hat{\phi})$$

$$a_{212}(\hat{z}) = \cos\theta(\hat{z})\sin\hat{\phi}(-\alpha_1 \cos\theta(\hat{z})\xi_4(\hat{z}) \\ + \sin\theta(\hat{z})(\alpha_3 \cos^2\hat{\phi} + \alpha_2 \sin^2\hat{\phi})\xi_3(\hat{z}))$$

$$a_{213}(\hat{z}) = \sin\theta(\hat{z})\sin\hat{\phi}(\alpha_1 \cos\theta(\hat{z}) - \alpha_3 \cos^2\hat{\phi}(\cos\theta(\hat{z}) - 1) \\ - \alpha_2(\cos\theta(\hat{z}) - \cos^2\hat{\phi}(\cos\theta(\hat{z}) - 1)) + \xi_2(\hat{z})\cos\theta(\hat{z})\sin\hat{\phi})$$

$$a_{312}(\hat{z}) = \cos\hat{\phi}\cos\theta(\hat{z})(\alpha_1 \cos\theta(\hat{z})\xi_4(\hat{z}) \\ + \sin\theta(\hat{z})(\alpha_3 \cos^2\hat{\phi} + \alpha_2 \sin^2\hat{\phi})\xi_3(\hat{z}))$$

$$a_{313}(\hat{z}) = \sin\theta(\hat{z})\cos\hat{\phi}(\alpha_1 \cos\theta(\hat{z}) - \alpha_2 \sin^2\hat{\phi}(\cos\theta(\hat{z}) - 1) \\ - \alpha_3(\cos\theta(\hat{z}) - \sin^2\hat{\phi}(\cos\theta(\hat{z}) - 1)) + \xi_2(\hat{z})\cos\theta(\hat{z})\cos\hat{\phi})$$

$$a_{122}(\hat{z}) = \sin\theta(\hat{z})\sin\hat{\phi}(-\alpha_1 \sin\theta(\hat{z})\xi_4(\hat{z}) + (\alpha_3 \cos^2\hat{\phi}(\cos\theta(\hat{z}) - 1) \\ + \alpha_2(1 + \sin^2\hat{\phi}(\cos\theta(\hat{z}) - 1)))\xi_3(\hat{z}))$$

$$a_{123}(\hat{z}) = \sin\theta(\hat{z})\sin\hat{\phi}(\alpha_1 \cos\theta(\hat{z}) - \alpha_3 \cos^2\hat{\phi}(\cos\theta(\hat{z}) - 1) \\ - \alpha_2(1 + \sin^2\hat{\phi}(\cos\theta(\hat{z}) - 1)) + \xi_1(\hat{z}))$$

$$a_{222}(\hat{z}) = \cos\theta(\hat{z})\sin^2\hat{\phi}(-\alpha_1 \sin\theta(\hat{z})\xi_4(\hat{z}) + (\alpha_3 \cos^2\hat{\phi}(\cos\theta(\hat{z}) - 1) \\ + \alpha_2(1 + \sin^2\hat{\phi}(\cos\theta(\hat{z}) - 1)))\xi_3(\hat{z}))$$

$$a_{223}(\hat{z}) = -\alpha_1 \sin^2\theta(\hat{z})\sin^2\hat{\phi} - \alpha_3 \cos^2\hat{\phi}\sin^2\hat{\phi}(\cos\theta(\hat{z}) - 1)^2 - \alpha_2(\cos\theta(\hat{z}) \\ - \cos^2\hat{\phi}(\cos\theta(\hat{z}) - 1))(1 + \sin^2\hat{\phi}(\cos\theta(\hat{z}) - 1)) + \xi_1(\hat{z})\cos\theta(\hat{z})\sin^2\hat{\phi}$$

$$a_{322}(\hat{z}) = \cos\theta(\hat{z})\sin\hat{\phi}\cos\hat{\phi}(\alpha_1 \sin\theta(\hat{z})\xi_4(\hat{z}) + (\alpha_3 \cos^2\hat{\phi}(\cos\theta(\hat{z}) - 1) \\ + \alpha_2(1 + \sin^2\hat{\phi}(\cos\theta(\hat{z}) - 1)))\xi_3(\hat{z}))$$

$$a_{323}(\hat{z}) = \cos\hat{\phi}\sin\hat{\phi}(-\alpha_1 \sin^2\theta(\hat{z}) - (\cos\theta(\hat{z}) - 1)(\alpha_3(\cos\theta(\hat{z}) \\ - \sin^2\hat{\phi}(\cos\theta(\hat{z}) - 1)) + \alpha_2(1 + \sin^2\hat{\phi}(\cos\theta(\hat{z}) - 1))) + \xi_1(\hat{z})\cos\theta(\hat{z}))$$

$$a_{132}(\hat{z}) = \sin\theta(\hat{z})\cos\hat{\phi}(\alpha_1 \sin\theta(\hat{z})\xi_4(\hat{z}) + (\alpha_2 \sin^2\hat{\phi}(\cos\theta(\hat{z}) - 1) \\ + \alpha_3(1 + \cos^2\hat{\phi}(\cos\theta(\hat{z}) - 1)))\xi_3(\hat{z}))$$

$$a_{133}(\hat{z}) = \sin\theta(\hat{z})\cos\hat{\phi}(\alpha_1 \cos\theta(\hat{z}) - \alpha_3(1 + \cos^2\hat{\phi}(\cos\theta(\hat{z}) - 1)) \\ - \alpha_2 \sin^2\hat{\phi}(\cos\theta(\hat{z}) - 1) + \xi_1(\hat{z}))$$

$$a_{232}(\hat{z}) = \cos\theta(\hat{z})\cos\hat{\phi}\sin\hat{\phi}(\alpha_1 \sin\theta(\hat{z})\xi_4(\hat{z}) + \alpha_2 \sin^2\hat{\phi}(\cos\theta(\hat{z}) - 1) \\ + \alpha_3(1 + \cos^2\hat{\phi}(\cos\theta(\hat{z}) - 1)))\xi_3(\hat{z}))$$

$$a_{233}(\hat{z}) = \sin\hat{\phi}\cos\hat{\phi}(-\alpha_1 \sin^2\theta(\hat{z}) - (\cos\theta(\hat{z}) - 1)(-\alpha_3(1 + \cos^2\hat{\phi}(\cos\theta(\hat{z}) - 1)) \\ + \alpha_2(\cos\theta(\hat{z}) - \cos^2\hat{\phi}(\cos\theta(\hat{z}) - 1))) + \xi_1(\hat{z})\cos\theta(\hat{z}))$$

$$a_{332}(\hat{z}) = \cos^2\hat{\phi}\cos\theta(\hat{z})(\alpha_1 \sin\theta(\hat{z})\xi_4(\hat{z}) + (\alpha_2 \sin^2\hat{\phi}(\cos\theta(\hat{z}) - 1) \\ + \alpha_3(1 + \cos^2\hat{\phi}(\cos\theta(\hat{z}) - 1)))\xi_3(\hat{z}))$$

$$a_{333}(\hat{z}) = -\alpha_1 \sin^2\theta(\hat{z})\cos^2\hat{\phi} - \alpha_3(\cos\theta(\hat{z}) - \sin^2\hat{\phi}(\cos\theta(\hat{z}) - 1)) \\ (1 + \cos^2\hat{\phi}(\cos\theta(\hat{z}) - 1)) - \alpha_2 \cos^2\hat{\phi}\sin^2\hat{\phi}(\cos\theta(\hat{z}) - 1)^2 \\ + \xi_1(\hat{z})\cos\theta(\hat{z})\cos^2\hat{\phi}$$

The functions $a_{ijk}(\hat{z})$ listed above are not as complicated as they might seem at first glance. There is overlap in the required calculations between the various functions which can be utilized in the coding of the GNF filter to expedite the computations.

Appendix E

EKF Gain Calculations

The terms needed to compute $F(\hat{x})$ are presented here. Let $l_{ij}(x)$ be the (i,j) th element of L_{EB} defined in (2.14). Define

$$\Delta_1^2 = x_1^2 + x_6^2 + x_{10}^2 \quad \text{and}$$

$$\Delta_2^2 = [x_6(x_{11} - g) - x_7x_{10}]^2 + [x_3x_{10} - x_2(x_{11} - g)]^2 + [x_2x_7 - x_3x_6]^2.$$

Nine of the nonzero elements of $F(\hat{x})$ are given by

$$F_{4i-1,4j}(x) = l_{ij}(x) \quad , i = 1, 2, 3 \text{ and } j = 1, 2, 3. \quad (E1)$$

The remaining nonzero terms are given by the formula

$$F_{4i-1,j}(x) = \frac{\partial f_i}{\partial x_j} + \sum_{k=1}^3 \frac{\partial l_{i,k}}{\partial x_j} x_{4k}, \quad i = 1, 2, 3 \text{ and } j = 2, 3, 6, 7, 10, 11. \quad (E2)$$

The non-zero derivatives $\partial l_{ik} / \partial x_j$ needed to evaluate (E2) are given by

$$\frac{\partial l_{11}(x)}{\partial x_2} = \frac{1}{\Delta_1} (l_{21}^2(x) + l_{31}^2(x))$$

$$\frac{\partial l_{21}(x)}{\partial x_2} = \frac{1}{\Delta_1} (-l_{11}(x)l_{21}(x))$$

$$\frac{\partial l_{31}(x)}{\partial x_2} = \frac{1}{\Delta_1} (-l_{11}(x)l_{31}(x))$$

$$\frac{\partial l_{11}(x)}{\partial x_6} = \frac{1}{\Delta_1} (-l_{11}(x)l_{21}(x))$$

$$\frac{\partial l_{21}(x)}{\partial x_6} = \frac{1}{\Delta_1} (l_{11}(x)^2 + l_{31}^2(x))$$

$$\frac{\partial l_{31}(x)}{\partial x_6} = \frac{1}{\Delta_1} (-l_{21}(x)l_{31}(x))$$

$$\frac{\partial l_{11}(x)}{\partial x_{10}} = \frac{1}{\Delta_1} (-l_{11}(x)l_{31}(x))$$

$$\frac{\partial l_{21}(x)}{\partial x_{10}} = \frac{1}{\Delta_1} (-l_{21}(x)l_{31}(x))$$

$$\frac{\partial l_{31}(x)}{\partial x_{10}(x)} = \frac{1}{\Delta_1} (l_{11}^2(x) + l_{21}^2(x))$$

$$\frac{\partial l_{12}(x)}{\partial x_2} = \frac{1}{\Delta_2} (l_{12}(x)((x_{11} - g)l_{22}(x) - x_7 l_{32}(x)))$$

$$\frac{\partial l_{22}(x)}{\partial x_2} = \frac{1}{\Delta_2} (-(x_{11} - g)(1 - l_{22}^2(x)) - x_7 l_{22}(x)l_{32}(x))$$

$$\frac{\partial l_{32}(x)}{\partial x_2} = \frac{1}{\Delta_2} (x_7(1 - l_{32}^2(x)) + (x_{11} - g)l_{32}(x)l_{22}(x))$$

$$\frac{\partial l_{12}(x)}{\partial x_3} = \frac{1}{\Delta_2} (l_{12}(x)(x_6 l_{32}(x) - x_{10} l_{22}(x)))$$

$$\frac{\partial l_{22}(x)}{\partial x_3} = \frac{1}{\Delta_2} (x_{10}(1 - l_{22}^2(x)) + x_6 l_{22}(x)l_{32}(x))$$

$$\frac{\partial l_{32}(x)}{\partial x_3} = \frac{1}{\Delta_2} (-x_6(1 - l_{32}^2(x)) - x_{10} l_{32}(x)l_{22}(x))$$

$$\frac{\partial l_{12}(x)}{\partial x_7} = \frac{1}{\Delta_2} ((x_{11} - g)(1 - l_{12}^2(x)) - x_3 l_{12}(x)l_{32}(x))$$

$$\frac{\partial l_{22}(x)}{\partial x_7(x)} = \frac{1}{\Delta_2} (l_{22}(x)(-x_3 l_{32}(x) + (x_{11} - g)l_{12}(x)))$$

$$\frac{\partial l_{32}(x)}{\partial x_7} = \frac{1}{\Delta_2} (-x_3(1 - l_{32}^2(x)) - (x_{11} - g)l_{32}(x)l_{12}(x))$$

$$\frac{\partial l_{12}(x)}{\partial x_7} = \frac{1}{\Delta_2} (-x_{10}(1 - l_{12}^2(x)) - x_2 l_{12}(x)l_{32}(x))$$

$$\frac{\partial l_{22}(x)}{\partial x_7} = \frac{1}{\Delta_2} (l_{22}(x)(x_2 l_{32}(x) - x_{10}(x)l_{12}(x)))$$

$$\frac{\partial l_{32}(x)}{\partial x_7} = \frac{1}{\Delta_2} (x_2(1 - l_{32}^2(x)) + x_{10}l_{12}(x)l_{32}(x))$$

$$\frac{\partial l_{12}(x)}{\partial x_{10}} = \frac{1}{\Delta_2} (-x_7(1 - l_{12}^2(x)) - x_3l_{12}(x)l_{22}(x))$$

$$\frac{\partial l_{22}(x)}{\partial x_{10}} = \frac{1}{\Delta_2} (x_3(1 - l_{22}^2(x)) + x_7l_{22}(x)l_{12}(x))$$

$$\frac{\partial l_{32}(x)}{\partial x_{10}} = \frac{1}{\Delta_2} (l_{32}(x)(x_3l_{22}(x) - x_7l_{12}(x)))$$

$$\frac{\partial l_{12}(x)}{\partial x_{11}} = \frac{1}{\Delta_2} (x_6(1 - l_{12}^2(x)) + x_2l_{12}(x)l_{22}(x))$$

$$\frac{\partial l_{22}(x)}{\partial x_{11}} = \frac{1}{\Delta_2} (-x_2(1 - l_{22}^2(x)) - x_6l_{22}(x)l_{12}(x))$$

$$\frac{\partial l_{32}(x)}{\partial x_{11}} = \frac{1}{\Delta_2} (l_{32}(x)(x_6l_{12}(x) - x_2l_{22}(x)))$$

$$\frac{\partial l_{13}(x)}{\partial x_2} = \frac{1}{\Delta_1 \Delta_2} (x_{10}(x_{11} - g) + x_6x_7 - l_{13}(x)(l_{11}(x)\Delta_2 + (x_7l_{32}(x) - (x_{11} - g)l_{22}(x))\Delta_1))$$

$$\frac{\partial l_{23}(x)}{\partial x_2} = \frac{1}{\Delta_1 \Delta_2} (-2x_2x_7 + x_3x_6 - l_{23}(x)(l_{11}(x)\Delta_2 + (x_7l_{32}(x) - (x_{11} - g)l_{22}(x))\Delta_1))$$

$$\frac{\partial l_{33}(x)}{\partial x_2} = \frac{1}{\Delta_1 \Delta_2} (-2x_2(x_{11} - g) + x_3x_{10} - l_{33}(x)(l_{11}(x)\Delta_2 + (x_7l_{32}(x) - (x_{11} - g)l_{22}(x))\Delta_1))$$

$$\frac{\partial l_{13}(x)}{\partial x_3} = \frac{1}{\Delta_1 \Delta_2} (-(x_6^2 + x_{10}^2) - l_{13}(x)(-x_6l_{32}(x) + x_{10}l_{22}(x))\Delta_1)$$

$$\frac{\partial l_{23}(x)}{\partial x_3} = \frac{1}{\Delta_1 \Delta_2} (x_2x_6 - l_{23}(x)(-x_6l_{32}(x) + x_{10}l_{22}(x))\Delta_1)$$

$$\frac{\partial l_{33}(x)}{\partial x_3} = \frac{1}{\Delta_1 \Delta_2} (x_2x_{10} - l_{33}(x)(-x_6l_{32}(x) + x_{10}l_{22}(x))\Delta_1)$$

$$\frac{\partial l_{13}(x)}{\partial x_6} = \frac{1}{\Delta_1 \Delta_2} (x_2x_7 - 2x_3x_6 - l_{13}(x)(l_{21}(x)\Delta_2 + (-x_3l_{32}(x) + (x_{11} - g)l_{12}(x))\Delta_1))$$

$$\frac{\partial l_{23}(x)}{\partial x_6} = \frac{1}{\Delta_1 \Delta_2} (x_2x_3 + x_{10}(x_{11} - g) - l_{23}(x)(l_{21}(x)\Delta_2 + (-x_3l_{32}(x) + (x_{11} - g)l_{12}(x))\Delta_1))$$

$$\frac{\partial l_{33}(x)}{\partial x_6} = \frac{1}{\Delta_1 \Delta_2} (-2x_6(x_{11} - g) + x_7 x_{10} - l_{33}(x)(l_{21}(x)\Delta_2 + (-x_3 l_{32}(x) + (x_{11} - g)l_{12}(x))\Delta_1))$$

$$\frac{\partial l_{13}(x)}{\partial x_7} = \frac{1}{\Delta_1 \Delta_2} (x_2 x_6 - l_{13}(x)(x_2 l_{32}(x) - x_{10} l_{12}(x))\Delta_1)$$

$$\frac{\partial l_{23}(x)}{\partial x_7} = \frac{1}{\Delta_1 \Delta_2} (-(x_2^2 + x_{10}^2) - l_{23}(x)(x_2 l_{32}(x) - x_{10} l_{12}(x))\Delta_1)$$

$$\frac{\partial l_{33}(x)}{\partial x_7} = \frac{1}{\Delta_1 \Delta_2} (x_6 x_{10} - l_{33}(x)(x_2 l_{32}(x) - x_{10} l_{12}(x))\Delta_1)$$

$$\frac{\partial l_{13}(x)}{\partial x_{10}} = \frac{1}{\Delta_1 \Delta_2} (x_2(x_{11} - g) - 2x_3 x_{10} - l_{13}(x)(l_{31}(x)\Delta_2 + (x_3 l_{22}(x) - x_7 l_{12}(x))\Delta_1))$$

$$\frac{\partial l_{23}(x)}{\partial x_{10}} = \frac{1}{\Delta_1 \Delta_2} (x_6(x_{11} - g) - 2x_7 x_{10} - l_{23}(x)(l_{31}(x)\Delta_2 + (x_3 l_{22}(x) - x_7 l_{12}(x))\Delta_1))$$

$$\frac{\partial l_{33}(x)}{\partial x_{10}} = \frac{1}{\Delta_1 \Delta_2} (x_2 x_3 + x_6 x_7 - l_{33}(x)(l_{31}(x)\Delta_2 + (x_3 l_{22}(x) - x_7 l_{12}(x))\Delta_1))$$

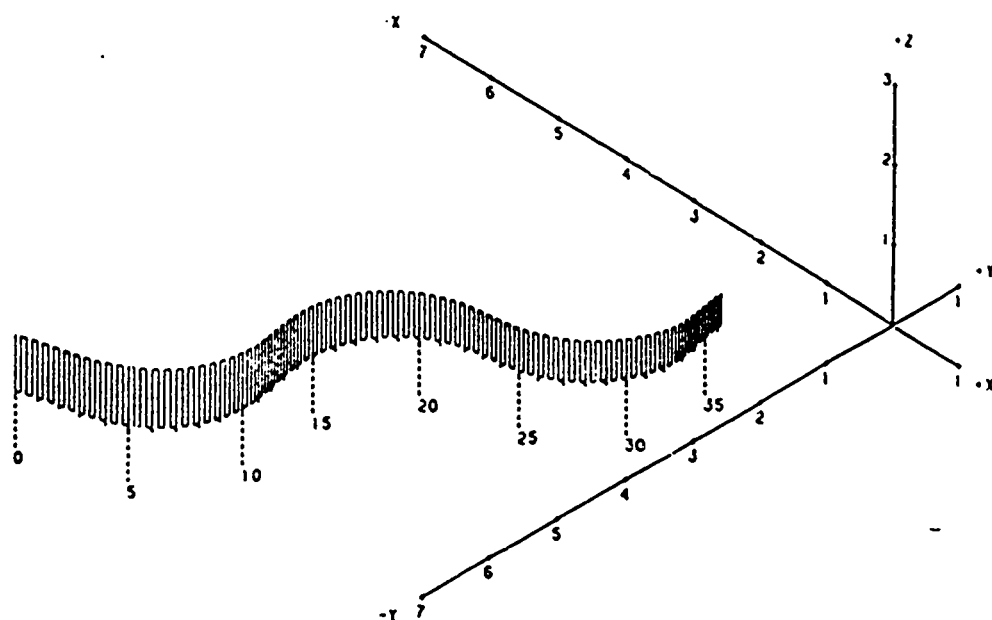
$$\frac{\partial l_{13}(x)}{\partial x_{11}} = \frac{1}{\Delta_1 \Delta_2} (x_2 x_{10} - l_{13}(x)(-x_2 l_{22}(x) + x_6 l_{12}(x))\Delta_1)$$

$$\frac{\partial l_{23}(x)}{\partial x_{11}} = \frac{1}{\Delta_1 \Delta_2} (x_6 x_{10} - l_{23}(x)(-x_2 l_{22}(x) + x_6 l_{12}(x))\Delta_1)$$

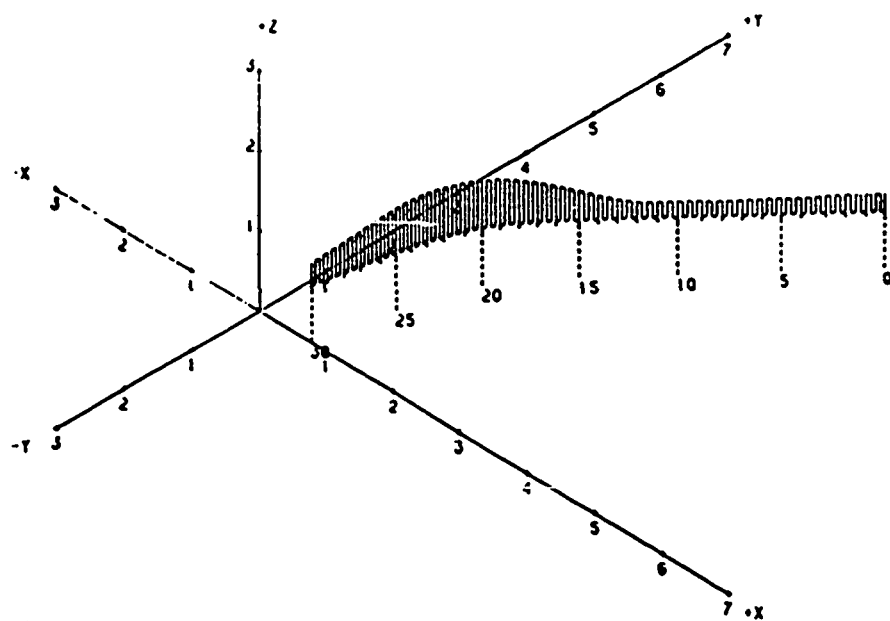
$$\frac{\partial l_{33}(x)}{\partial x_{11}} = \frac{1}{\Delta_1 \Delta_2} (-(x_2^2 + x_6^2) - l_{33}(x)(-x_2 l_{22}(x) + x_6 l_{12}(x))\Delta_1)$$

The above terms are substituted into (E2) and evaluated at the most current estimate of the state yielding $F(\hat{x})$.

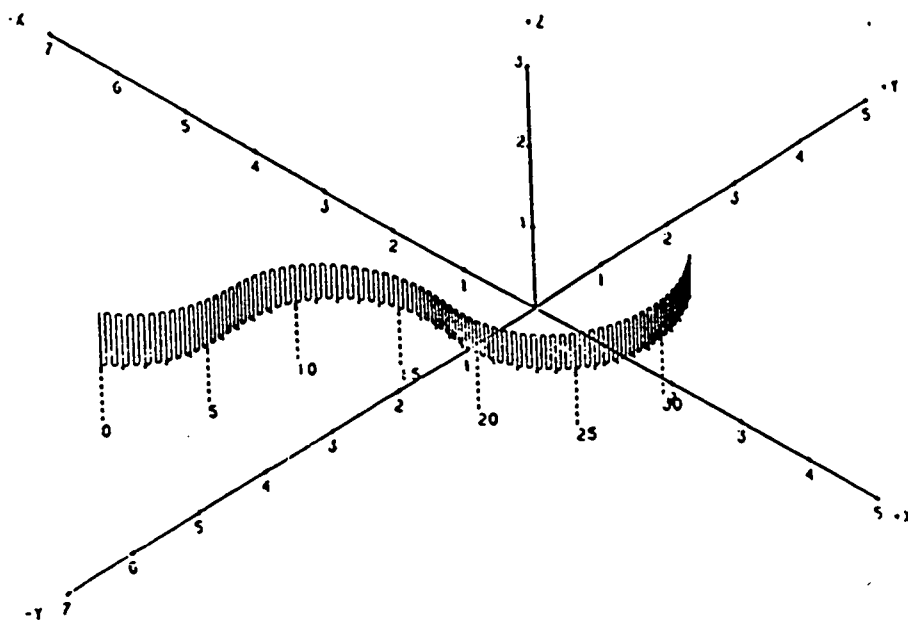
Appendix F*** Actual Aircraft Trajectories**

A898.RAW

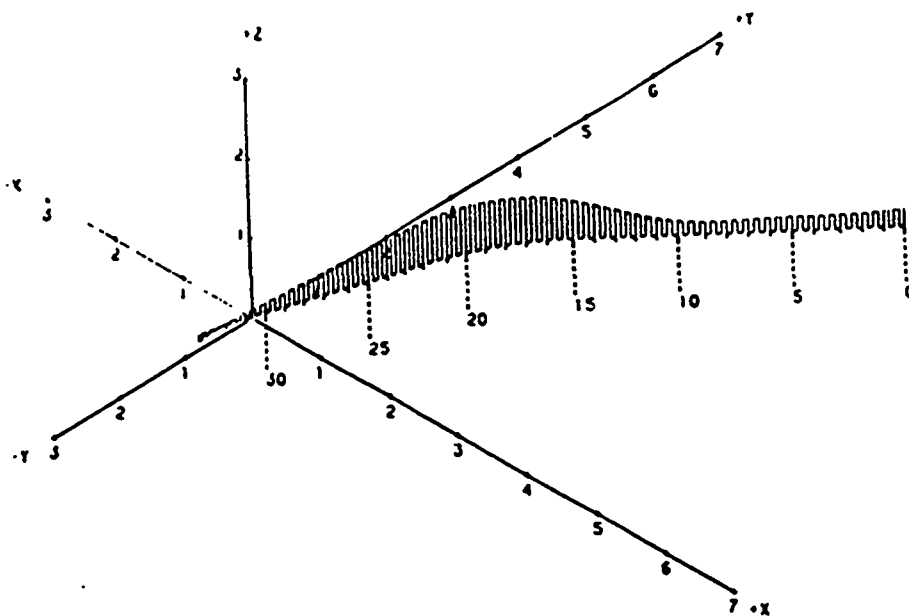
IZK898.SIM

B501.RAW

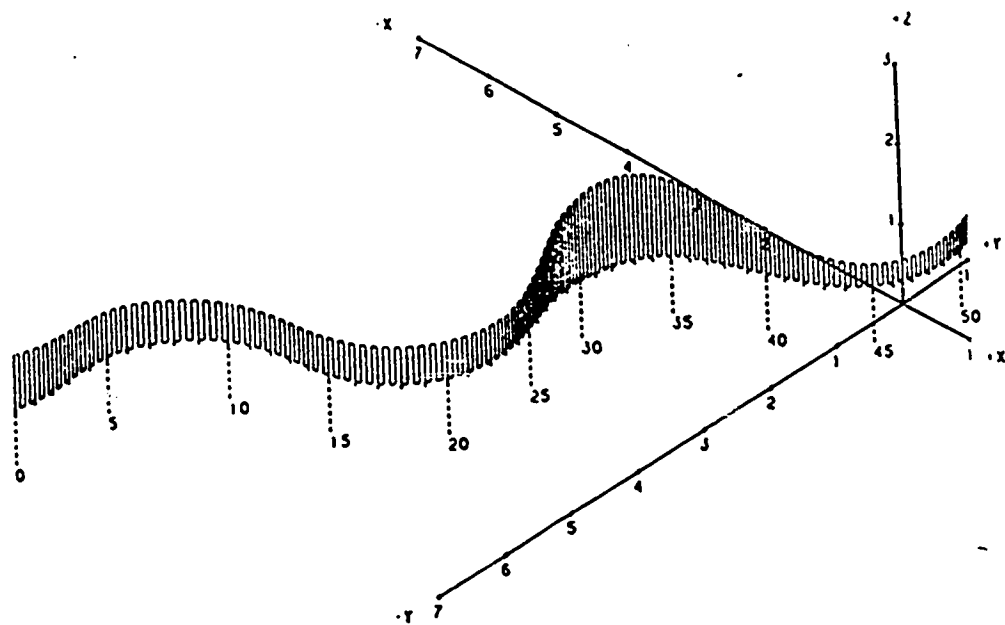
IZK501.SIM

C899.RAW

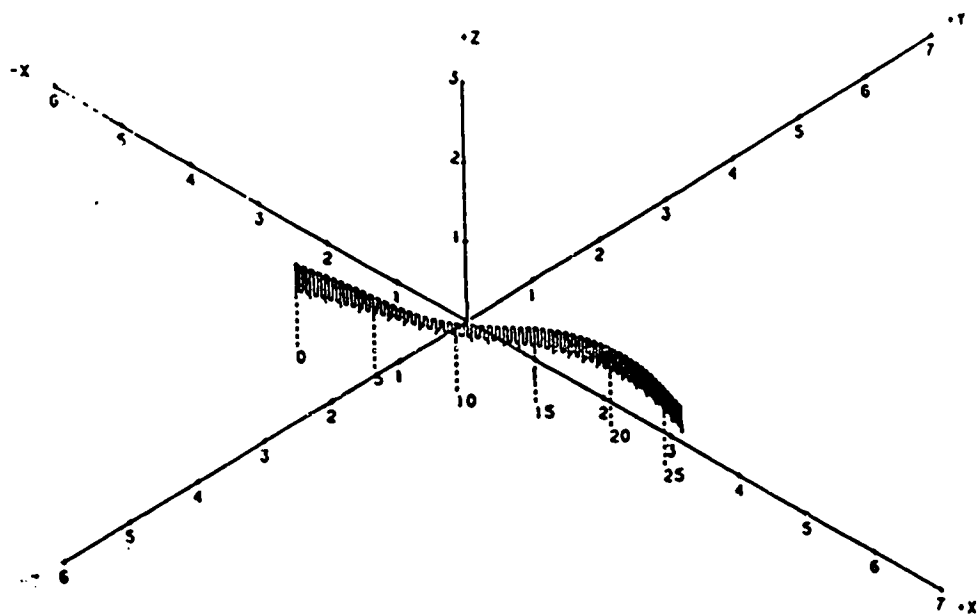
IZK899.SIM

DS02.RAW

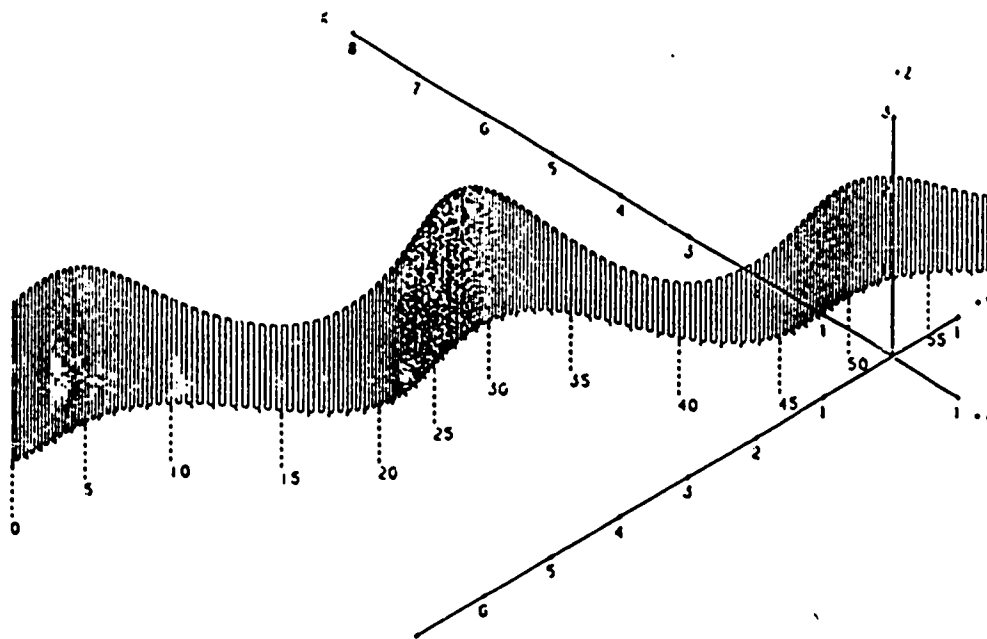
IZK502.SIM

E900.RAW

IZK900.SIM

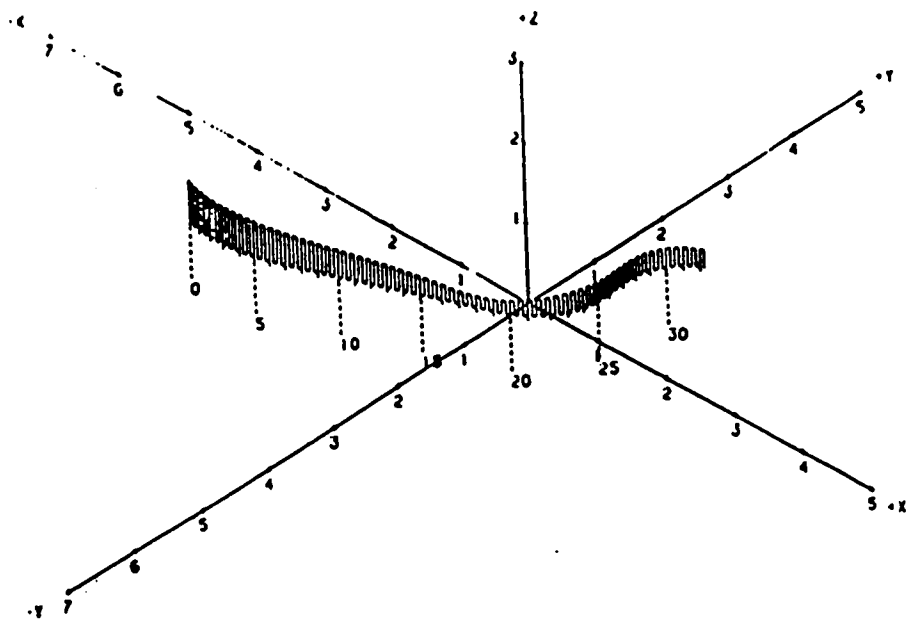
F506.RAW

IZK506.SIM



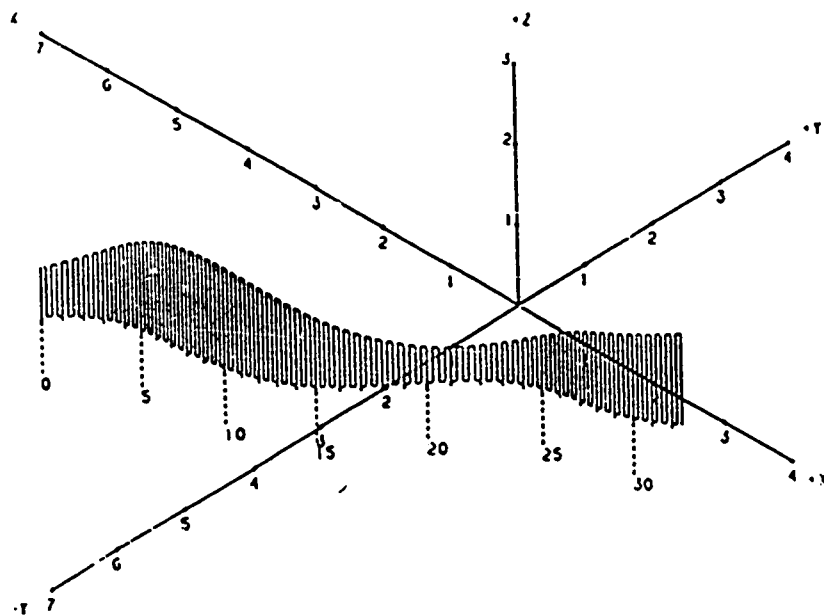
G902.RAW

IZK902.SIM



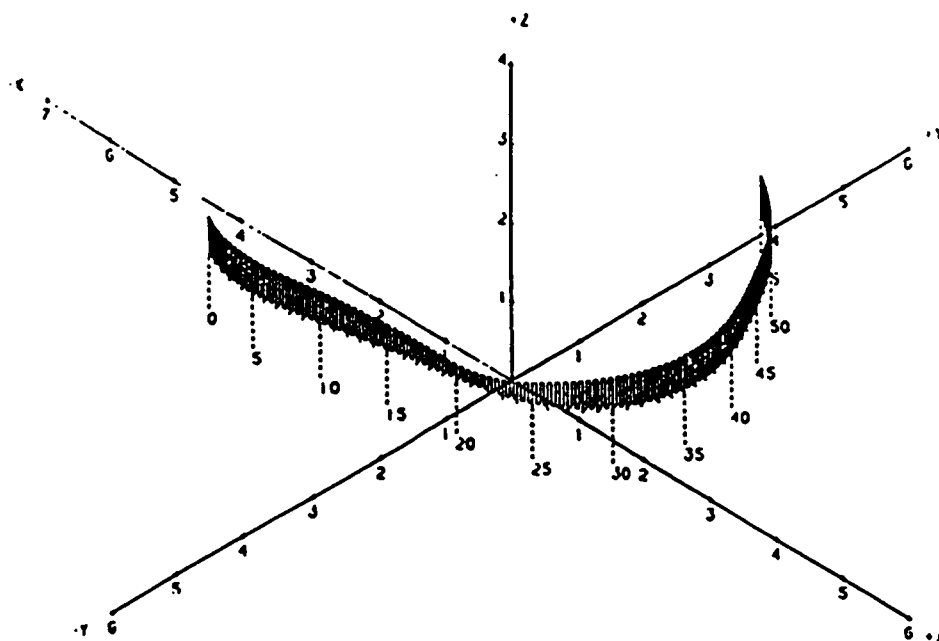
H508.RAW

IZK508.SIM



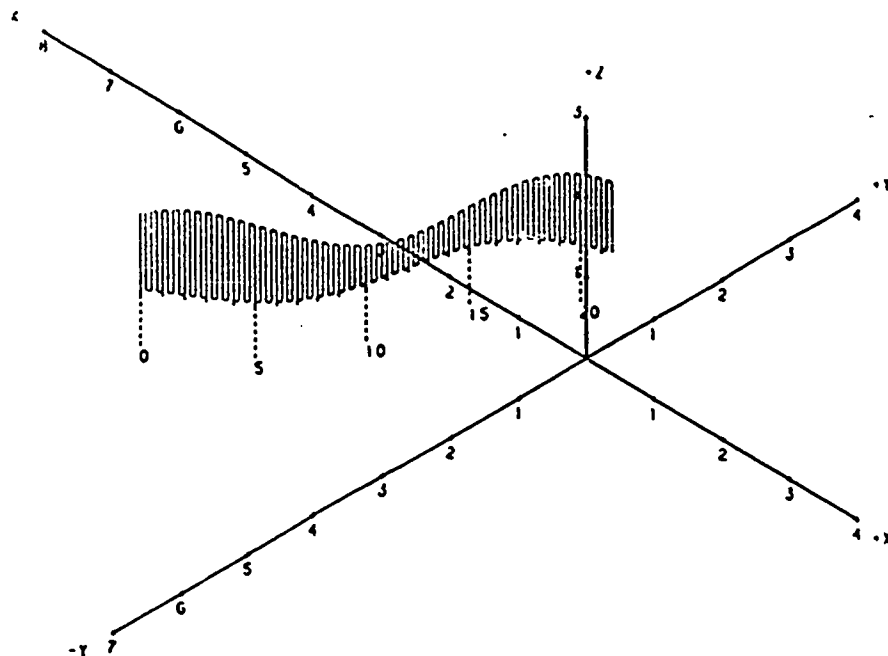
I903.RAW

IZK903.SIM

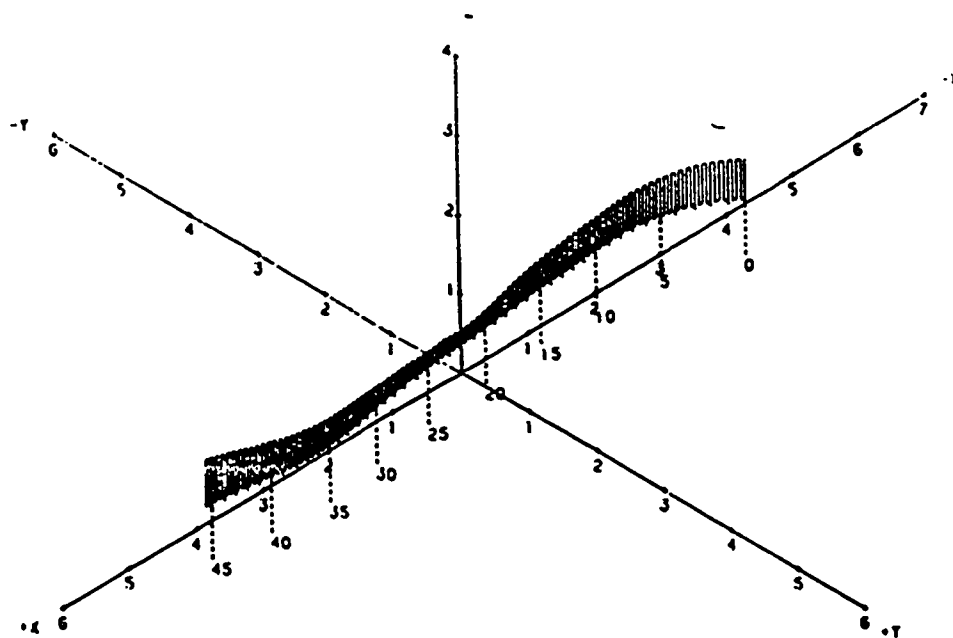


JS10.RAW

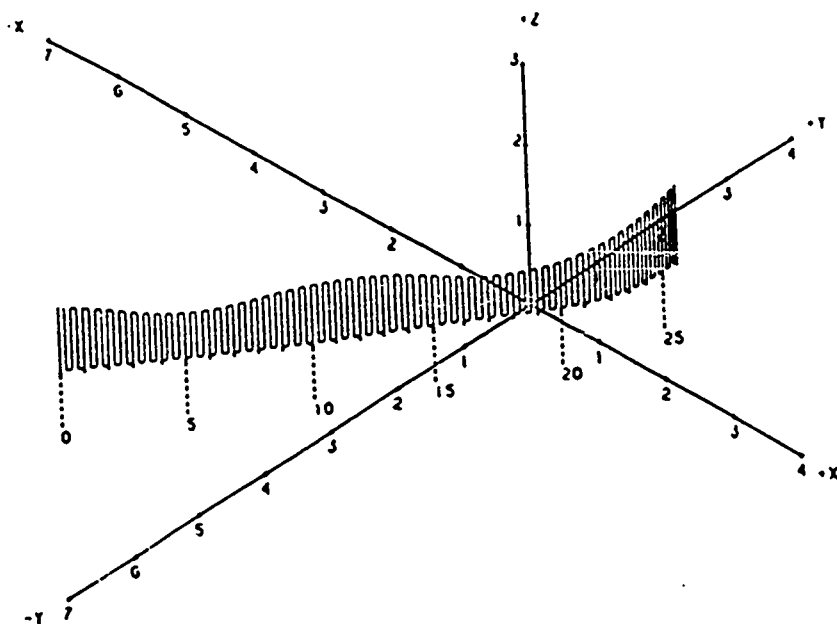
IZK510.SIM



K904.RAW IZK904.SIM

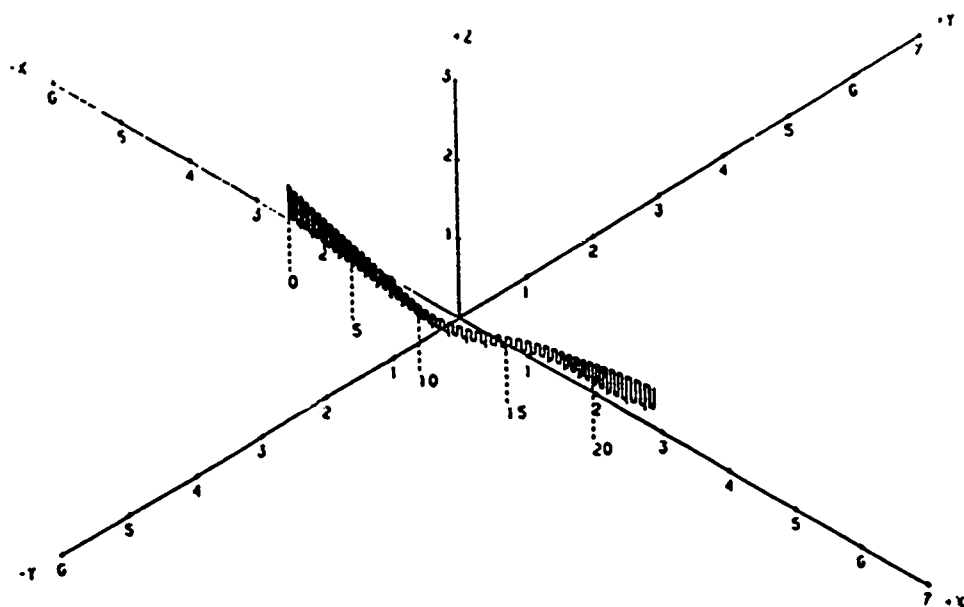


L512.RAW IZK512.SIM



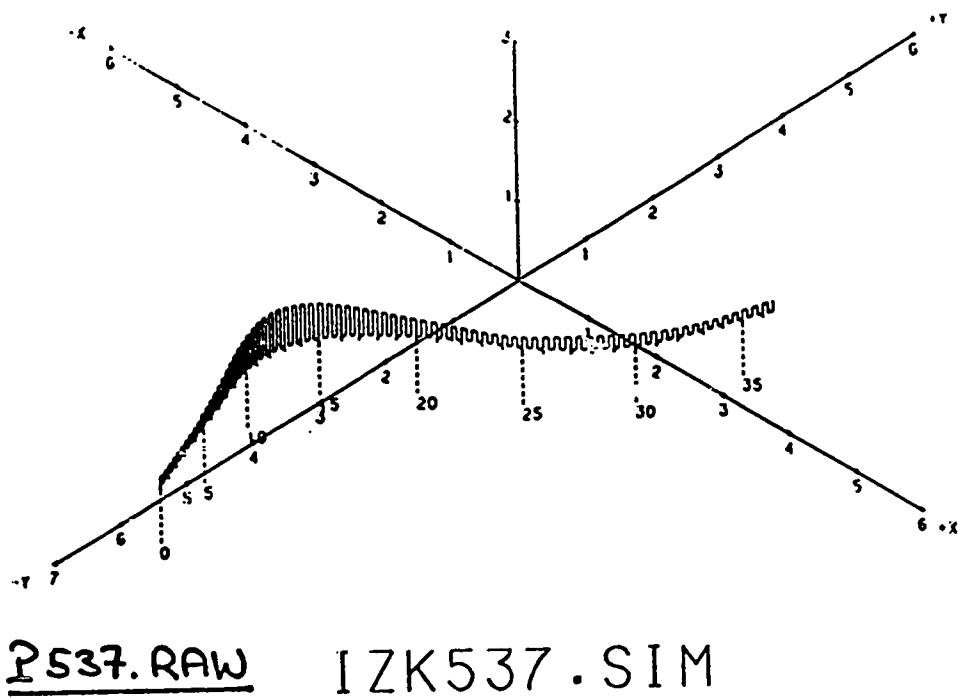
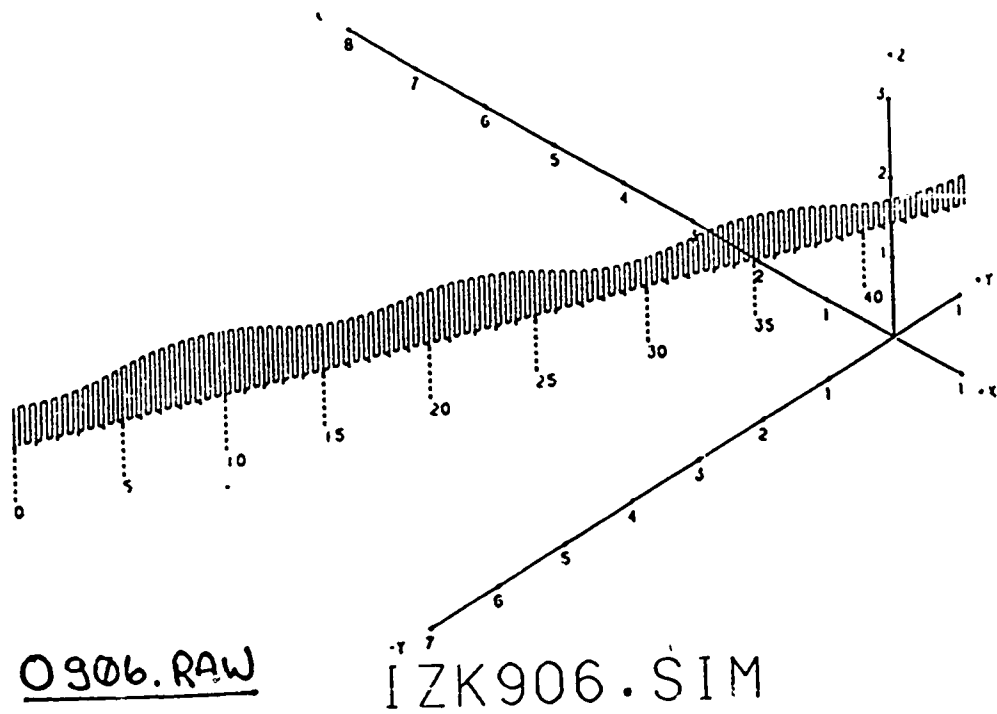
M305.RAW

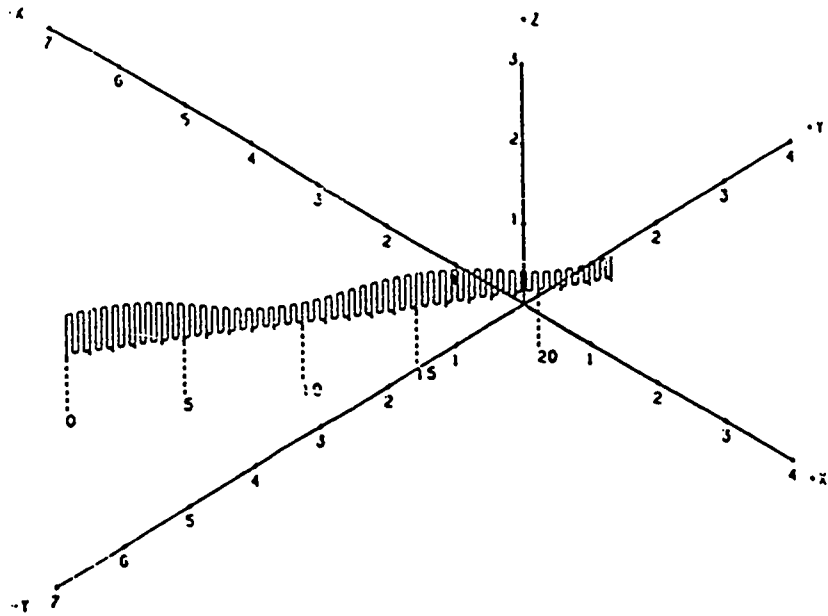
IZK905.SIM



N514.RAW

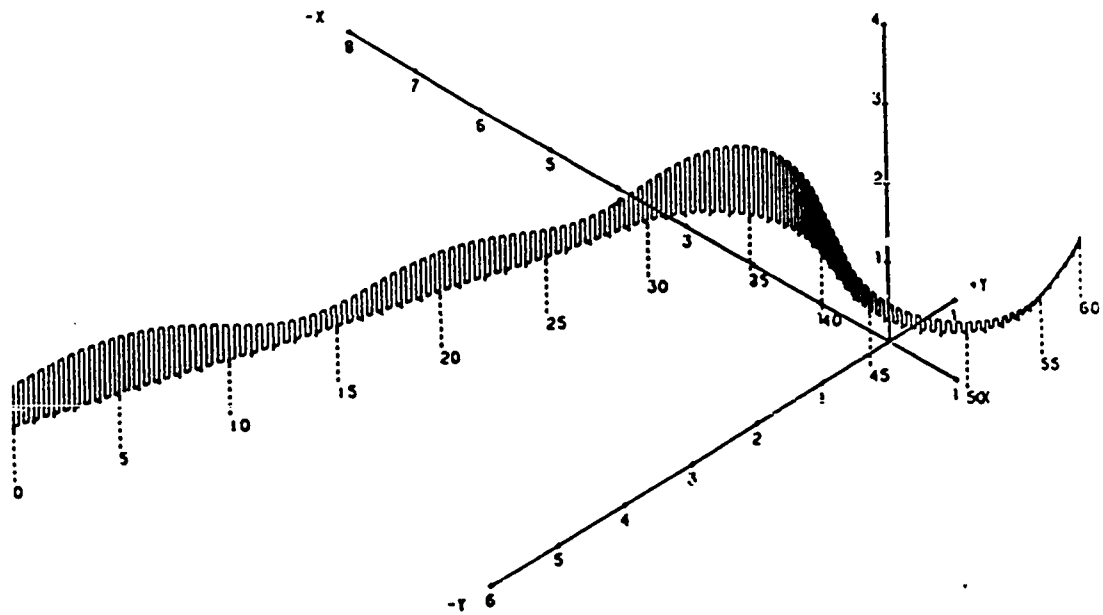
IZK514.SIM





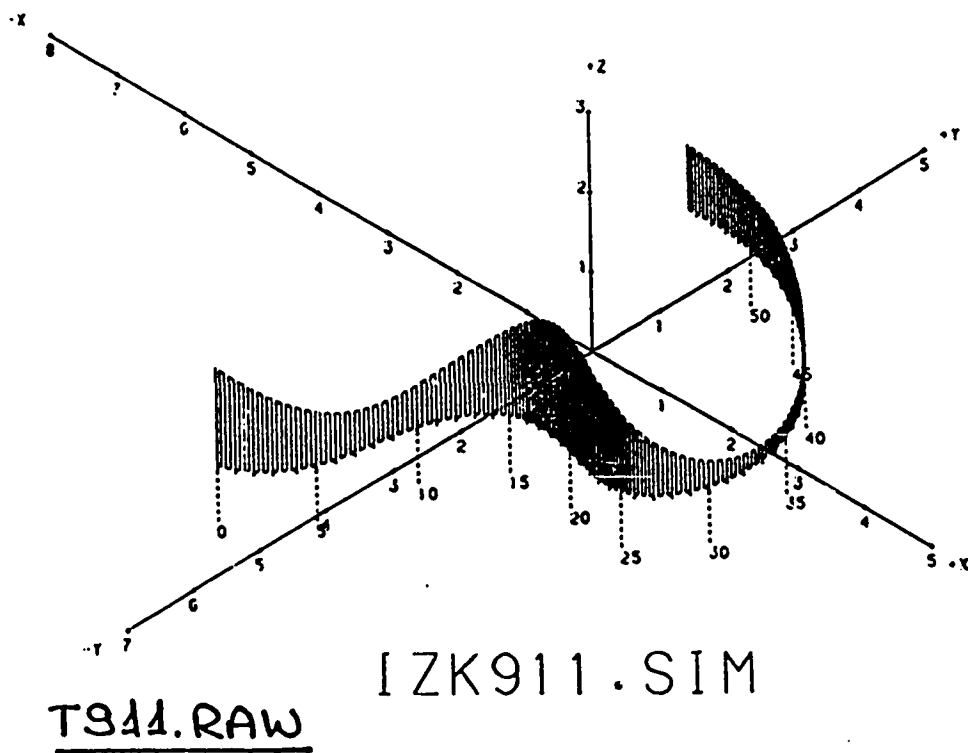
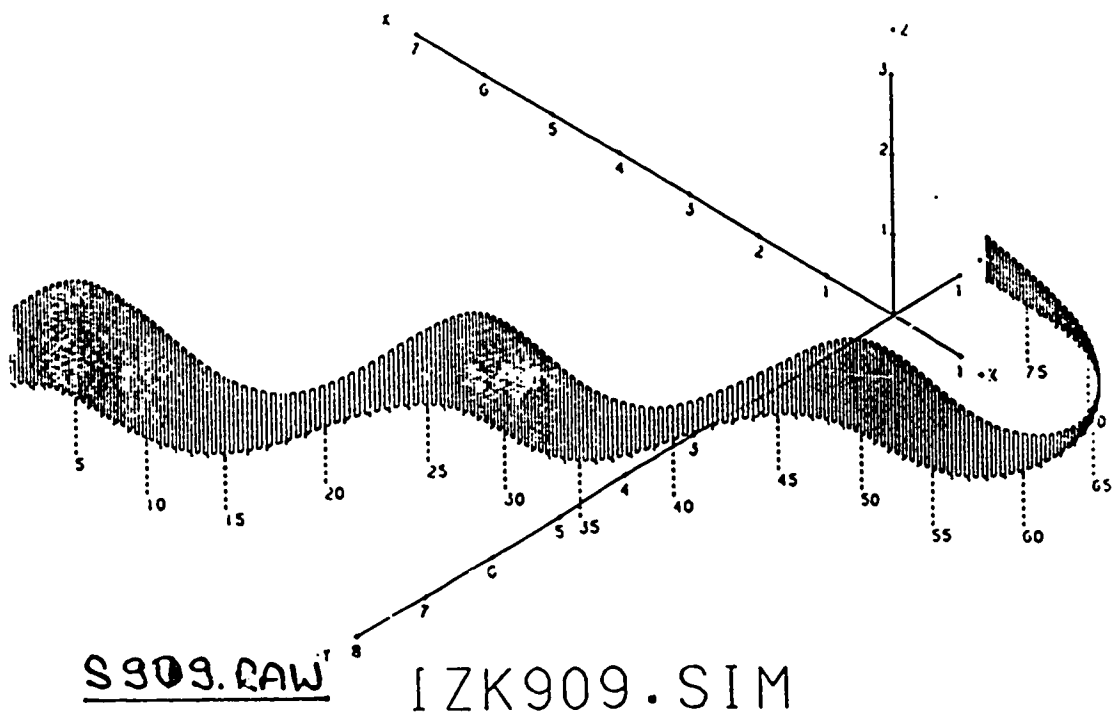
Q907.RAW

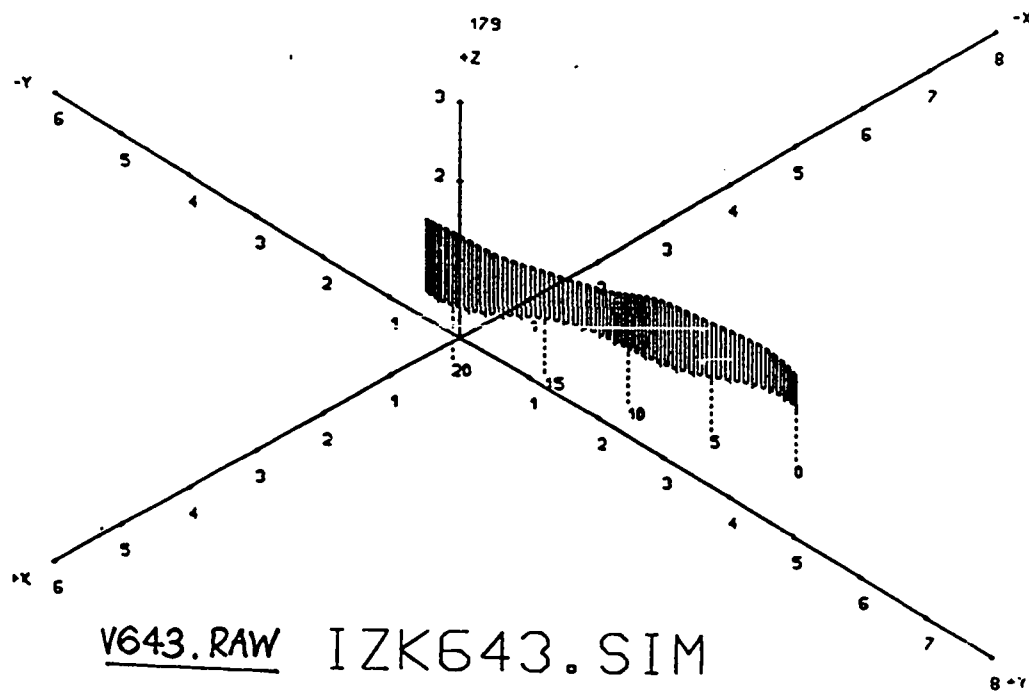
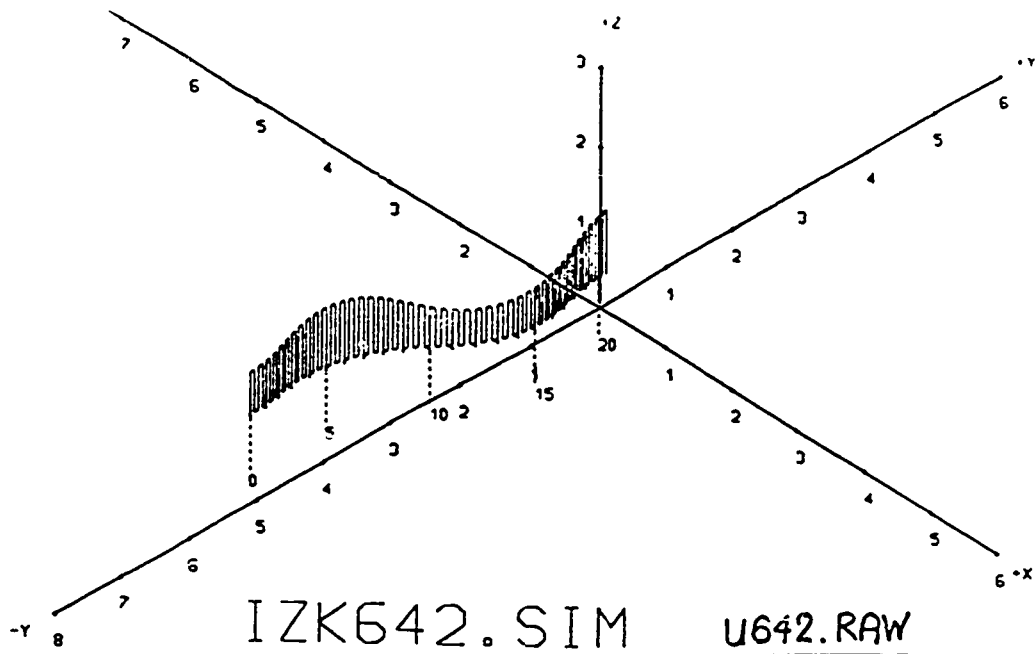
IZK907.SIM

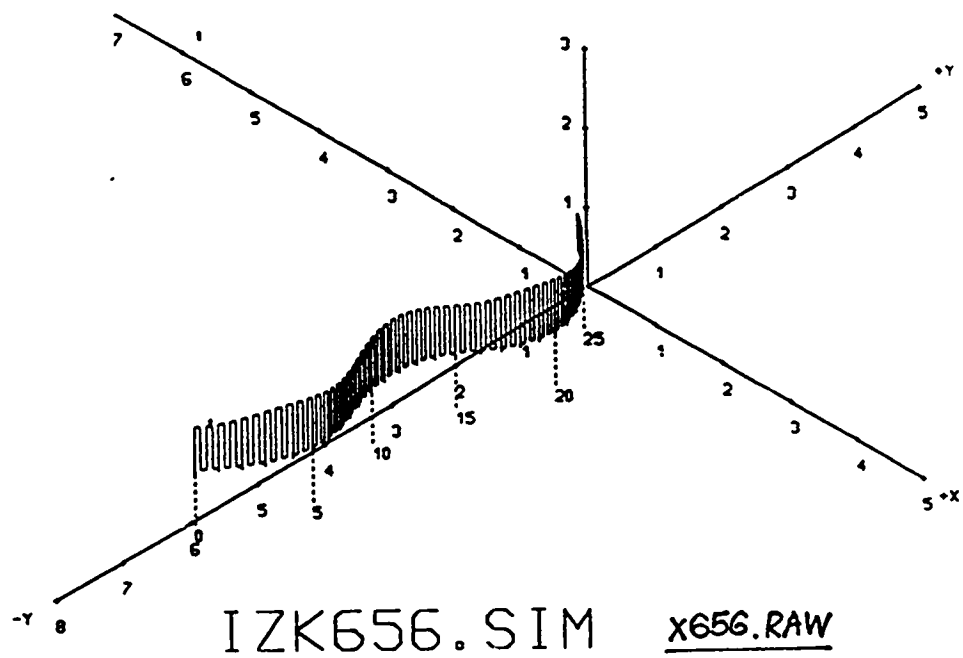
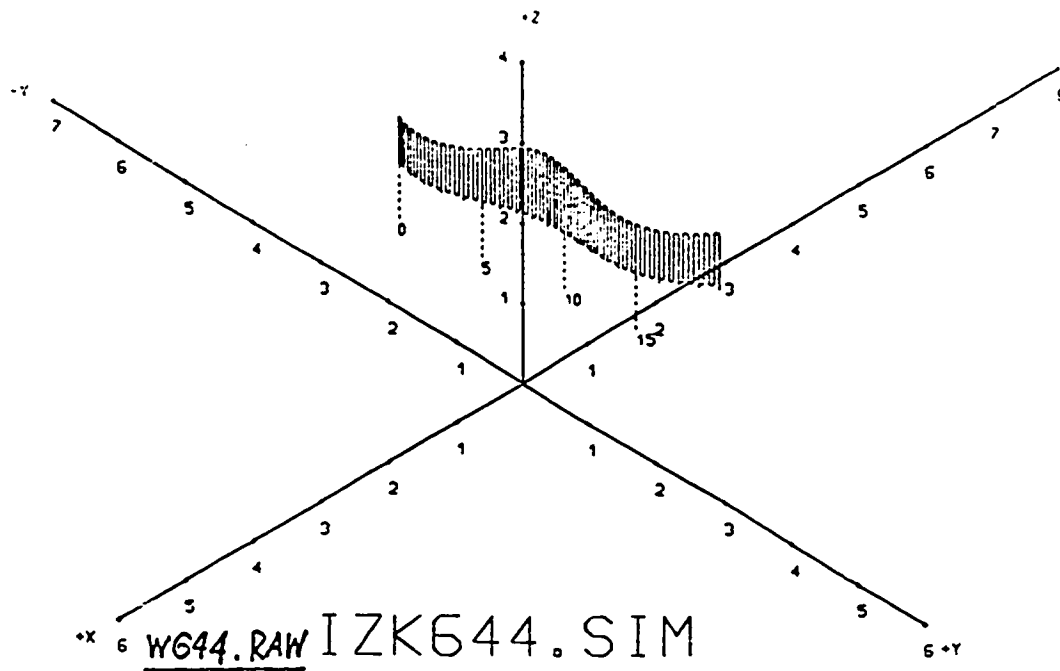


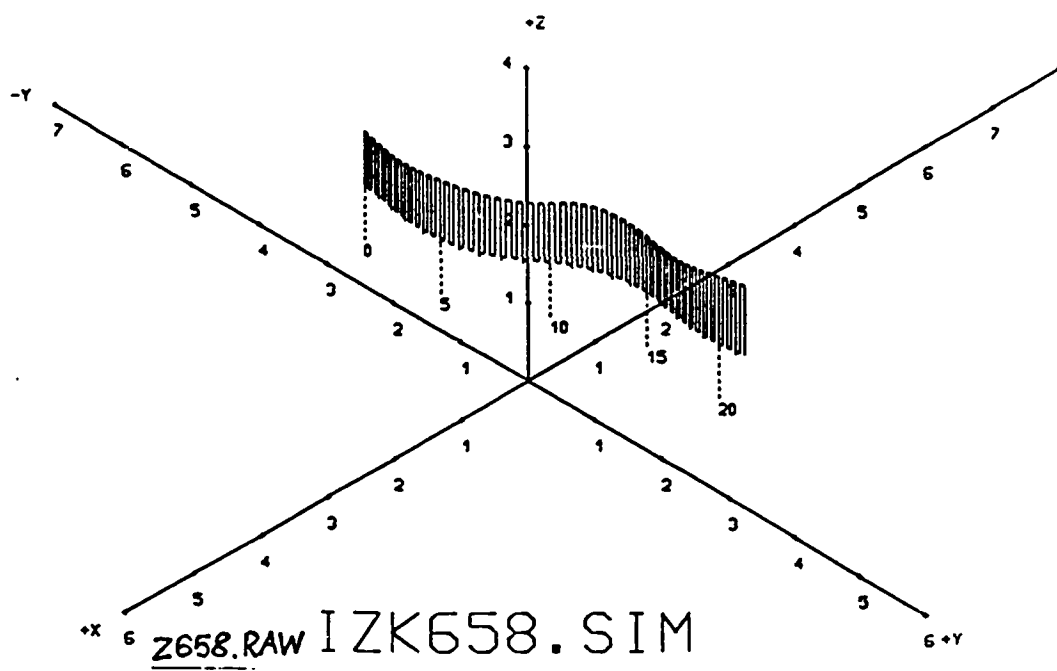
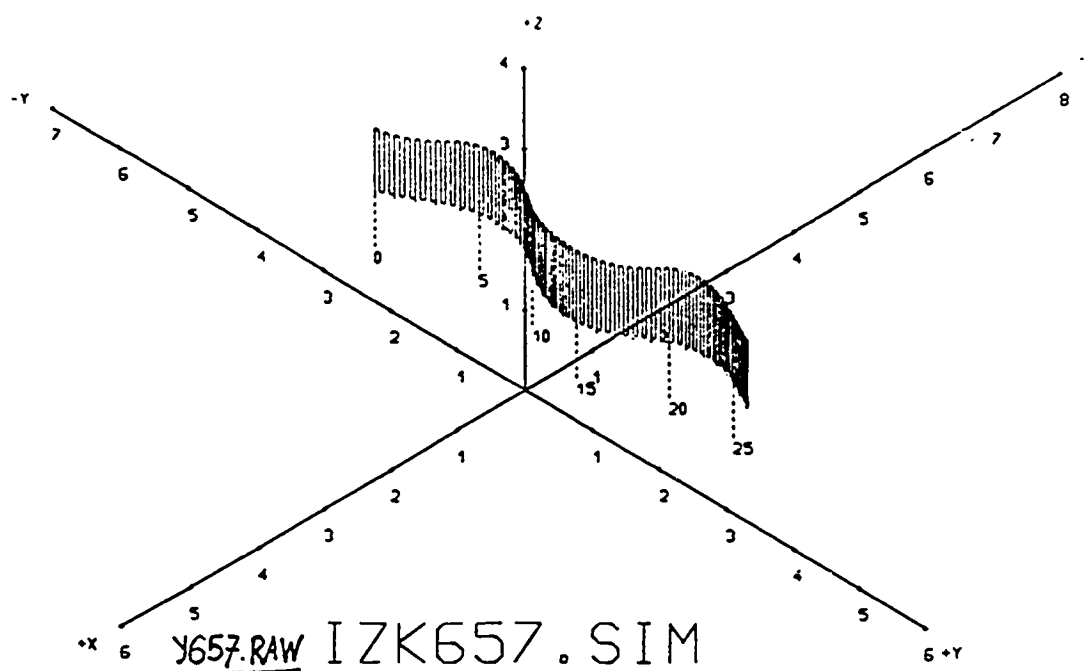
R908.RAW

IZK908.SIM









Bibliography

- [1] R. F. Berg, "Estimation and Prediction for Maneuvering Target Trajectories," IEEE AC-28, 303-313, March 1983.
- [2] D. Bestle, M. Zeitz, "Canonical form Observer design for non-linear time-variable systems," Int. J. Control, Volume 38, Number 2, 419-431, 1983.
- [3] R. H. Bishop, A. C. Antoulas, "Nonlinear Observers: Theory and Applications," Rice University, Report Number TR8805, April 1988.
- [4] C. B. Chang, J. A. Tabaczynski, "Application of State Estimation to Target Tracking," IEEE AC-29, Number 2, 98-109, February 1984.
- [5] Contraves, Personal Communication, 1986.
- [6] B. Etkin, *Dynamics of Atmospheric Flight*, John Wiley & Sons, Inc., New York, 1972.
- [7] R. Frezza, S. Karahan, A. J. Krener, M. Hubbard, "Application of An Efficient Nonlinear Filter," Analysis and Control of Nonlinear Systems, 223-237, 1988.
- [8] A. Gelb, *Applied Optimal Estimation*, The M.I.T. Press, Cambridge, Massachusetts, 1974.
- [9] N. H. Gholson, R. L. Moose, "Maneuvering Targer Tracking Using Adaptive State Estimation," IEEE Trans. Aerosp. Electron. Syst., May 1977.
- [10] R. Hermann, A. J. Krener, "Nonlinear Controllability and Observability," IEEE AC-22, Number 5, 728-740, 1977.
- [11] L. R. Hunt, M. Luksic, and R. Su, "Exact Linearizations of Input-Output Systems," Int. J. Control, Volume 43, Number 1, 247-255, 1986.
- [12] A. H. Jazwinski, *Stochastic Processes and Filtering Theory*, Academic Press, New York, 1970.
- [13] R. E. Kalman, J. E. Bertram, "Control System Analysis and Design Via the "Second Method" of Lyapunov, I. Continuous-Time Systems," Journal of Basic Engineering, 371-393, June 1960.
- [14] S. R. Kou, D. L. Elliott, T. J. Tarn, "Exponential Observers for Nonlinear Dynamic Systems," Information and Control, Volume 29, 204-216, 1975.

- [15] S. R. Kou, D. L. Elliott, T. J. Tarn, "Observability of Nonlinear Systems," *Information and Control*, Volume 22, 89-99, 1973.
- [16] A. J. Krener, "The Asymptotic Approximation of Nonlinear Filters by Linear Filters," *Theory and Applications of Nonlinear Control Systems*, 359-378, 1986.
- [17] A. J. Krener, A. Isidori, "Linearization by output injection and nonlinear observers," *Systems and Control Letters*, Volume 3, Number 1, 47-52, 1983.
- [18] A. J. Krener, S. Karahan, M. Hubbard, "Approximate Normal Forms of Nonlinear Systems," *IEEE Proceedings of the 27th Conference on Decision and Control*, 1223-1229, December 1988.
- [19] A. J. Krener, W. Respondek, "Nonlinear Observers with Linearizable Error Dynamics," *SIAM J. Control and Optimization*, Volume 23, Number 2, 197-215, March 1985.
- [20] J. Kushner, *Stochastic Stability and Control*, Academic Press, New York, 1967.
- [21] P.S. Maybeck, *Stochastic Models, Estimation and Control Volume I*, Academic Press, 1979.
- [22] A. Miele, *Flight Mechanics, Volume 1, Theory of Flight Paths*. Addison-Wesley Publishing Company, Inc., Reading, Massachusetts, 1962.
- [23] R. L. Moose, "Adaptive Estimator for Passive Range and Depth Determination of a Maneuvering Target(U)," *U.S. Naval J. Underwater Acoustics*, July 1973.
- [24] R. L. Moose, H. F. Vanlandingham, D. H. McCabe, "Modeling and Estimation for Tracking Maneuvering Targets," *IEEE Trans. Aerosp. Electron. Syst.*, AES-15, Number 3, 448-456, May 1979.
- [25] J. R. Munkres, *Topology A First Course*, Prentice-Hall, Inc., New Jersey, 1975.
- [26] B. O'Neill, *Elementary Differential Geometry*, Academic Press, New York, 1966.
- [27] A. R. Phelps, A. J. Krener, "Computation of Observer Normal Form Using Macsyma", *Analysis and Control of Nonlinear Systems*, C. I. Byrnes, C. F. Martin, and R. E. Sacks (editors), Elsevier Science Publisher B. V., North Holland, 1988.
- [28] J. B. Pearson, "A Note on Nonlinear Filtering," *IEEE AC-13*, Number 1, 103-105, February 1968.

- [29] R. A. Singer, "Estimating Optimal Tracking Filter Performance for Manned Maneuvering Targets," *IEEE Trans. Aerosp. Electron. Syst.*, AES-6, 420-436, 1970.
- [30] R. A. Singer, K. W. Behnke, "Real-Time Tracking Filter Evaluation and Selection for Tactical Applications," *IEEE Trans. Aerosp. Electron. Syst.*, AES-7, No. 1, 100-110, January, 1971.
- [31] F. E. Thau, "Observing the state of non-linear dynamic systems," *Int. J. Control*, Volume 17, Number 3, 471-479, 1973.
- [32] J. S. Thorp, "Optimal Tracking of Maneuvering Targets," *IEEE Trans. Aerosp. Electron. Syst.*, AES-9, July 1973.
- [33] M. Vidyasagar, *Nonlinear Systems Analysis*, Prentice-Hall Inc., New Jersey, 1978.
- [34] B. L. Walcott, M. J. Corless, S. H. Zäk, "Comparative study of non-linear state-observation techniques," *Int. J. Control*, Volume 45, Number 6, 2109-2132, 1987.
- [35] J. Weilenmann, Data package containing the aircraft maneuver trajectory data base, Contraves AG, August 30 1988.
- [36] D. E. Williams, B. Friedland, "Target Maneuver Detection and Estimation," *Proceedings of the 27th Conference on Decision and Control*, Austin, TX December 1988.